Optimal Control of Marine Propulsion Diesel Engine During Transient Loading Operation:

Application for Smoke Opacity Reduction through Manifold Air Injection Avoiding Compressor Surge

George Papalambrou

Doctoral Thesis

School of Naval Architecture and Marine Engineering
National Technical University of Athens

Supervisor: Professor N. P. Kyrtatos

September 2008

Contents

Contents iii

List of Figures vii

List of Tables xi

1 Introduction 3

1.1 Problem Formulation 3

1.2 Smoke Emissions in Diesel Engines 4

1.2.1 Smoke Formation 5

1.2.2 PM and Smoke Density (Opacity) Measurement . . . 7

1.2.3 Emission Legislation 8

1.3 Review of Previous Work 10

1.3.1 Air Injection 10

1.3.2 Predictive Control Applications in Combustion Engines 11

1.4 Thesis Contributions 12

2 Experimental Engine Setup 15

2.1 Engine Testbed 15

2.2 Instrumentation 16

2.3 Data Acquisition System 18

2.4 Engine Hierarchical Control System 19

2.4.1 The Air Injection Controller 20

2.4.2 The Engine Controller 20

2.5 Engine Operation 21

2.6 Air Injection 24

2.7 Compressor 24
2.8 Setting Up the Experiments 25
2.9 Summary 26

3 Identification of Engine Model **33**
3.1 System Identification 33
3.2 Identification Methods 35
3.2.1 Parametric Identification 36
3.2.2 Subspace Identification 36
3.2.3 Nonlinear Identification 36
3.3 Model Structures 37
3.3.1 Transfer Function and Polynomial Models 37
3.3.2 State Space Models 39
3.3.3 Performance quality criteria 40
3.4 System Identification for Engine Model 40
3.4.1 Data Scaling 41
3.4.2 Measurement Schedule 42
3.4.3 Transfer Function Results 44
3.4.4 Subspace Results 50
3.4.5 Nonlinear Identification Results 50
3.5 Summary 51

4 Model Predictive Controller **57**
4.1 Formulation of Model Predictive Control 57
4.1.1 Application Fields 58
4.1.2 The Basic Elements 59
4.1.3 Unconstrained MPC 61
4.1.4 Constrained MPC 63
4.1.5 State Estimation 65
4.1.6 Tuning Parameters 66
4.1.7 Advantages, Drawbacks, Limitations 66
4.2 Models for MPC 67
4.2.1 Step and Pulse Response 68
4.3 Stability and Robustness 69

4.3.1 Stability in Predictive Control 69
4.3.2 Robustness in Predictive Control 69
4.4 Nonlinear Model Predictive Control 70
4.5 Summary 71

5 Control of Smoke Density (Opacity) 73
5.1 Control Systems in Marine Diesel Engines 74
5.2 Controller Design 74
5.2.1 Control Objectives 74
5.2.2 Tuning 75
5.3 Implementation of Control Algorithms 78
5.4 Performance of Predictive Controllers 81
5.4.1 Results from Pressure Control 83
5.4.2 Results from Opacity Control 90
5.5 Summary 98

6 Conclusions and Future Work 101

References and Bibliography 105

Appendices 115
.1 Instrumentation and Controllers 115
.2 Compressor Instability 120

List of Figures

1.1 Soot mass fraction .vs crank angle in diesel engine 6

2.1 The test-bed with engine and brake 16
2.2 The instrumentation diagram of the engine testbed 27
2.3 The opacimeter as connected to the engine exhaust line . . . 28
2.4 The AVL Indiset 620 28
2.5 The computer architecture for control and data acquisition . 29
2.6 The engine digital controller 29
2.7 The air injection supply line as it enters the intake manifold . 30
2.8 The air injection supply line with sensors and actuator 30
2.9 The turbocharger compressor side at engine testbed 31
2.10 The cabinet in the Control room 31

3.1 Block diagram of the engine model, as used in system identification 41
3.2 Measured engine responses during the Base test. Air injection is not applied. 43
3.3 Measured engine responses during the A1 test. Air injection is applied for 4 sec 44
3.4 Measured engine responses during the A2 test. Air injection is applied for 8 sec 45
3.5 Measured engine responses during the B1 test. Air injection is applied in pulses. 46
3.6 Open loop step input for opacity, input 1 (fuel) 48
3.7 Open loop step input for opacity, input 2 (pressure) 49
3.8 Bode frequency response for opacity, with input fuel 50

3.9 Bode frequency response for opacity, with input air injection 51
3.10 Residuals for opacity 52
3.11 Open-loop identified and measured opacity 52
3.12 Open loop step input for pressure 53
3.13 Bode frequency response for pressure, with input air injection 53
3.14 Residuals for pressure, Pengin 54
3.15 Open-loop identified and measured pressure 54
3.16 The identified nonlinear Hammerstein-Wiener model 55

4.1 Predictive control: the basic idea 60
4.2 Block diagram of a MPC with state feedback without constraints 63
4.3 Block diagram of a MPC with constraints and state feedback 65

5.1 The simulated MPC in closed-loop configuration 76
5.2 Simulated MPC, standard 77
5.3 Simulated MPC, with $P = 10,\ 20,\ 50$ 78
5.4 Simulated MPC, $R = 1,\ 10,\ 100$ 79
5.5 Simulated MPC, $T_s = 0.05,\ 0.1,\ 0.2$ sec 80
5.6 MPC block diagram 81
5.7 Relay element in controller for air injection 82
5.8 The digital filter for Pengin channel in action 83
5.9 Bode plot of the digital filter for pressure 84
5.10 Predictive controller for pressure in intake manifold (MPC I) 85
5.11 Controlled and manipulated variables, MPC I, set point 1 . . 86
5.12 Opacity and fuel rack variables, MPC I, set point 1 87
5.13 Control output and the relay switching, MPC I, set point 1 . 88
5.14 Controlled and manipulated variables, MPC I, set point 2 . . 89
5.15 Opacity and fuel rack variables, MPC I, set point 2 90
5.16 Control output and the relay switching, MPC I, set point 2 . 91
5.17 Predictive controller for opacity (MPC II) 92
5.18 Controlled and manipulated variables, MPC II, setting a . . . 93
5.19 Constraint and fuel rack variables, setting a 94
5.20 Control output and the relay switching a 95

5.21 Controlled and manipulated variables, MPC II, setting b . . . 96
5.22 Constraint and fuel rack variables, setting b 97
5.23 Control output and the relay switching b 98
5.24 Comparison for opacity, MPC II 99
5.25 Comparison for intake manifold pressure, MPC II 100
5.26 Comparison of opacity with air injection under MPC control (top) and without air injection 100

1 The various sensors at engine 116
2 The AVL amplifier rack 117
3 Surge avoidance 122

List of Tables

2.1 Sensors and actuators at testbed 17

3.1 Transfer functions from control and disturbance inputs to outputs 47

5.1 Parameters of the experimental controllers 82

Abstract

The reduction of smoke emissions and improvement of load acceptance in a turbocharged marine diesel engine, during transient operation involving rapid load increases, were considered in the present work. Model predictive control (MPC) was used in a system for external compressed air injection directly in the air manifold. Concurrently, the aim was to avoid surge in the turbocharger compressor upstream of the air manifold.

Previous work in the Laboratory of Marine Engineering/NTUA had proved experimentally the applicability of the air injection method for smoke reduction and had also investigated the compressor surge behavior via engine performance simulations.

Compressor system surge is a self-excited limit cycle oscillation, characterized by large amplitude pressure rise and mass flow fluctuations. It starts to occur when the pressure rise and mass flow characteristics for constant speed exceed certain values determined by characteristics of the compressor and load. A surge avoidance method was used , where stable operation was achieved by operating the compressor at a safe distance, defined as surge margin, from the unstable region.

In MPC, a dynamical model of the process is used to construct and solve an optimization problem aiming to achieve prescribed performance, under constraints on input/output variables. MPC is widely accepted in the process industry and recently has been considered for the control in combustion engines, despite the high computational overhead.

Due to the difficulty of deriving a process model from first principles for the smoke density (opacity), system identification was used in order to derive control models relating air injection and fuel to opacity and intake

manifold pressure. Air injection was considered as manipulated variable, and opacity as controlled variable. The fuel was considered as measured disturbance. Intake manifold pressure was related to compressor instability. In the MPC, the objective function was the minimization of smoke density (opacity), with constraint not to exceed a limit in intake manifold pressure.

Experiments at the Laboratory were performed on a full scale marine diesel engine, with two different types of predictive controllers. Results comparing the opacity under air injection model predictive control with the standard engine operation, i.e. without air injection, during the same transient were presented. It can be seen that with air injection, opacity was reduced considerably. The peak value remained the same in both cases, about 80%. However, in the case with air injection, this peak dropped considerably after about 0.5 sec to a steady value of about 40%, until the end of disturbance.

The significant reduction obtained in the full scale testbed experiments demonstrated the effectiveness of the proposed system of controlled air injection for smoke abatement during engine transients, as well as the suitability of the control method used.

Acknowledgments

First and foremost, I would like to thank my supervisor Professor N. Kyrtatos for his guidance in this research effort. He gave me the freedom to follow my own research ideas and additionally he entrusted me the entire engine test-bed for all the required experimental runs. He justified the thesis research objectives so as to be respected challenges for experimentation, arranged for all the details during these four years with endless optimism despite the difficulties, and provided instructive comments and suggestions.

I thank also the other two members of the Committee, Professors C. Frangopoulos and K. Kyriakopoulos for their support and very constructive comments during our meetings.

In particular I would like to thank Dr. N. Alexandrakis, who as test-bed manager made possible to operate the complete engine with total success. He provided the basic ideas for data acquisition and hardware signal conditioning and set-up the appropriate measurement devices-often of his own construction.

I thank also Dr. L. Kaiktsis, for his assistance in the part related to the smoke emissions.

This work is devoted to my wife Sophia and sons Ilias and Konstantinos, for all their support and those evenings with weekends that I was not with them.

Chapter 1

Introduction

The focus of this thesis is on the reduction of exhaust smoke density (opacity) during load transient in a diesel engine by injecting external compressed air directly into the intake manifold. A performance constraint related to turbocharger compressor instability is imposed: the pressure in the engine intake manifold should not exceed certain limits. Model-based control theory was used, with two elements. The first is the requirement of a suitable engine model for prediction. The second is the minimization of a cost function related to opacity, subject to constraints.

In this chapter the stage is set up with the formulation of the problem, presentation of information on smoke and the method of opacity measurement and finally review of air injection and model-based control applications related to diesel engines.

1.1 Problem Formulation

The main problem under consideration is the mismatch of air to fuel, when a large load is suddenly applied to a turbocharged diesel engine. During such a transient, the engine speed initially drops. The speed controller will command the fuel actuator to provide more fuel, anticipating the deviation from its set point. As this is conventionally a fast hydraulic/electric system, it will respond promptly. On the other hand, engine air cannot be admitted as fast. Of concern here is the *turbocharger lag*, which refers to the inability

of turbocharger to respond rapidly to changes in load and engine speed changes, due to its rotating inertia. Consequently the turbocharger lag can be a problem during transient operation, as the compressor flow and pressure may not be sufficient to meet engine breathing requirements during the lag period. Marine diesel engines are used for 99% of all ships. In marine diesel propulsion, the turbocharger, the engine, and the propeller operation are optimized to achieve the rated power and maximum torque output. Thus, the turbocharger size is determined for high engine torque output which usually leads to large inertia and effective flow area and consequently slow air flow response [SS00].

According to a recent study [LLG+08] large cargo ships emit more than twice as much soot as previously estimated, and tugboats emit nearly twice as much soot for the amount of fuel used than other commercial vessels. Tugboats are typical vessels with large load transients.

During a load increase, due to poor combustion from the fuel/air mismatch, excessive exhaust smoke may be caused, and engine has a limited responsiveness. Several methods and devices have been proposed, in an effort to reduce such smoke emissions. One possible measure is the forced external increase of air flow to the engine. In this work external compressed air is injected directly into the intake manifold, downstream of the turbocharger compressor.

One drawback is the possible cause of instability or even surge in the compressor due to the sudden increase of its downstream pressure and subsequent opposite flow.

1.2 Smoke Emissions in Diesel Engines

The need for compliance to low regulatory limits on emissions has brought considerable advances in the understanding of the smoke and soot and particulate formation mechanism. In this section the smoke formation process and the measurement of opacity are reviewed, as well as the applicable legislation for marine transportation.

1.2.1 Smoke Formation

The present work is concerned about the relation of smoke emissions and diesel engines. Diesel engines have relatively low engine-out emissions in hydrocarbons and carbon monoxide emissions. The main pollutant species in the diesel exhaust are Nitrogen Oxides (NOx) due to the high pressures and temperatures during combustion, smoke and Particulate Matter (PM). As in spark ignition engines, the air/fuel ratio is one primary factor that affects pollution formation; others are the injection timing and pressure. Smoke and PM emissions are caused when insufficient oxygen is admitted to the engine to fully burn the fuel. On the other hand, excess of oxygen raises the combustion temperature and increases the NOx emissions.

Diesel particulate matter (PM) is a complex mixture of solid and carbonaceous material, unburned hydrocarbons and inorganic compounds. The measured amount of absorbed and condensed matter strongly depends on the cooling conditions: temperature, cooling rate, residence time in the conditioning and sampling devices, etc.

Exhaust particulate matter (PM) composition of marine diesel operation can be summarized by following fractions [CIM08]:

$$PM = Soot + SOF + IF \tag{1.1}$$

where Soluble Organic Fraction (SOF) refers to organic material and IF (Inorganic Fraction) to volatile, semi-volatile and non-volatile compounds like sulphates and nitrates, metals and water.

Soot is produced during incomplete combustion. Ash originates from fuel and lube oil (additives, impurities) as well as engine wear and corrosion products. Volatile species are accumulated on the particles as exhaust gas cools down during the travel through the exhaust duct and any measurement system. In addition to the change of particulate composition and mass, the volatile matter buildup affects the physical properties of the particle e.g. mobility diameter (drag). All liquid and gas fuel operated combustion processes generate small size particulates - the diesel engine is not unique in this respect.

A non-homogeneous air/fuel mixture causes the formation of soot and PM. When the outlet layer of a fuel droplet begins to burn, its core becomes

so hot that cracking processes begin. The shorter hydrocarbon chains are not easily inflammable such that some escape combustion and appear at the exhaust port as soot particles [GO04].

Soot is mostly carbon, and the emissions of soot are determined by existence of two phenomena: *formation* and *oxidation*. In the ideal case of complete combustion of hydrocarbon fuel with stoichiometric air, the exhaust gas would be composed of the chemical species carbon dioxide (CO_2), water, (H_2O) and molecular nitrogen (N_2). However, in real combustion, as chemical reactions never proceed completely and boundary conditions are non-ideal, formation of new products like carbon monoxide (CO), unburned hydrocarbons (HC), nitrogen oxides (NOx) and particulate matter (PM) -approximated as soot- may take place.

The soot mass fraction history within a diesel engine combustion is shown in Figure 1.1, from [Sti03]. Soot appears shortly after start of combustion, it rises to maximum near TDC and falls rapidly as a result of oxidation.

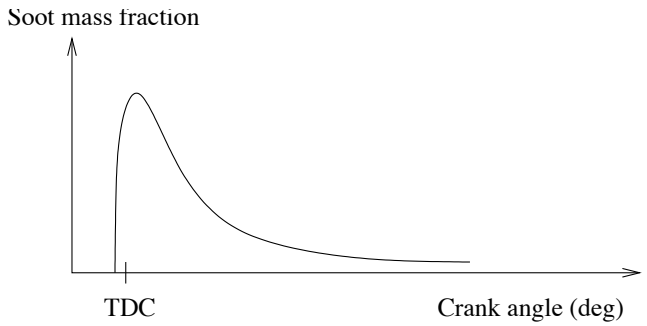

Figure 1.1: Soot mass fraction .vs crank angle in diesel engine, [Sti03]

Details from experimental investigations for soot formation in diesel engines can be found in [Boc94] and [Hey98]. As general reference on the subject, physical and chemical fundamentals for soot formation in flames, can be found in [Boc94] while in [WMD99] a coupled treatment of chemical reaction and fluid flow related to combustion, with pollutant models is given.

1.2.2 PM and Smoke Density (Opacity) Measurement

Particulate emissions (PM) are defined by the measurement method and the understanding and knowledge of used methods are essential. The methods are many and are based on measuring various physical/chemical characteristics of the particle at different temperatures and pressures. Emission regulations are based on different measurement methods (i.e. regulators are defining particulates in different ways). By definition, smoke is visible (white, grey, blue, black, brown and yellow).

Particulate Matter from marine engines can be measured according to two completely different measurement methods i.e. the dilution method and the direct measurement method (dry dust method) [CIM08].

For the dilution method, recommended is ISO 8178: Reciprocating internal combustion engines - Exhaust emission measurement.

For the measurement of smoke, the following methods can be used:
1. Filter Smoke Number, with recommended methods:

- ISO 8178-3: Reciprocating internal combustion engines exhaust emission measurement, method 2: Smoke measurement by a filter-type smoke meter.

- ISO 10054: Internal combustion compression ignition engines measurement apparatus for smoke from engines operating under steady-state conditions filter type smoke meter.

As the above methods are not suitable for transient (dynamic) measurements of the present work, they were not taken into consideration.
2. Smoke Density, with recommended methods:

- ISO 8178-3: Reciprocating internal combustion engines exhaust emission measurement, method 1: Smoke measurement by an opacimeter.

- ISO 11614: Reciprocating internal combustion compression ignition engines - apparatus for measurement of the opacity and for determination of the light absorption coefficient of the exhaust gas.

Smoke opacity meters (opacimeters) measure the optical properties of diesel exhaust and quantify the visible black smoke emissions with the use

of physical phenomena like the extinction of a light beam by scattering and absorption [MK06].

In opacity measurements, light extinction occurs in engine exhaust gas charged with soot particulates. The light extinction is described according to the Beer-Lambert Law

$$\frac{E}{E_o} = e^{-KL} \tag{1.2}$$

where E is the light intensity of scattered light, E_0 is the light intensity of emitted light, K is the extinction coefficient, L is the light path or measuring length, which in our case equals to 0.430 m.

Opacity is defined as

$$Opacity = 1 - \frac{E}{E_o} = 1 - e^{-KL} \tag{1.3}$$

Units for opacity are usually in percentage values, where 0% is for clear air and 100% is for black smoke.

Areas of concern in the opacity measurement, can be the insufficient resolution of measuring devices in the very low levels of opacity close to those of proposed legislation, insensitivity to small particles having size around 50 nm and cross-sensitivity to nitrogen dioxide, which could cause bias [MK06]. In general, the path length affects measurement; an infinite path length has 100% opacity. It is also known that there exists bad correlation of opacity measurements with other particulate matter (PM) measurement parameters such as mass. PM determination is mostly based on gravimetric methods as mentioned above. In general, opacity below 2% is not visible to bare eye, where as opacity with values higher than 5% present clearly visible plumes of smoke.

1.2.3 Emission Legislation

For the particulate matter and smoke and specifically for large engines including marine engines, the current legislation holds as follows, from [Kyr07].

The International Maritime Organization (IMO), has not imposed any limits yet. However, for the future there are proposals under review, with possible inclusion in Tier II 2010. Limits are yet unspecified.

In Europe there are some 'local' regulations for waterborne transport. Two such examples are River Rhine and Bodensee (Lake Constance), regulations. EU also has Stage (Tier) IIIA regulations, where the limit in PM is 0.2 to 0.5 g/kWh, depending on engine size. ISO 8178 specifies the measurement and evaluation methods for particulate exhaust emissions from internal combustion engines under steady-state and transient conditions.

In the USA, existing Environmental Protection Agency (EPA) regulations, referred to as Tier 2 standards, include standards for emissions of PM, NOx, hydrocarbons (HC) and carbon monoxide (CO) from locomotive and marine diesel engines. For PM, the limit is 0.2 to 0.5 g/kWh, depending on engine size. Particulates are also defined according to the ISO 8178 measurement method.

The EPA recently (2008) adopted new air emission standards aiming to dramatically reduce emissions of diesel particulate matter (PM) and nitrogen oxide (NOx) from locomotives and marine diesel engines [Age08]. The final rule consists of a three-part emission control strategy. First, it tightens emissions standards for existing locomotives and large marine diesel engines when they are re-manufactured. Second, it sets near-term engine-out emissions standards, referred to as Tier 3 standards, for newly-built locomotives and marine diesel engines; this starts in 2009. Third, it sets longer-term standards, referred to as Tier 4 standards, for newly-built locomotives and marine diesel engines. These standards are based on the application of high-efficiency catalytic aftertreatment technology and would phase-in beginning in 2014 for marine diesel engines. These standards are enabled by the availability of ultra-low sulfur diesel fuel with sulfur content capped at 15 parts per million, which will be available by 2012. These marine Tier 4 engine standards apply only to commercial marine diesel engines above 600 kW (800 hp).

EPA estimates 90% PM reductions from Tier 4 engines meeting the new standards, compared to current engines meeting the current Tier 2 standards. According to EPA, by 2030 this program will reduce annual emissions of PM by 27,000 tons and those emission reductions continue to grow beyond 2030 as fleet turnover is completed.

1.3 Review of Previous Work

Various primary (on-engine) methods such as those affecting combustion and secondary (exhaust gas-aftertreatment) such as scrubbers, filters and trap methods exist for PM and smoke abatement.

The enforced independent increase of boost pressure for smoke reduction during transient, is covered here.

1.3.1 Air Injection

The method under study in this thesis is the supply of external compressed air to the engine intake manifold during transient load application in order to match the required increase in fuelling.

Compressed air has been used to inject the fuel in some early diesel engines [Moh51].

Compressed air directly injected to the cylinders is used for startup of all large marine engines, but operates at very low rotational speeds.

Direct injection of air in the cylinder is also possible during the closed cycle, but the required valving and timing constraints are quite significant at high engine speeds.

In [MIO94], it was shown that with the injection of air into a modified pre-chamber it is possible to alter the combustion characteristics and hence the products of combustion. Experimental results showed that with optimum injection timing, it is possible to have improved combustion process and reduction of both PM and CO, with reasonably low NOx.

Compressed air injected directly onto the turbocharger compressor blades has often been used to drive the compressor wheel like a turbine so that it spins faster during transient load increases and the air is also added to the air flow to the engine. Several commercial applications of this concept exist with large marine turbocharger manufacturers such as ABB and MAN ('jet assist'). Fatigue loading of the blades limits the application to very short bursts of air injection [CVKA05].

In [LKK05], engine performance simulations also investigated the use of air injection on the compressor wheel during transient and showed the potential improvements in engine response.

Initial related work [PAK+07] has proved experimentally the applicability of the air injection method on compressor and in manifold for smoke reduction in a similar engine setup, but also highlighted the dangers of an uncontrolled airflow.

1.3.2 Predictive Control Applications in Combustion Engines

Until today, Model Predictive Control (MPC) has been studied in several applications with internal combustion engines. In [OdR07], MPC is applied for the model-based control of air path in a diesel engine, using VGT [1] and EGR [2]. Simulated and experimental results confirm that the proposed strategy improves the dynamics of the air path and reduces calibration work load. The model of the air path system was identified using prediction error methods.

In [HRFA06], nonlinear model predictive control (NMPC) was applied to control a diesel engine with VGT and EGR valve. The overall control objective was to regulate the set point of the air-to-fuel ratio and amount of recirculated exhaust gas in order to obtain low exhaust emission values and low fuel consumption without smoke generation. Simulation results showed the advantages and disadvantages, while the achieved performance was comparable to other control methods. The mean-value engine model was based on first principles, as derived in [Jun03].

In [vEL01], MPC with constraints was applied to a laboratory gas turbine installation, succeeding in real time implementation. Two models were used: one was based on physics equations for compressible fluid flow and the other - a lumped parameter model- in which flow was neglected and the fluid inertia was lumped in a single volume. Steady state set-point and transient tracking of reference trajectories performed satisfactorily.

In [FLD06], NMPC was applied in a gasoline engine having as objective the tracking of desired torque profile without increment in emissions, with the throttle and the EGR valve as manipulated variables. Simulated studies showed improvements in engine control, while the average run time needed for NMPC optimization was around 10 msec.

[1] VGT: Variable Geometry Turbine

[2] EGR: Exhaust Gas Recirculation

In [HOO+06], Generalized Predictive Control (GPC) was used as control method for the air-fuel ratio system, while system identification was applied for the derivation of the models for both the engine and the catalyst system. Experiments in full-scale vehicle proved the validity of the proposed design and control approach.

In [Ben04], MPC strategy was applied in an Homogeneous Charge Compression Ignition (HCCI) engine for the control of combustion phasing so that it occurs at a certain crank angle degree. Dual fuels and VVA[3] were used as actuators. The models of engine dynamics were obtained by system identification. Experiments demonstrated that MPC was able to solve the problem of load control and simultaneous minimization of fuel consumption and emissions, satisfying four constraints on the control and output variables, with success.

In [BBA02], the feasibility of constrained MPC is investigated for a turbojet aircraft engine. It is a simulated study where the real plant was represented by a physics-based large and complicated model. The constrained MPC used a simplified real-time model while an Extended Kalman Filter was used to reconstruct states and reduce noise. Results showed potential for better performance than the standard production controller; however the average execution time was about seventy times higher than the required fuel control loop time.

A more detailed description of MPC is given in Chapter 4.

1.4 Thesis Contributions

The issue of exhaust opacity reduction and the issue of avoidance of turbocharger instabilities during engine transients have been individually considered for over thirty years in engine applications. The main contribution of this thesis is the study of the combination of those two issues as a performance index (to minimize opacity) and a constraint (to avoid certain operating limits) in the framework of a model-based advanced control system.

[3]VVA: Variable Valve Actuators

A comprehensive framework for large engine controller design is provided, which covers both the aspect of model building from experimental data and that of controller design. From the extensive coverage found in the literature in these two areas, information applicable to our problem configuration is presented.

Models which describe the transient variations of opacity and pressure in the engine intake manifold, with inputs the fuel and air injection supply are derived using system identification. Different methods were used and various model structures have been tested.

The supporting experimental work was carried out on a state-of-the-art full size diesel engine test-bed. The rapid prototyping of a real-time controller as part of an existing engine controller is presented.

As a whole, the point of view was towards the integration of control engineering issues with diesel engine operation. Issues of concern were the suitability of various engine variables for control, applicability and capacity of identified plant models, the benefit of an advanced control system and the integration of a control subsystem in the whole automation of the powerplant.

The thesis is divided in four main chapters that describe the experimental setup, the model identification, the controller framework and the results of model predictive control study. Following the introduction with a brief background on soot emissions and a review of previous work on air injection and model predictive control presented in Chapter 1, the content of the next chapters is summarized below.

Chapter 2 describes the test-bed with diesel engine at the Laboratory of Marine Engineering at NTUA. An air injection pipework and associated valving was added, in order to supply external compressed air in the intake manifold during a transient. The systems for air injection and engine control and also for measurement and data acquisition are detailed.

Chapter 3 describes the system identification part of the study. Methods and model structures are established. From the experimental data, models suitable for controller design are derived. Air injection is considered as an input, opacity is considered as output, the fuel is taken as a measured disturbance and air pressure in the engine manifold is also modeled, in order

to be used as a constraint.

Chapter 4 describes the model based controller, in necessary details: formulation, cost function, constraints, model structures, issues of stability and finally the nonlinear model predictive control.

Chapter 5 describes the closed-loop model predictive control for opacity reduction. A constrained optimization problem is solved and two different controller cases are studied. Both controllers were implemented on the testbed. Experimental results from engine loading sequences demonstrate the opacity reduction achieved.

Chapter 6 presents conclusions and some possible future directions of the relevant research.

Chapter 2

Experimental Engine Setup

The experiments described in this thesis were performed on a marine diesel engine at the Laboratory of Marine Engineering, at the National Technical University of Athens. The test engine is based on a modified MAN B & W Holeby 5L16/24, which was appropriately adapted to accept the air injection system. Three computer systems were operated respectively for the engine and brake control, the air injection control and the measurement and data acquisition.

This chapter describes the experimental setup, the sensors, the actuators and the computer systems.

2.1 Engine Testbed

The heart of the test-bed is the MAN B & W Holeby 5L16/24 engine, modified for advanced research applications. It is a 5-cylinder, 4-stroke turbocharged diesel engine having a maximum power of 500 kW and a nominal speed of 1200 rpm. The cylinder bore is 160 mm and the stroke 240 mm. The engine in its commercial form is mainly used for ship-board electric power generation and small ship propulsion. In the experimental setup, the engine is coupled to an electric dynamometer, AEG GC 40.22-M, with shaft power of 488 kW, speed of 20-1200 rpm and capability for 4-quadrant operation in the load/speed plane. The connection between the engine and the dynamometer is realized via a shaft of 2.5 m length and 145 mm diameter

and a flexible coupling. The engine test-bed is shown in Figure 2.1.

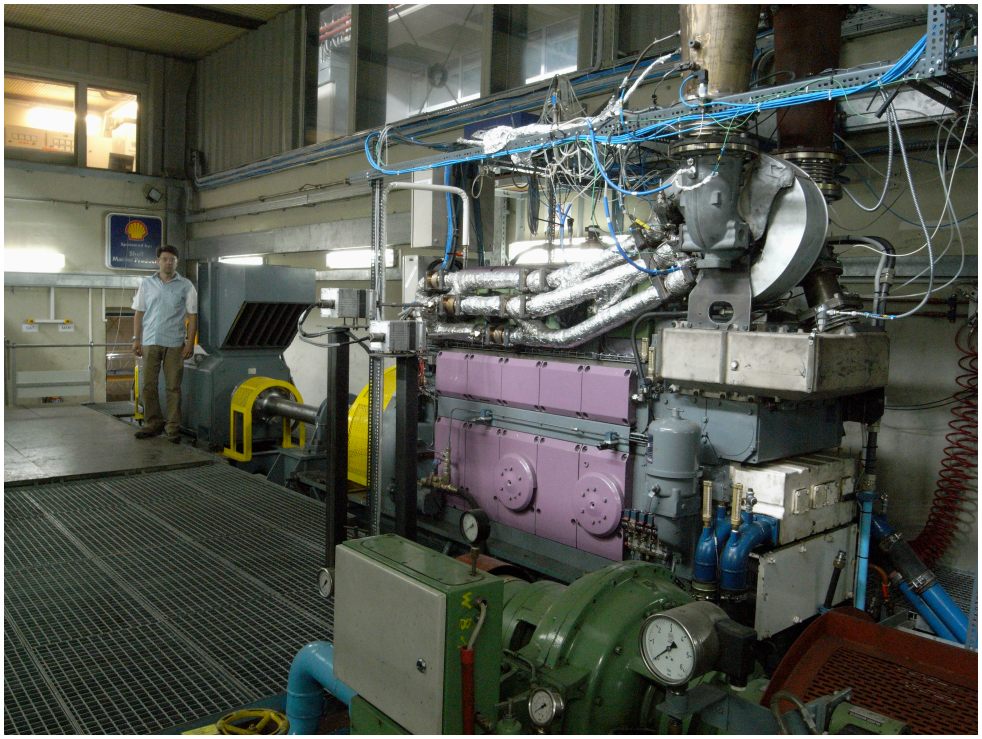

Figure 2.1: The test-bed with engine and brake

2.2 Instrumentation

The engine testbed with sensors and actuators are shown in the instrumentation diagram of Figure 2.2. Table 2.1 provides the sensor identification number and description of operation.

In this chapter only the opacity measurement is described. Descriptions of measurement instrumentation for pressures, temperatures, speed, shaft torque and other engine variables can be found in Appendix .1.

Smoke Opacity Measurement

The opacity in the exhaust gas is measured with an AVL 439 opacimeter [AVLa]. A probe of 1 m length and 10 mm in diameter is mounted in the

Table 2.1: Sensors and actuators at testbed

Number	Sensor/Actuator Description
DPT 1	Differential pressure intake air
PT 1	Pressure intake air
TT 1	Temperature intake air
DPT 2	Differential pressure intake air, compressor exit
PE 101	Compressor in pressure
TE 101	Compressor in temperature
PE 102	Compressor out pressure
TE 201	Intercooler in temperature
TE 303	Charge air temperature
PE 303	Charge air pressure
ZT 403	Rack position
PE 401	Pressure cylinder 1
ME 402	Engine torque
SE 402	Engine speed
TE 504	Turbine in temperature upper manifold
TE 503	Turbine in temperature middle manifold
PE 502	Turbine in pressure lower manifold
PT 501	Turbine in pressure lower manifold Abs
TE 501	Turbine in temperature lower manifold
PE 505	Exhaust pressure cylinder 1
PE 506	Exhaust pressure cylinder 1 Static
SE 601	Turbocharger speed
PT 701	Turbine out pressure Abs
PE 702	Turbine out pressure
TE 701	Turbine out temperature
OPA 701	Opacity
PT 901	Air injection pressure
TE 901	Air injection temperature
FT 901	Air injection mass flow
ZS 901	Air injection valve command
FY 403	Fuel actuator command
FT 901	Brake command

engine exhaust line and draws off sample exhaust gas. The gas is routed to the opacimeter through a conditioning tube. Heated air is supplied around the tube up to the sensing probe, thus ensuring that the gas sample has constant temperature as it enters the opacimeter. Inside the device, a measuring chamber of defined measuring length and non-reflecting surface is filled homogeneously with exhaust gas. Two halogen lamps at the one end of chamber provide the light source necessary for the measurements. The detector unit equipped with green filter is on the other side of the chamber. The loss of light intensity between the light source and the detector is measured and from it the opacity of the exhaust gas is calculated. The calculation is based on the Beer-Lambert Law. The exhaust gas passes through two pumps which maintain a constant measurement flow from 40 to 49 lt/min, before it exits back to the exhaust line. The continuous measurement values are available as analog output signal from the opacimeter. The output rate is 50 Hz.

A 'zeroing' procedure is performed every half hour of measurement in order to evaluate the 'zero intensity value' E_0, required in calculations. During zeroing, ambient air at 100^o C is fed in the chamber and a mean value of light intensity E_0 is measured.

The opacimeter at engine testbed is shown in Figure 2.3.

2.3 Data Acquisition System

The engine data acquisition system (DAQ) acquires and stores measured data during test runs, which after the session end are post-processed. It comprises a PC with DAQ software and the AVL Indiset hardware [AVLb]. The total number of analog inputs reaches 48 channels. From these, 16 channels can perform fast data acquisition especially for crank angle resolution and the remaining 32 channels sample at 0.1 sec, for cycle resolution.

The PC is equipped with the AVL IndiCom software which carries out the channel parameterizing, the measurements and the display of data. The PC also contains a National Instruments PCI-6071E data acquisition board providing the input and output signals, connected to the PCI bus. This DAQ card provides up to 32 differential analog input channels, with 12-bit

resolution, with configurable sampling rate up to 1 MS/s per channel. The input signal ranges are from -10V to +10V.

The AVL 620 provides dedicated channels that allow it to synchronize with external systems for the starting of a measurement session as well as crank angle degree mark signals. In our case, the external trigger is supplied by the engine digital control system, type Woodward ATLAS.

The AVL system achieves high performance data acquisition due to the *circular buffer* data storage. In this type of structure, a fixed-size buffer continuously reads data as if it were connected end-to-end, like a ring. In the case that the buffer becomes full, when new data arrives, then it starts overwriting the oldest data.

The AVL Indiset 620 hardware is shown in Figure 2.4.

2.4 Engine Hierarchical Control System

The engine hierarchical control system is formulated in a top-down structure.

On top, there is the air injection control system. In the middle there is the engine control system, with the local closed-loop controllers of engine speed and brake torque. The respective actuators (fuel governor and thyristors of dynamometer brake) are at the lowest level.

With a full scale experimental setup of this magnitude, safety is a primary concern. As stated in [Mac04], while considering model predictive controller (MPC) as an advanced controller, with MPC implemented on top of traditional local controllers, we can experiment with this (new) advanced control technology safely; should it starts misbehaving, it is possible to disable it either manually or automatically as in our case, and still hold the engine safely at previous set-points.

In the framework of this experimental work, the existing engine control system was modified so as to accept an additional shutdown trigger. Two pressure sensors PT 301, PT 302, provided redundant pressure measurements from the intake engine manifold. They were analog inputs to the Woodward ATLAS engine controller. If the pressure in the intake manifold exceed the safety limits, the engine was shutdown. This was considered a necessary precaution, as a large increment in the manifold pressure could

severely damage the engine. This imposed limit is related to the constraint of the MPC controller. During the complete testing schedule, the emergency shutdown did not come into operation a single time, as the air injection control system behaved faultlessly. The robust engine control system thus provided a safe environment, as it protected the engine in a lower level, allowing room for MPC experimentations.

The complete computer architecture is shown in Figure 2.5.

The individual systems are described in the following sections.

2.4.1 The Air Injection Controller

The air injection control layer was set up for the present experiments; it comprised two personal computers (PCs), as a host and a target, one DAQ card and MATLAB software environment. The software environment chosen to develop the air injection controller was the MathWorks Development Environment. This tool-set consists of a number of components including the following:

- MATLAB: provides high-level modeling/scripting language
- Simulink: provides visual modeling environment that uses block interconnections
- Real-Time Workshop: compiles Simulink models for to C language for real-time applications
- xPC: a real-time operating system, enables use of PC hardware and Commercial-Off-The-Shelf data acquisition cards as a real-time target.

A similar approach is common in rapid prototyping environments; for example a comparable setup is followed in [Sou04] for the control of an HCCI engine.

More details on the air injection controller can be found in Appendix .1

2.4.2 The Engine Controller

The engine is controlled by a digital control system, type Woodward ATLAS. At the heart of the ATLAS PC is a Pentium processor, running VxWorks

real time operating system (OS). This OS is designed to control the proper timing of all application code so that the dynamic performance of the final control system is absolutely guaranteed. Each piece of application code is scheduled under a rate group of up to 5 milliseconds cycle time. The hardware platform is based on the industry standard PC/104 bus structure. The PC/104 modules are stacked onto the backplane in order to add inputs/outputs like analog inputs of 0-5V, 4-20mA, analog outputs of 4-20 mA, discrete inputs and relay outputs. The application software is based on graphical (i.e. interconnected blocks) programming.

The engine control system integrates the engine speed and the brake torque control loops. The engine speed loop maintains the speed set point by varying the fuel quantity with the fuel actuator. It is implemented as Proportional-Integral-Derivative (PID) controller, with scheduling of its three parameters on engine speed. The torque loop controls the brake torque with the thyristors phasing, following the torque setpoint. As sensor, the actual shaft torque measurement is utilized. Also a Proportional-Integral-Derivative controller is used, scheduling its three parameters on torque.

Figure 2.6 shows the engine controller ATLAS with its PC/104 format.

2.5 Engine Operation

The engine comprises the engine block, the turbocharger and sensors with actuators. One camshaft drives the valves and one activates the fuel pump in the fuel injection system. Figure 2.2 shows the principal components of the test-bed engine to which the control strategy is applied.

The turbocharger system consists of the exhaust gas receiver, the turbocharger, the charging air inter-cooler and the charging air receiver. The turbine wheel is driven by the engine exhaust gas and the radial turbine wheel drives the turbocharger centrifugal compressor, which is mounted on the common shaft. The compressor draws air from ambient through a filter and discharges via a watercooled charge air cooler to the air receiver. From the charging air receiver the air can be admitted to each cylinder through the inlet valves. From the exhaust valves the exhaust gas is led via the exhaust manifold, through the turbine and further to the exhaust outlet

silencer and exhaust stack.

With reference to Figure 2.2, a description of engine operation can be as follows. Clean air is drawn into the compressor 100; after its exit the compressed air is then cooled by an intercooler 200. In the inlet duct to the compressor and nearby to a Venturi nozzle, respectively the pressure PT1, diaphragm differential pressure DPT1, and temperature TT1 are measured. With these three sensors, the fresh air mass flow is calculated, according to ISO 5167 [1]. The intercooler cools the compressed air in order to decrease its density. It is desirable that the charge air has a high density as this allows a greater mass of air to be induced in the engine cylinders. The intercooled air is admitted into the engine block via the inlet manifold 300. The pressure of the inlet manifold air as it enters the inlet manifold is measured by a pressure sensor PE102 which produces signal MAP indicative of the manifold air pressure. The temperature of the inlet manifold air as it enters the inlet manifold is measured by a temperature sensor TT303 which produces a signal MAT indicative of the manifold air temperature. The engine block 200 comprises the cylinder block with five cylinders, with pistons, valve train and crankshaft. The engine speed is measured by a twin-laser arrangement system SE402, which reads successive black and white markings on the engine flywheel, with a resolution of 0.5 degrees.

The fuel injection system supplies the required fuel to the engine for burning. Each cylinder is provided with a respective fuel injector pump unit, high pressure pipe and injection valve. The fuel that is injected in each cylinder is adjusted by continuous movement of the fuel pump rack. The angular position of the fuel rack is measured with an encoder of 13-bit gray scale, ZT403. The rack movement is actuated by the fuel actuator FY403. This is a Woodward UG-Actuator, which takes a given electrical input signal and converts it to a proportional hydraulic output-shaft position to control engine fuel flow. It produces 42 degrees of rotary output. In the test engine, the control action is on the fuel rate and not on the injection timing. The injection timing cannot be modified, as it depends on the cam profile.

[1] ISO 5167: Measurement of fluid flow in circular cross-section conduits running full using pressure differential devices-Part 3: Nozzles and Venturi nozzles.

The exhaust manifold is of the semi-pulse type and is split in three streams out of the five cylinders and enters a triple-entry turbine, ABB prototype turbo, type TPS-48X. Two butterfly valves, type Woodward Glo-Tech, driven by Woodward ProAct rotary actuators segment the exhaust pipes, forming the pulse-exhaust system. This system utilizes the exhaust pressure pulse energy and at higher loads and lower engine speeds leads to improved overall turbocharger efficiency.

The speed of the turbocharger shaft is measured with a Hall-effect type speed sensor SE601. The exhaust gas after its passage through the turbine exits via the stack to the atmosphere. A small part of the exhaust gas from the engine is sampled by the opacimeter OPA701, which measures the exhaust gas opacity. The installation of the opacimeter is showed in Figure 2.3.

The engine is connected to an electric dynamometer (brake), type AEG GC 40.22-M, with shaft power of 488 kW, and speed of 20-1200 rpm. The brake 800 is a DC [2] machine, connected to the power system of the Laboratory, with three phase dual converter. The dual converter-DC machine system allows brake operation in four quadrants of the torque-speed plane. This means, that the machine can drive and be driven bidirectionally. Additionally, field control enables the machine to be operated with speeds two to three times above its nominal no-load speed. The brake is capable of applying any time series of dynamic load to the MAN B&W L16/24 engine. The shaft torque measurement ME402 provides the actual torque applied to the engine. More details for the torque measurement can be found in Appendix .1. The electric dynamometer is controlled by the respective controller MY801 in closed-loop.

In a compression-ignition engine, only air is inducted in the cylinders. Just before combustion, the fuel is injected in the cylinder. Load control is achieved by varying the amount of fuel in each cycle. A/F ratio is the ratio of air mass flow rate to fuel mass flow rate admitted to the engine. Consequently, the A/F ratio varies depending on the engine load. A/F typical values range from 18 to 70 while the stoichiometric $(A/F)_s$ value for

[2] Direct Current

light diesel is 14.5. Also relevant is the fuel/air equivalence ratio ϕ, defined as $\frac{(F/A)_{actual}}{(F/A)_s}$. When the AF ratio is less than 20 then, particulate matter (soot) is evident is exhaust gas [Hey98].

2.6 Air Injection

In the air injection operation external compressed air is supplied to the engine intake manifold. With this action, the required quantity of air that matches the supplied fuel is provided, during transient operation, independent of the turbocharger response and the respective boost pressure and related airflow. In this way the air charging of the engine is improved, reducing the smoke emissions during the transient.

In the testbed, air injection is accomplished with a dedicated air injection line, 1 inch in diameter, which receives compressed air from a 350 lt reservoir (air bottle), stored at 30 bar pressure supplied from air compressors. This 30 bar pressure is reduced to a suitable level; for our runs it was set at 9 bar. The actuator for the air supply is a solenoid valve, ZS901, type Burkert 281. The valve commands are coming from the air injection controller. The air line is equipped with pressure (PT901), temperature (TE901) and mass flow (FT901) measurements, which are logged by the DAQ system.

The engine testbed with air injection line is shown in Figure 2.7.

2.7 Compressor

The engine testbed is equipped with ABB TPS-48X prototype experimental turbocharger. It is shown in Figure 2.9.

When air is independently injected the intake manifold pressure will increase so that the engine air flow is expected to increase. However, the turbocharger compressor which also feeds the intake manifold will be suddenly subjected to an increased pressure. If the compressor cannot withstand the higher pressure field downstream then the compressor may experience partial or even total flow reversal. This instability phenomenon is known as compressor surge. A more detailed description of this instability is given in Appendix .2.

The unsteady fluid-dynamic excitation of the compressor results in additional periodic load on the blades causing vibration and fatigue. Further due to the rapid changes of compressor demand torque during surge, the severe reversals of torsional loading could eventually lead to failure of turbocharger shaft [LTK03], [TK02].

It is therefore important in the proposed control arrangement to avoid the occurrence of compressor surge by appropriately controlling the air injection so as to restrict the pressure rise in the manifold in a way that the compressor operates safely away from surge.

2.8 Setting Up the Experiments

The existing engine testbed required several modifications and adaptions prior to setting up the arrangements for the needs of the present research study. The related work is summarised below.

- Set-up of the closed-loop dynamometer imposed torque control and its scheduling and tuning on-site the parameters of the PID controller using the Ziegler-Nichols methods. Details of the tuning can be found in [Pap06c]. The shaft torque measurement system is described in [Ale06].

- Set-up of the data acquisition environment by parameterizing the AVL platform and post processing the experimental data. In several cases the data acquired in crank-angle resolution were 'aligned' with data in time resolution. For this purpose routines in MATLAB and Perl language were written.

- Design of the re-wiring of the field signals and reconstruction of the electrical cabinets that hosted the acquisition hardware. Commissioning of the signal lines for sensors and actuators.

- Set-up of the real-time air injection controller in the MATLAB platform. Modified the existing engine controller application in order to interconnect to the 'higher lever' control layer of the air injection controller.

The new cabinet in the Control room with the field wiring and signal conditioning and isolation modules is shown in Figure 2.10.

2.9 Summary

In this chapter, the testbed with experimental diesel engine 5L16/24 was described. A modification allowed compressed air to be injected in the intake manifold through a solenoid valve. Information on smoke opacity measurement was provided, as it is the basic feedback signal. The data acquisition system that performed the logging of experimental data for further processing was also presented. Next the engine control system was described. It comprised the air injection controller and the engine controllers for speed and brake torque. The first controller was designed and set up to implement the model-based control theory used. The engine controllers were used during the engine operation under load transients, holding the speed constant at 1200 rpm and applying the desired torque load. A description of engine operation was given introducing the various sensors and actuators available in the testbed. Finally the behaviour of a compressor under instability was introduced. Later we shall use the idea of avoiding instability by means of keeping manifold air pressure under certain limits, at specific operating conditions.

With this setup, experiments were designed and run in order to provide experimental data suitable for system identification. Identification and derivation of control models are the subjects of the next chapter.

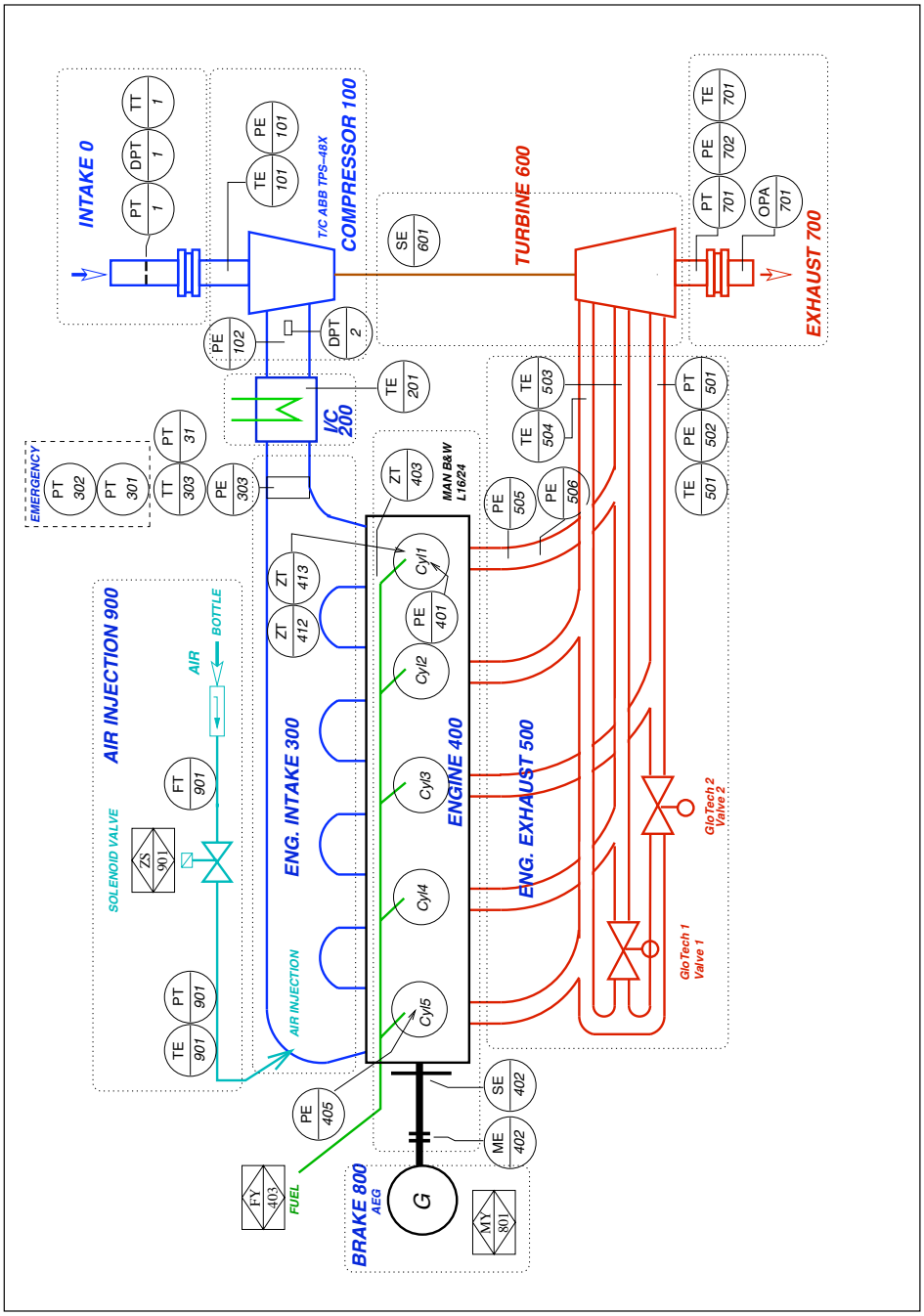

Figure 2.2: The instrumentation diagram of the engine testbed. Sensors are shown in circles and actuators in rectangles

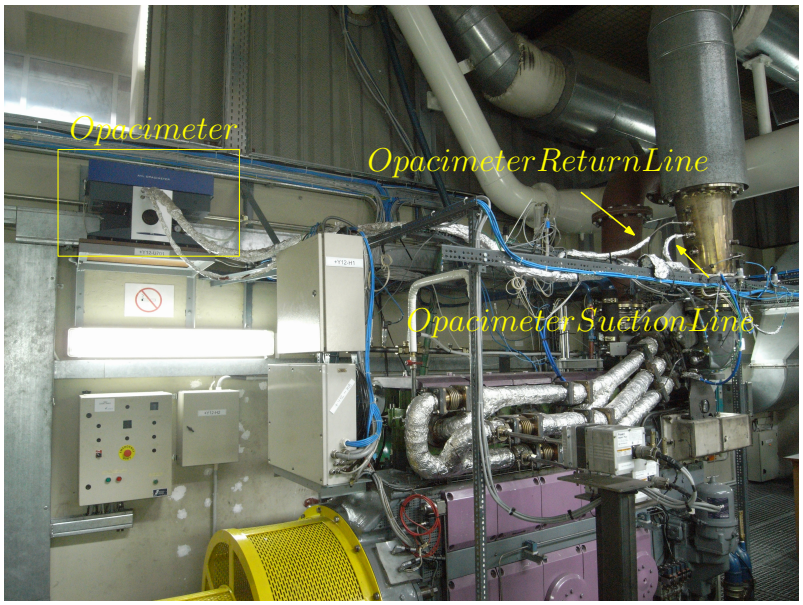

Figure 2.3: The opacimeter as connected to the engine exhaust line

Figure 2.4: The AVL Indiset 620

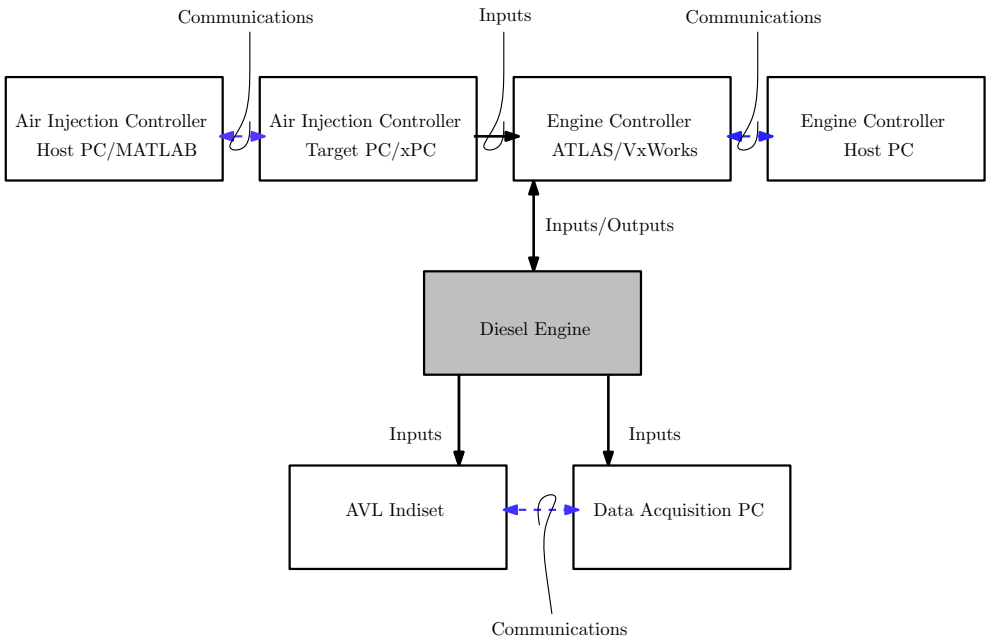

Figure 2.5: The computer architecture for control and data acquisition

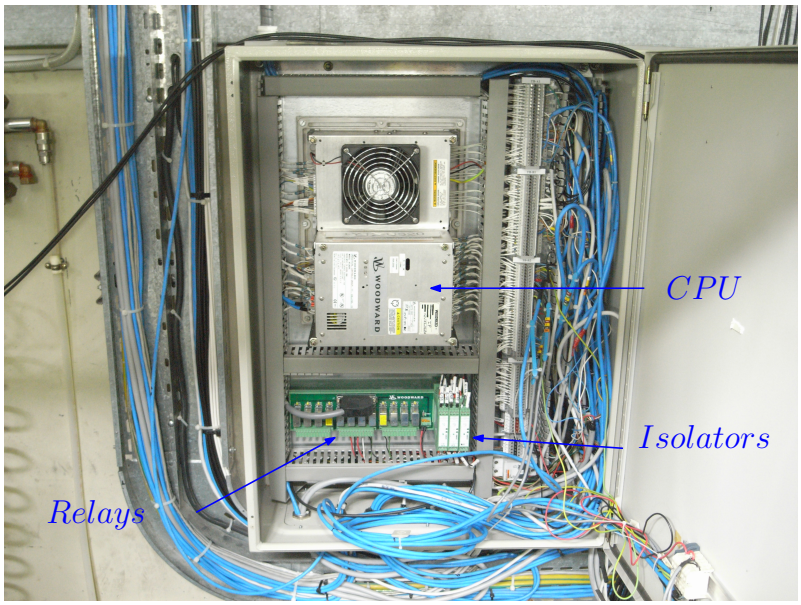

Figure 2.6: The engine digital controller

Figure 2.7: The air injection supply line as it enters the intake manifold at the right side

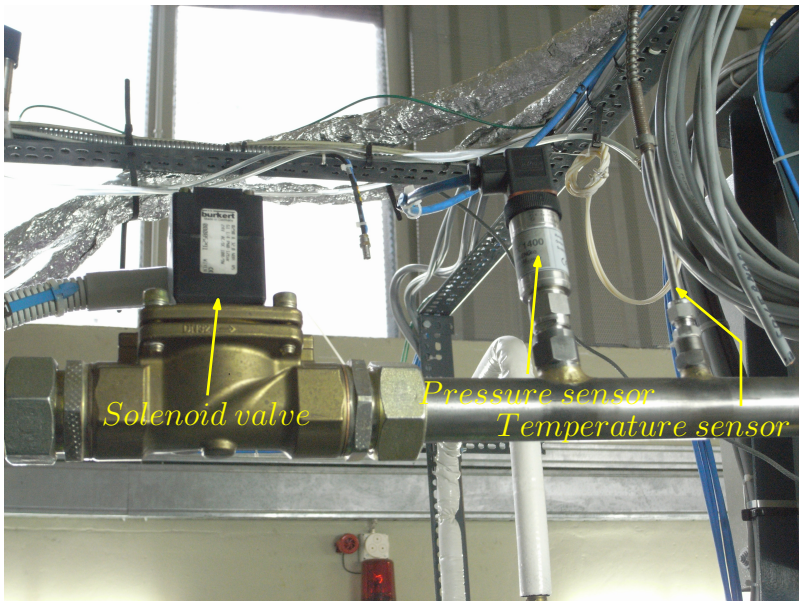

Figure 2.8: The air injection supply line with sensors and actuator

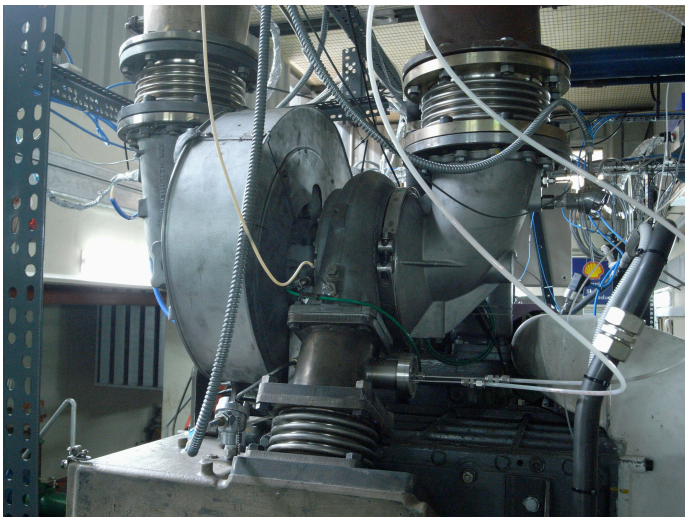

Figure 2.9: The turbocharger compressor side at engine testbed

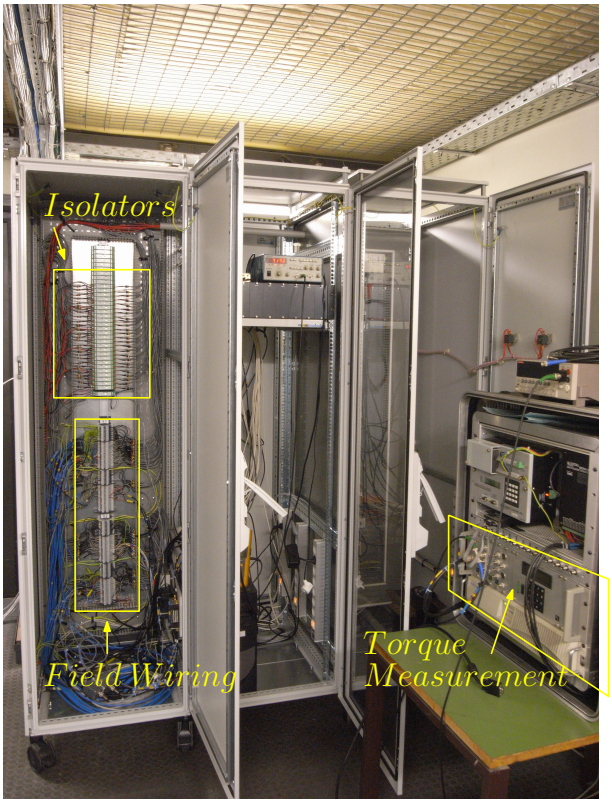

Figure 2.10: The cabinet in the Control room

Chapter 3

Identification of Engine Model

The requirement of an engine model that will predict the plant behaviour and can be used inside the controller has been declared. In this thesis, the derivation of such an engine model is based on system identification.

Chapter 3 is divided in two parts. In the first part, the framework for the identification methods (parametric, subspace and nonlinear) and the structure of models (transfer functions, state-space and Hammerstein-Wiener) is established in a broad sense. In the second part, the identified models that relate selected inputs to outputs, as required by the controller, are presented. Opacity is considered a controlled variable as the aim is to minimize it, while the control action is the air injection supply. As the fuel is not directly controlled, the fuel rack position is measured and considered as a measured disturbance. The engine model will be an important part of the model predictive controller, as it will be shown in Chapter 4.

3.1 System Identification

In model predictive control (MPC), an explicit linear model is required to predict future plant outputs. A linearized model can be obtained either with first-principles modelling or with system identification.

Sometimes a *first-principles* nonlinear model of the plant is available.

That is, a model in which the equations are obtained from a knowledge of the underlying physical, chemical and thermodynamic processes. Such a model consists of a (large) collection of differential- algebraic equations, containing non-smooth elements such as switches (case statements) and look-up tables [Mac04].

Typically such models are developed for the purposes of detailed simulation, operator training or even safety certification. Linearized models can then be obtained from a first-principles nonlinear model. In simple cases, this can be done analytically, but in complex cases it has to be done with the aid of computer software. Perturbations are applied to the nonlinear model, and the Jacobian matrices are estimated numerically. Alternatively, the nonlinear model can be used to generate simulation data for particular operating conditions, and then to apply system identification techniques to this data, as if it had been obtained from the actual plant.

Often for control purposes this framework is too complicated to be useful. The quality of a model is dictated by the ultimate goal it serves; there is a trade-off between model complexity and accuracy [vOdM96].

System identification can be defined as the process of obtaining a model for the behavior of a plant, based on input and output plant data. Most commonly, it is obtained by performing tests on the plant which involve injecting known signals, such as steps, multi-sines, pseudo-random or others, at the plant inputs, and recording the resulting plant outputs.

In transient response testing the system is excited with known impulse and step function and the output is recorded. Often the noise will distort the measured system output. In this case the transient test signal is applied repeatedly and the resulting responses are averaged to obtain a smoothed estimate [Wel93].

Linearized models can then be obtained by using the techniques of system identification, in which first a certain parametrized model class is predefined by the user. Then using methods which range from simple curve-fitting to sophisticated statistically based, suitable numerical values are assigned to the parameters so as to fit as closely as possible to recorded data. Finally there is a validation step in which the model is tried out on experimental data that were not used in the system identification experiment.

Compared to models obtained from physics, system identification models have a limited validity and working range; in some cases they have no direct physical meaning, or represent only the input-output behavior of the plant, carrying no information about its internal structure. Models obtained in this way are often called *black box* models [Mac04]. As an advantage, they are relatively easy to obtain and more importantly are simple enough to make model-based control system design mathematically and practically tractable. Typical problems can be the choice of model structure, the time-varying nature of many systems and underestimated measurement features like sensors, sampling times or filters.

The literature on system identification is enormous. In particular, most aspects of identification theory and algorithms are covered respectively in [Lju99] and [Lju07]. The subspace method with industrial applications is covered in [vOdM96] and [KCM02], while identification using Markov parameters is covered in [Jua94] and [Mos95]. Some material on system identification specifically for the process industries can be found in [HS97] and [ZB93]. Finally, identification specifically for generalised predictive control (GPC) is covered in [HB85] and [WZ91].

3.2 Identification Methods

Most methods of system identification rely on iterative, nonlinear optimization to fit parameters in a pre-selected model structure, so as to best fit the observed data [Lju99]; these are known as *parametric* methods. An alternative class of identification methods is the *subspace methods*, which are 'one-shot' rather than iterative and rely on linear algebra rather on optimization. They are particularly effective for multivariable systems and can be used with arbitrary input-output-data and not just with step or pulse responses [KM99]. For the case that a nonlinear model is required, Hammerstein-Wiener models are commonly used.

The above methods were used in the present work and are a particular choice from a wide collection, as one can use also Instrumental Variables, Maximum Likelihood, Impulse response analysis (Markov parameters) or others.

3.2.1 Parametric Identification

The method for estimating the vector of θ parameters has the general term *prediction error* method, PEM. Prediction error ϵ is defined as

$$\epsilon(t, \theta_*) = y(t) - \hat{y}(t|\theta_*) \tag{3.1}$$

between the measured output and the predicted output of the model. Norm V_N is used

$$V_N(\theta, z^N) = \frac{1}{N} \sum_{t=1}^{N} l(\epsilon_F(t, \theta)) \tag{3.2}$$

Then the estimate $\hat{\theta}_N$ is defined as the minimization of function $V_N(\theta, z^N)$. Typical solution method is *least squares*.

With parametric estimation, process models were derived for inputs and outputs. This model type is chosen for its advantages: the model coefficients have a physical interpretation and it provides delay estimation.

Different model structures were created by the selection of the number of poles, and zeros and the addition of time delay. Thus first-, or second-order model were straightforward to estimate.

3.2.2 Subspace Identification

The term subspace identification refers to a class of algorithms with main characteristic the approximation of subspaces generated by the rows or columns of some block matrices of the input and output data.

Popular subspace identification method [vOdM96] is Numerical algorithm for Subspace System IDentification (N4SID), implemented in the Identification toolbox of MATLAB [Lju07].

3.2.3 Nonlinear Identification

A nonlinear relationship between input and output provides richer possibilities to describe nonlinear systems.

In the case that a nonlinear model is required, nonlinear identification methods can be used. Two possible choices can be the Nonlinear ARMAX model (NARMAX) and the Hammerstein-Wiener models. In this thesis the second option was considered, as the initial attempts with the former did

not give workable models. In the Hammerstein-Wiener theory, the nonlinear model is represented with three terms, a nonlinear term for input, a linear model and a nonlinear term representing the output. For the input term a piecewise nonlinearity was considered , which relates to the linear and ramp-like limit of the actual fuel command. For the output term, a saturation nonlinearity was considered , which is similar to the upper high limit of the opacity measurement, which is 100%. Finally for the linear model a relation with two zeros as numerator and three poles as denominator was considered.

With the availability of a nonlinear model, nonlinear model predictive control can be an alternative to (linear) model predictive control, in cases that an improved quality of forecasting is required.

3.3 Model Structures

In this section, the two basic forms of model structures that are the outcome of the identification methods are presented. In general it is feasible to obtain from the structure of one model the structure of the other, successfully. For example in the case of availability of a model in transfer function form representing a step response, then a state-space model can be easily obtained. However that model would be of large dimension in states in order to incorporate all the responses and possible delays.

3.3.1 Transfer Function and Polynomial Models

A process model in continuous time is

$$G(s) = e^{-sT_d} \frac{K_p}{1 + sT_p} \tag{3.3}$$

where K_p is the static gain, T_p is the time constant, T_d is the time delay, in the case of a first-order system. In the case of a second order system, the transfer function becomes

$$G(s) = e^{-sT_d} \frac{K_p}{1 + 2s\zeta T_w + s^2 T_w^2} \tag{3.4}$$

where ζ is the damping and T_W is the time constant.

To acquire a *polynomial representation* of a transfer function, a linear, time invariant model can be described as

$$y(k) = G(q)u(t) + H(q)e(t) \tag{3.5}$$

where

$$G(q) = \sum_{k=1}^{\infty} g(k)q^{-k} \tag{3.6}$$

$$H(q) = 1 + \sum_{k=1}^{\infty} h(k)q^{-k} \tag{3.7}$$

Then $G(q), H(q)$ is parametrized as rational functions, with parameters the coefficients of numerators and denominators. A simple way is to use the linear difference equation known as *equation error model*

$$y(t)+a_1y(t-1)+...+a_{n_a}y(t-n_a) = b_1u(t-1)+...+b_{n_b}u(t-n_b)+e(t) \tag{3.8}$$

The parameter vector is

$$\theta = [a_1\ a_2\ ...\ a_{n_a}\ b_1\ b_{n_b}]^T \tag{3.9}$$

With the introduction of

$$A(q) = 1 + a_1q^{-1} + ... + a_{n_a}q^{-n_a} \tag{3.10}$$

$$B(q) = b_1q^{-1} + ... + b_{n_b}q^{-n_b} \tag{3.11}$$

finally $G(q)$ and $H(q)$ have the form

$$G(q,\theta) = \frac{B(q)}{A(q)} \tag{3.12}$$

$$H(q,\theta) = \frac{1}{A(q)} \tag{3.13}$$

In the case that a delay of n_k samples from u to y exists, then the above becomes

$$A(q)y(t) = q^{-n_k}B(q)u(t) + e(t) \tag{3.14}$$

PEM has the following structure

$$A(z^{-1})y(k) = z^{-d}\frac{B(z^{-1})}{F(z^{-1})}u(k) + \frac{C(z^{-1})}{F(z^{-1})}e(k) \tag{3.15}$$

where similarly d is the time delay, and A, B, C, D, F are polynomials.

The above form is also known as ARX model, where AR is for the autoregressive part $A(q)y(t)$ and X for the extra input $B(q)u(t)$.

The structure in AutoRegressive Moving Average with eXogenous input (ARMAX) is

$$A(z^{-1})y(k) = z^{-d}B(z^{-1})u(k) + C(z^{-1})e(k) \tag{3.16}$$

where d is the time delay, and A, B, C are polynomials. $u(k)$ and $y(k)$ are the control and output sequence of the plant respectively.

The poles of a linear system are the roots of the denominator of the transfer function G. The poles have a direct influence on the dynamic properties of the system. The zeros are the roots of the denominator of G. Poles and zeros are equivalent ways to describe the coefficients of a linear difference equation, like the ARX model. Poles are associated with the output side and zeros are associated with the input side.

The general equation of a linear dynamic system is given by

$$y(t) = G(z)u(t) + v(t) \tag{3.17}$$

In this equation, G is an operator that takes the input to the output and captures the system dynamics, and v is the additive noise term. The poles of a linear system are the roots of the denominator of the transfer command G. The poles have a direct influence on the dynamic properties of the system. The zeros are the roots of the numerator of G. Zeros and poles are equivalent ways of describing the coefficients of a linear difference equation, such as the ARX model. Poles are associated with the output side of the difference equation, and zeros are associated with the input side of the equation. The number of poles is equal to the number of sampling intervals between the most-delayed and least-delayed output. The number of zeros is equal to the number of sampling intervals between the most-delayed and least-delayed input.

3.3.2 State Space Models

In state-space (SS) model form the relation between input, noise and output signals is written as a system of first-order differential or difference equations,

using the auxiliary state vector $x(t)$ or $x(k)$ in discrete time [Lju99].

The SS models in discrete time, have the structure

$$x(k+1) = Ax(k) + Bu(k) \tag{3.18}$$

$$y(k) = Cx(k) + Du(k) \tag{3.19}$$

SS models usually come from Subspace Identification methods.

In discrete time, the models have the form

$$x(k+1) = \Phi x(k) + \Gamma_u u(k) + \Gamma_d d(k) + \Gamma_w w(k) \tag{3.20}$$

$$y(k) = y(k) + z(k) = Cx(k) + D_u u(k) + D_d d(k) + D_w w(k) + z(k) \tag{3.21}$$

where x is a vector of n state variables, u represents the n_u manipulated variables, d represents n_d measured but freely-varying inputs (i.e., measured disturbances), w represents n_w unmeasured disturbances, y is a vector of n_y plant outputs, z is measurement noise, and Φ, Γ_u , etc., are constant matrices of appropriate size. The variable $y(k)$ represents the plant output before the addition of measurement noise.

3.3.3 Performance quality criteria

The following two criteria can be considered in order to assess the model performance quality.

1. Loss Function: value of the identification criterion at the estimate. Normally equal to the determinant of the covariance matrix of the prediction errors, that is, the determinant of Noise Variance.

2. Akaike's Final Prediction Error (FPE): defined as $\frac{(1+d/N)}{(1-d/N)}$, where d is the number of estimated parameters and N is the length of the data record.

3.4 System Identification for Engine Model

As output variables are considered those plant variables by which one obtains information about the internal state of the process. As input variables, the variables that independently can induce change in the internal conditions

of the system are considered. Finally, measured disturbance variables are those over which one does not have control, but are measurable [OR94].

In this context, 'opacity' is considered as an output (controlled) variable as the aim is to minimize it, while as input (and control action) the 'air injection supply' is used. As the fuel is not directly controlled, but the 'fuel rack position' can be measured, it is considered as a measured disturbance.

With a small modification of the above, for *identification purposes, fuel rack position is considered as input.* This is done often: there may be signals associated with the process that rightly are considered as inputs, in the sense that they affect the system, even though it is not possible to manipulate them [Lju99]. If they are measurable, it is then highly desirable to include them among the measured input signals and treat them as such when building models, even though from an operational point of view they should rather be considered as (measurable) disturbances.

Thus, the model has as inputs the fuel and the air injection and as outputs the opacity and the manifold pressure. Figure 3.1 shows the model with inputs-outputs. Also, shapes of the test signals are shown, as explained subsequently.

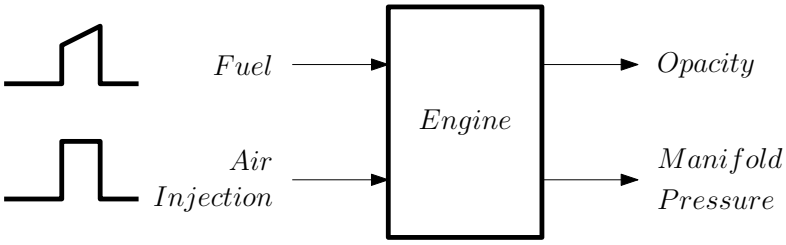

Figure 3.1: Block diagram of the engine model, as used in system identification

3.4.1 Data Scaling

Scaling is very important in practical applications as it makes the model analysis simpler and helps to avoid numerical errors [SP96]. The idea is to make input and output data of similar order, usually less than one in magnitude. A judgement must be made from the start of the design process

about the required performance of the control system. The references and disturbances were divided by their maximum expected values and the outputs by the maximum allowed change. These values were, for rack=0.6%, for air injection pressure=400 kPa, for opacity=60% and for intake manifold pressure=2 bar.

3.4.2 Measurement Schedule

During the identification procedure, the input variables excited the engine and the outputs together with the inputs were recorded. Unit steps and Pseudo-Random-Binary-Signal (PRBS) were used as test signals for the inputs. PRBS had appropriate frequency so as to provide sufficient time for the actuator and the engine to respond and focused on the low- to mid-frequency range identification. The air injection input was actuated with the test signal while the fuel command was given by the engine speed closed loop controller.

Base test: In the base test, air injection was not used. A load step was applied to the engine, which run at constant speed of 1200 rpm. The load was increased from 0 to 47.5% (1890 Nm), and was kept high for 10 sec. All the engine parameters were recorded, so as to allow comparison later on, when the air injection was applied in various ways.

Test A1: In the A1 test, air injection was applied for 4 sec, with a pressure of 9 bar. A load step was applied to the engine, which run at constant speed of 1200 rpm. The load was increased from 0 to 47.5% (1890 Nm), and was kept high for 10 sec. All the engine parameters were recorded, with main focus on opacity and intake manifold pressure. In this test, compressor instability did not occur.

Test A2: In the A2 test, air injection was applied for 8 sec, with a pressure of 9 bar. A load step was applied to the engine, which run at constant speed of 1200 rpm. The load was increased from 0 to 47.5% (1890 Nm), and was kept high for 10 sec. All the engine parameters were recorded, with main focus on opacity and intake manifold pressure. The objective was to disturb the engine, with the supply of compressed air for double duration than the previous test. In this test, compressor instability occurred, as

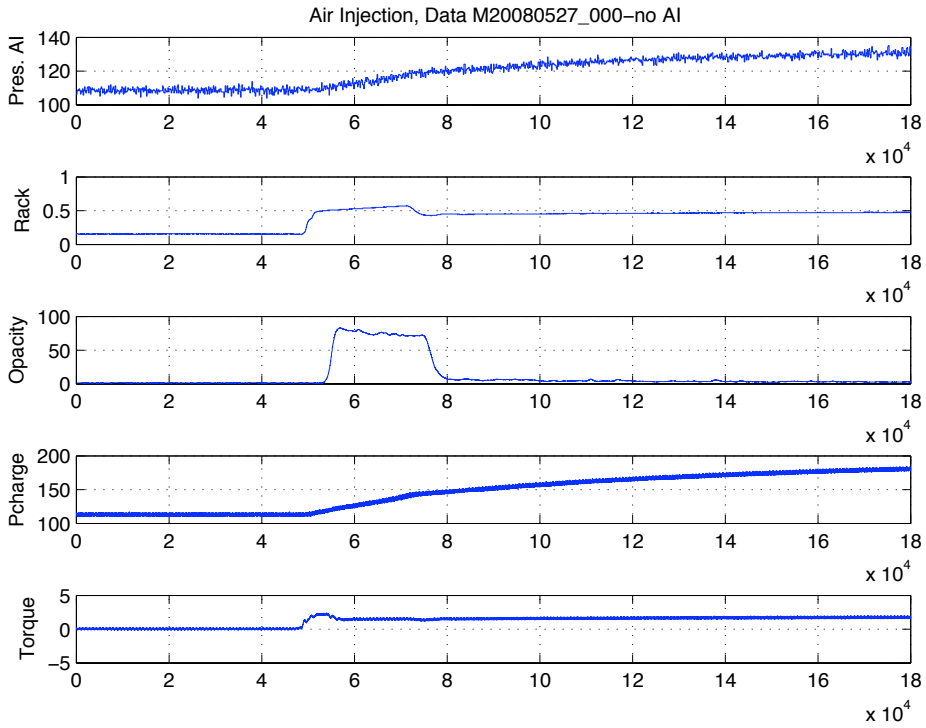

Figure 3.2: Measured engine responses during the Base test. Air injection is not applied.

was observed in the affected engine variables (mainly in pressures). When compressor surge occurs, it is also externally evident in the experimental installation by load noise (banging) due to the flow reversals.

Test B1: In B1 test, air injection was applied for 8 sec, with a pressure of 9 bar. The load was kept constant at 20% (800 Nm). The engine run at constant speed of 1200 rpm. The air injection command was a pseudo-random binary signal in appropriate frequency, in order to excite the engine. All the engine parameters were recorded, with main focus to see the response of intake manifold pressure.

Measurements from the four tests are shown in Figures 3.2,3.3,3.4,3.5 respectively. In all cases data are scaled (normalised). In these Figures, the jet pressure shows the behavior of the step command in tests Base, A1, A2

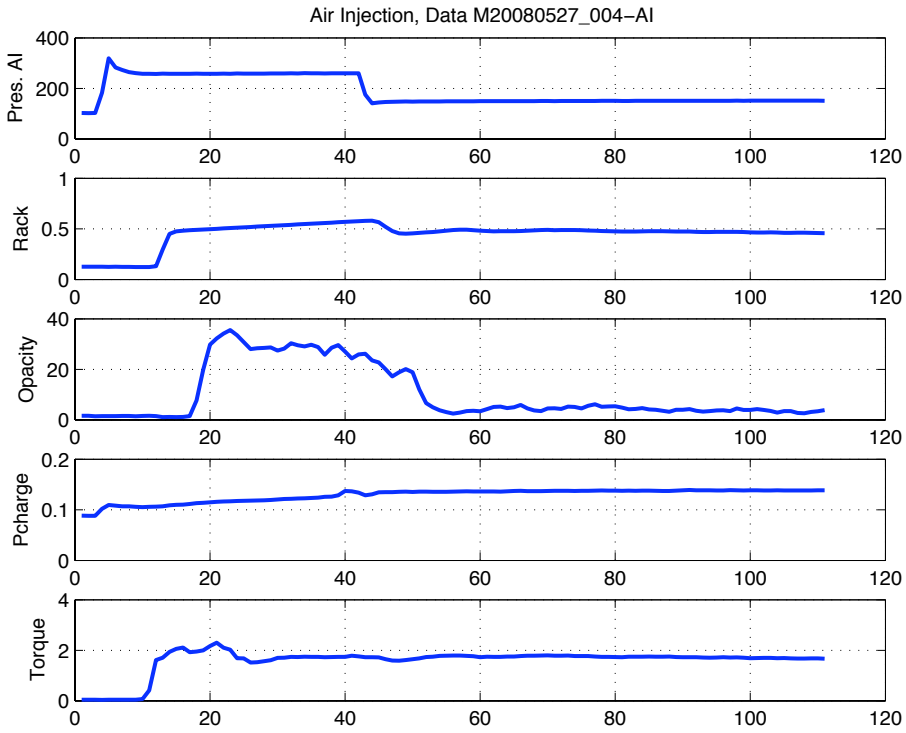

Figure 3.3: Measured engine responses during the A1 test. Air injection is applied for 4 sec

and the behavior of the binary signal (PRBS) in test B1. Engine variables of interest for identification are (apart from the air injection) the fuel,labeled as rack, opacity and pressure in intake manifold, labeled as pengin. For the fuel trace, a pattern that is a result of the fuel limiter operation can be observed. Although the load is applied rapidly, the action of the fuel actuator follows an inclined response and at about 0.8 it diverts and supplies considerable less fuel. Torque describes the step loading that is applied to the engine and eventually is responsible for the shape of the fuel (rack) variable.

3.4.3 Transfer Function Results

The transfer function from each input to output is as follows.

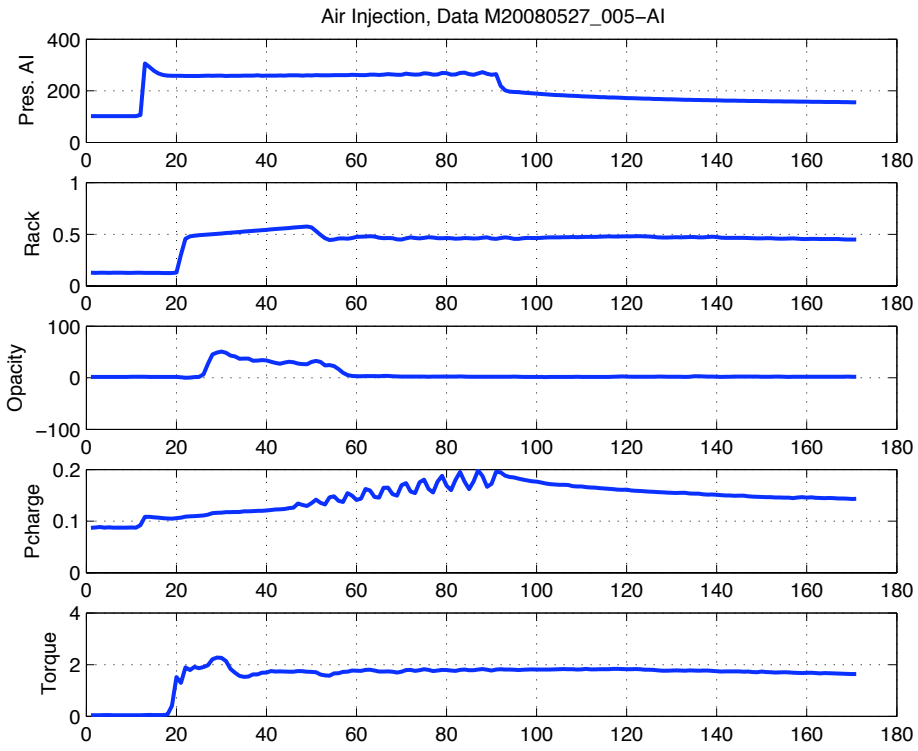

Figure 3.4: Measured engine responses during the A2 test. Air injection is applied for 8 sec

$$\begin{bmatrix} opacity \\ pressure_{intake\,manifold} \end{bmatrix} = \begin{bmatrix} G_{11} & G_{12} \\ G_{21} & G_{22} \end{bmatrix} \begin{bmatrix} fuel \\ air\ injection \end{bmatrix} \tag{3.22}$$

or equivalently

$$opacity = G_{11}\ fuel + G_{12}\ air\ injection \tag{3.23}$$

$$pressure_{intake\,manifold} = G_{22}\ air\ injection \tag{3.24}$$

with $G_{21} = 0$.

The transfer function from $air\ injection$ to $pressure_{intake\,manifold}$ is modelled as a first order lag with delay

$$G_{22}(s) = e^{-sT_d}\ \frac{K_p}{1 + T_p\ s} \tag{3.25}$$

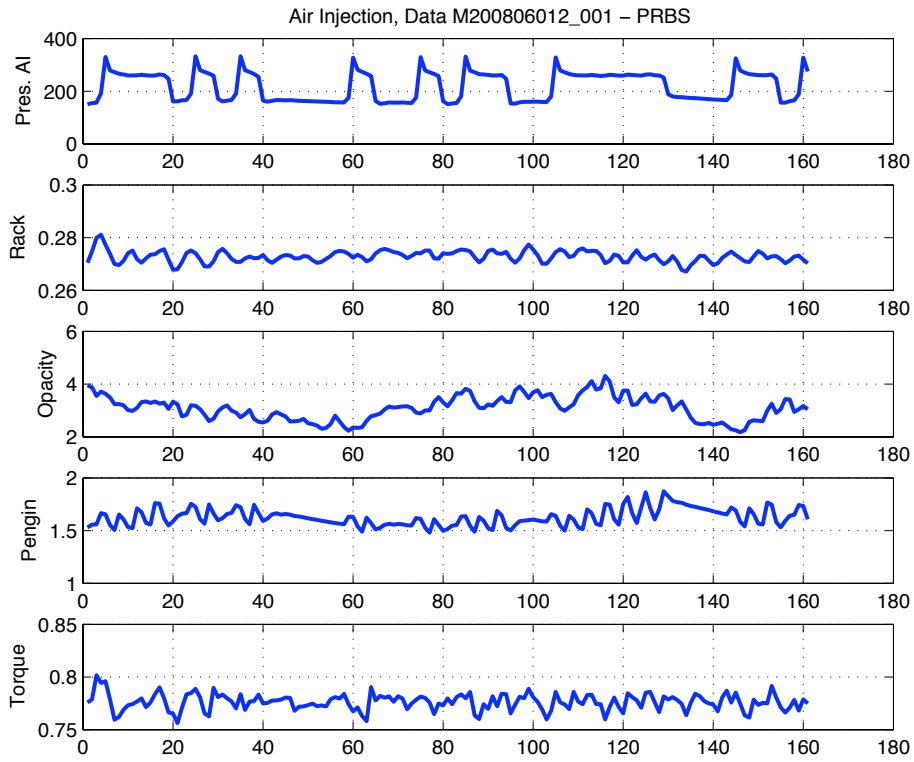

Figure 3.5: Measured engine responses during the B1 test. Air injection is applied in pulses.

where T_p is the time constant and T_d is the delay.

The transfer function from *rack* and *air injection* to *opacity* is modelled as second-order transfer functions with delay and zero

$$G_{11}(s), G_{12}(s) = e^{-sT_d}\ K_p\ \frac{1 + T_z s}{(1 + T_{p1} s)(1 + T_{p2} s)} \tag{3.26}$$

whereT_d is the delay, T_z is the zero and T_{p1}, T_{p1} are the poles. Table 3.1 shows the transfer functions.

Regarding the statistics of the identified transfer functions, these are as follows.

For $G_{22}(s)$, $K_p = 4.35 \pm 0.567$, T_{1p}=10.957 $\pm$ 4.779.

Table 3.1: Transfer functions from control and disturbance inputs to outputs

	u_1 $(air\ injection)$	u_2 $(fuel)$
y_1 (pressure)	$e^{-0.0487\ s}\ \frac{4.35}{1+10.957s}$	0
y_2 (opacity)	$e^{-0.600\ s}\ \frac{0.0754(1-25.747s)}{(1+15.288s)(1+5.3397s)}$	$e^{-0.340\ s}\ \frac{0.021955(1+193.18s)}{(1+2.4374s)(1+0.4901s)}$

For $G_{11}(s)$, $K_p = 0.0219 \pm 0.683$, T_{1p}=2.437 $\pm$ 0.45, T_{2p}=0.4901 $\pm$ 0.954, T_d=0.340 $\pm$ 0.308, T_z=193.18 $\pm$ 18.036.

For $G_{12}(s)$, K_p = 0.0754 $\pm$ 0.683, T_{1p}=15.288 $\pm$ 4.4245, T_{2p}=5.3397 $\pm$ 0.954, T_d=0.600 $\pm$ 0.0308, T_z=-25.989 $\pm$ 0.36.

The open loop poles are all stable. The open loop zero for the transfer function of opacity to pressure is non-minimum-phase, while for the transfer function of opacity to fuel it is left-hand-plane zero.

The uncertainty of the identified models in transfer function form can be considered from the statistics. For some model parameters, the estimate was not precise. This is due to the extend that the particular identification data for that combination of input-output did not provide adequate or rich information, so that the errors were significant. For the cases that the fuel is involved as variable in identification the problem in identification becomes ill-conditioned, as the respective fuel data come from closed-loop control operation.

Figures 3.6 and 3.7 show the nominal unit **step responses** of the identified transfer function for opacity, input 1 (fuel) and input 2 (pressure) respectively. Both Figures show that the engine model is asymptotically stable. It can be seen, for the input 2 (pressure) the effect of the non-minimum-phase zero, which causes inverse response.

The **Bode frequency response** for opacity with input fuel, is shown

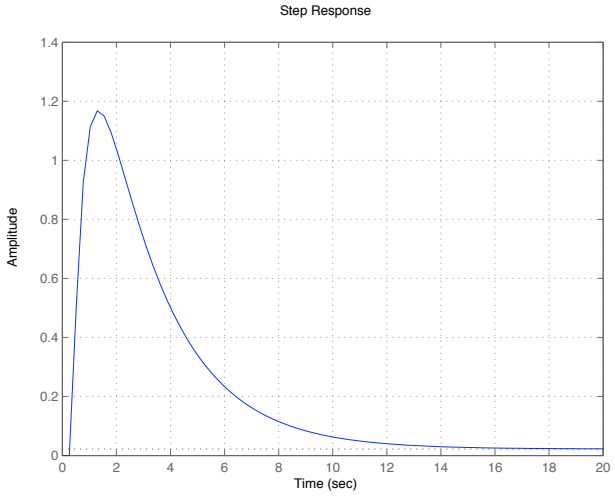

Figure 3.6: Open loop step input for opacity, input 1 (fuel)

in Figure 3.8, while for opacity with input air injection the respective Figure is 3.9.

It can be seen that for input fuel, the magnitude is a little higher that 0 db, which indicates that, for the scaled magnitudes, 1% of fuel will increase opacity more than 1%, for a range of frequencies from 0.5 to 5 rad/s.

In the **residual analysis** for this identified model, residuals are differences between the one-step-predicted output from the model and the measured output from the validation data set. Thus, residuals represent the portion of the validation data not explained by the model. Figure 3.10 shows the autocorrelation function and the 99% confidence bounds for validation data for opacity. It can be seen that in general the model is acceptable, as the correlation curves lie between the confidence level.

Figure 3.11 shows the identified and measured opacity data.

It can be seen that the fit in general is good. The model succeeds in capturing the dynamics, though it does not capture the initial high peak of opacity signal.

Figure 3.12 shows the nominal unit **step responses** of the identified transfer function for pressure. It can be seen that the engine model is

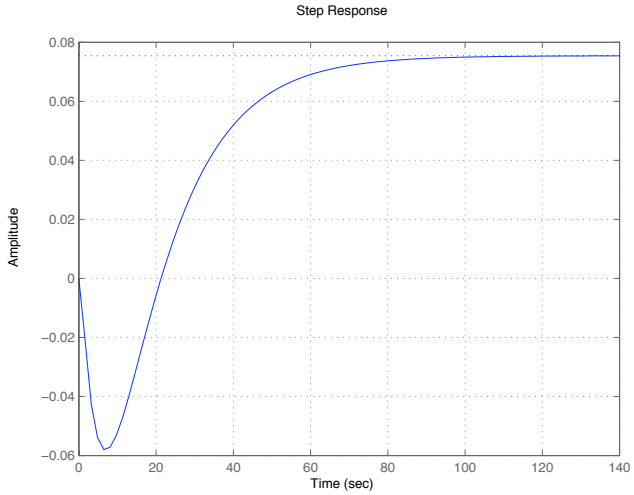

Figure 3.7: Open loop step input for opacity, input 2 (pressure)

asymptotically stable.

The **Bode frequency response** for pressure with input air injection, is shown in Figure 3.13. The input is the air injection pressure and the output is the manifold pressure.

It can be seen that in the low frequency range (below 0.08 rad/s) the amplification from input to output is about 12 dB. For frequencies higher than 0.08 rad/s, output is attenuated.

Figure 3.14 shows the autocorrelation function and the 99% confidence bounds for validation data for pressure.

It can be seen that in general the model is almost acceptable, as only the cross-correlation lies between the confidence level.

Figure 3.15 shows the identified and measured pressure data.

It can be seen that the model captured the average dynamics of the pressure variation, during air injection action, with success. With this type of model structure, the dominant dynamics in the upper part of response were captured, though in the lower part, the model failed to follow the initial rapid rise. Also it can be seen that the high frequency oscillations due to instability were not captured. However this was not a problem during the

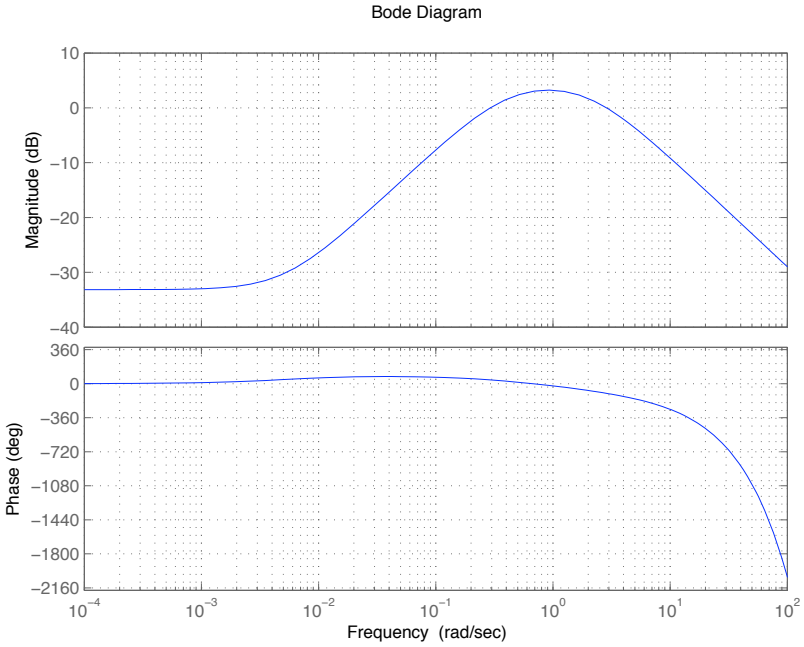

Figure 3.8: Bode frequency response for opacity, with input fuel

experiments, as the pressure signal was filtered and the oscillations were removed.

3.4.4 Subspace Results

Subspace identification method n4sid, from MATLAB, was used for the identification of engine model with this method. The identified model was used as internal model of controller MPC I, in Chapter 5.

3.4.5 Nonlinear Identification Results

The identified nonlinear Hammerstein-Wiener models are shown in Figure 3.16. Data from step responses were used in order to identify these models. The models presented a nonlinear relation between opacity and fuel and between air injection and intake manifold pressure. As a next step, a nonlinear model predictive controller (NMPC) was simulated for performance with the

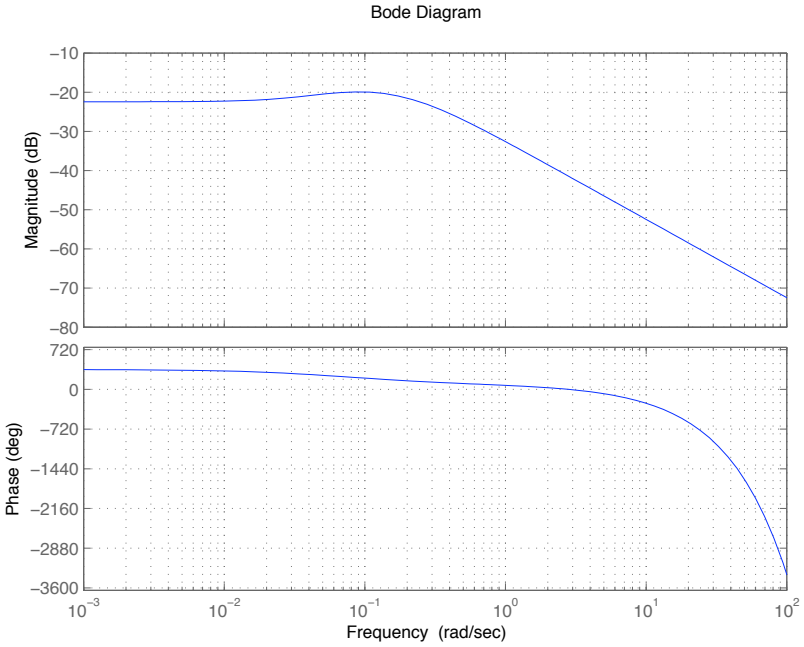

Figure 3.9: Bode frequency response for opacity, with input air injection

identified models. More information can be found in [PK08]. Information about NMPC is presented in Chapter 4.

3.5 Summary

System identification was the subject of this chapter. Three model structures were identified and results were presented. The models were in the linear forms of transfer function and state-space and also in nonlinear form, that of Hammerstein-Wiener. Statistics of the models were also provided, which show the quality of the various models. In some cases, large variances were observed. As these are linear models, their validity is only for a region close to the operating point around which process data was collected and system identification was performed.

The aim was to capture the dominant dynamic relations between the inputs like air injected air and fuel and the outputs such as exhaust opacity

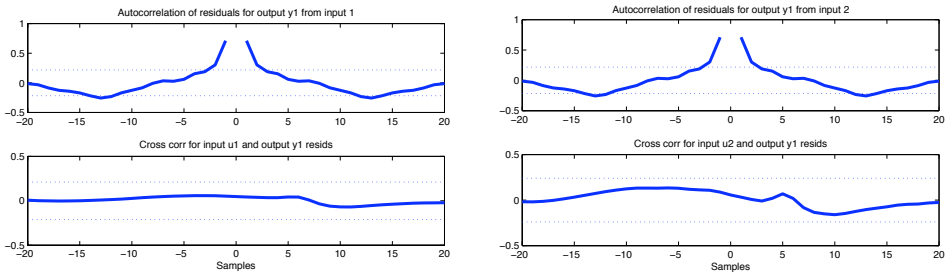

(a) Residuals for opacity, input 1

(b) Residuals for opacity, input 2

Figure 3.10: Residuals for opacity

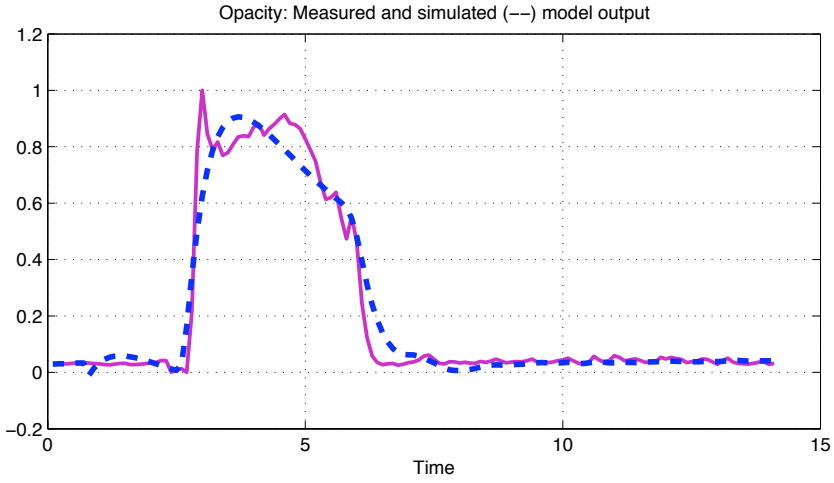

Figure 3.11: Open-loop identified and measured opacity

and pressure in intake manifold.

These models are required for operation of the model predictive controller, as this is formulated in the next chapter and is further implemented in Chapter 5.

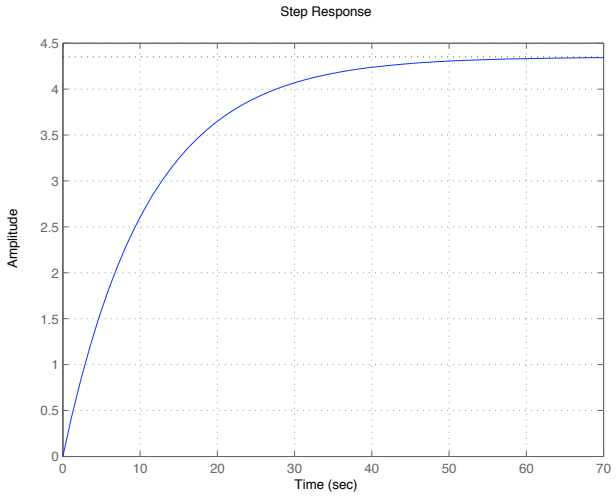

Figure 3.12: Open loop step input for pressure

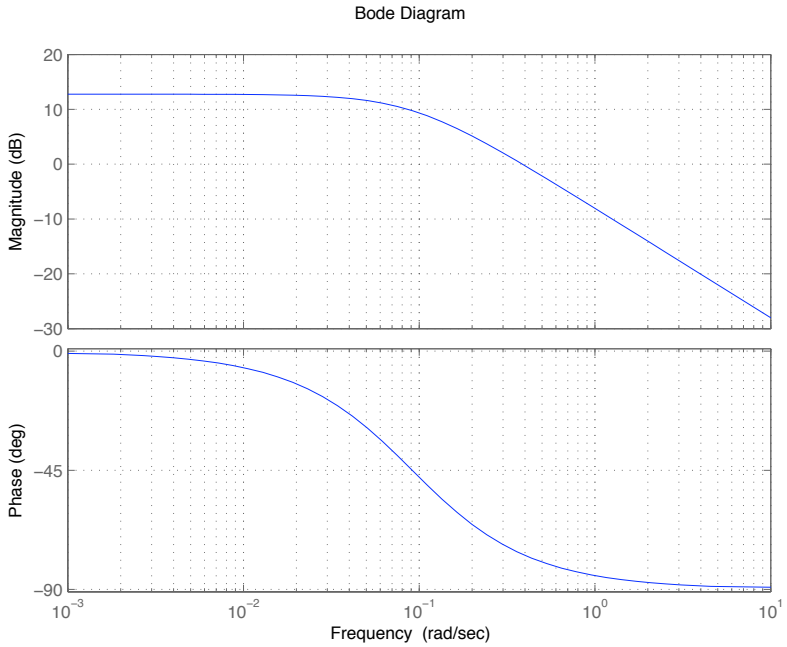

Figure 3.13: Bode frequency response for pressure, with input air injection

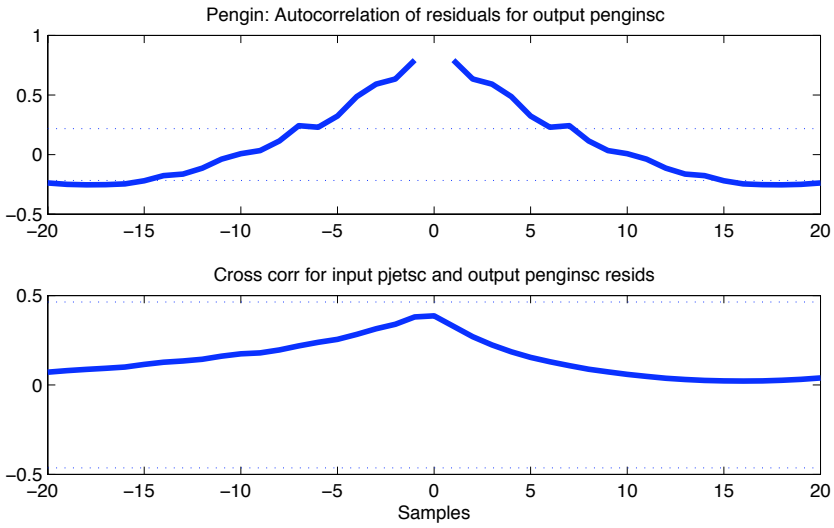

Figure 3.14: Residuals for pressure, Pengin

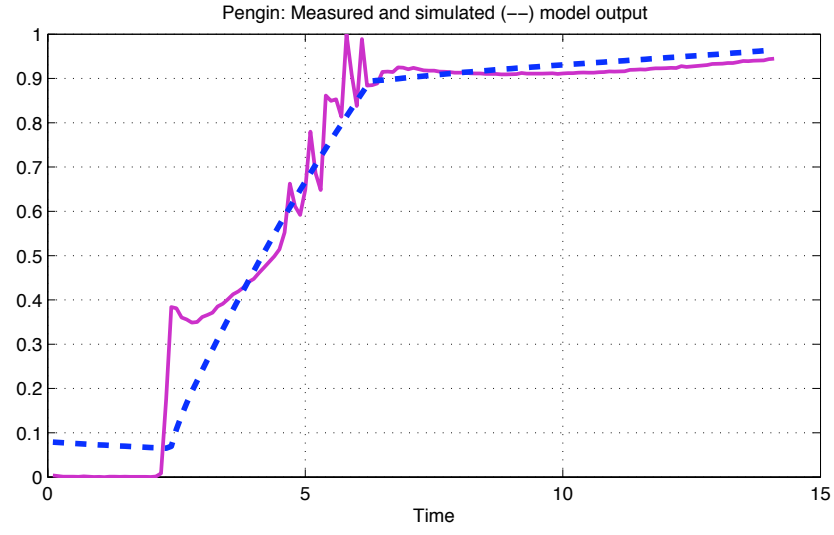

Figure 3.15: Open-loop identified and measured pressure

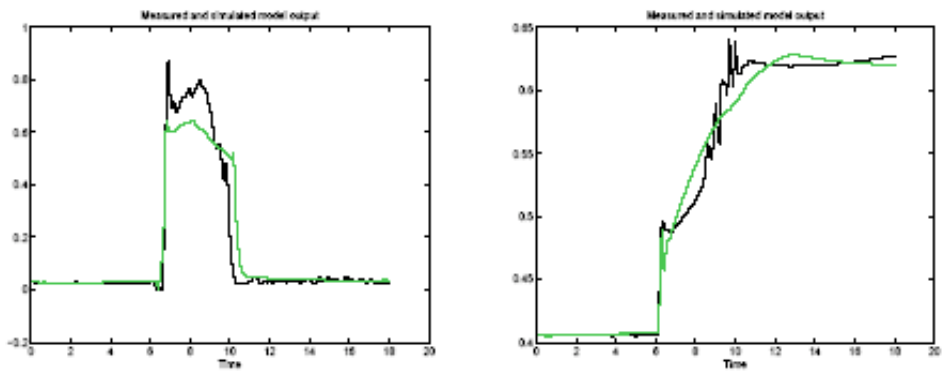

Figure 3.16: The identified nonlinear Hammerstein-Wiener model

Chapter 4

Model Predictive Controller

The purpose of this chapter is to present a self-contained brief coverage on Model Predictive Control (MPC). The basic concepts are introduced and the formulation of problem as constrained optimal control over a receding horizon is provided.

The Chapter outline is as follows. The formulation with unconstrained and constrained MPC and optimization issues is given in the beginning, followed by model structures and state estimation. Further on, the significant issues of stability and robustness are presented. The important approach of nonlinear MPC is presented next. Various applications are reviewed in order to give a feel of the diverse coverage of the control method. The theory and methods presented in Chapter 4 will be used in Chapter 5, for the design and implementation on the experimental engine of the predictive controllers for opacity reduction in the testbed engine.

4.1 Formulation of Model Predictive Control

Model Predictive Control is based on minimization of a performance index of the predicted response of a system, over a future horizon. The main idea is to use a model of the plant to predict the future evolution of the system. The model used, often called internal model, is a linearized model of the nonlinear plant. MPC computes the optimal current and future control inputs by minimizing the difference between set-points and future outputs

predicted from the given plant model [LYM06].

An important reason for the success of MPC is the handling of process constraints. In the design of control systems, the most common way to deal with constraints, is to consider linear systems and fix things up in an ad-hoc way, after the design. On the contrary, with MPC methodology, the constraints are part of the problem formulation, and are considered during control system design [Mac04].

4.1.1 Application Fields

The first-generation MPC systems were developed by industrial practitioners in 1970s for petrochemicals and quickly found wide success, as MPC tackled constraints and multivariable cases efficiently. An adaptive MPC theory known as Generalized Predictive Control (GPC) appeared in 1987. The total number of MPC industrial applications exceeded 4600 by end of 1999, according to a 2003 survey paper [QB03]. This number had grown more than twice since a previous survey back in 1997 by the same authors.

Representative applications that have utilized MPC are aircraft flight control, steam generators and utility boilers, catalytic cracking petrochemical units, batch and hydrocracker reactors, pulp and paper industry, distillation columns. [OR94]. A literature review on applications of MPC and nonlinear NMPC in combustion engines was given in paragraph 1.3.2.

In [VSP04] MPC was used for air flow management in a fuel cell system study, where it found an optimum balance between the use of fuel cell and capacitor during fast transients.

MPC was used for the regulation of the temperature of the super-conducting magnets of Large Hadron Collider accelerator at CERN [VCM99].

MPC can also be found in vibration suppression applications, with voice coil as actuator, as in [BO03].

Generalized Predictive Control (GPC) was studied in aeroelastic control of tilt rotor aircrafts, as in [KJB00].

Implementation of MPC in reconfigurable embedded hardware (Field Programmable Gate Array-FPGA) is studied in [LYM06] .

Informative reviews of MPC theory and practices can be found in text-

books such as [Mac04], and also in [CB00], [SEM04], [BMR07], [Mos95].

A related tutorial is presented in [Raw00] and a related review in [QB03], [BM99] and [ML99]. Information on NLMPC can be found in textbooks [KC01], [HS97] and in the review paper [AFN04]. GPC is covered in [CMT87a] and [CMT87b].

4.1.2 The Basic Elements

The basic concept of predictive control is presented below, from [Mac04]. Figure 4.1 shows the basic elements. The time is discrete, with the current sampling instant labeled as integer k. Then at current time k, the plant output is $y(k)$ (also is the latest measurement available), with $y(k-1)$, $y(k-2)$, ... , the previous history of the *output trajectory*. Also shown is the *set-point trajectory*, which is the trajectory that the output should follow; the values of which are marked as $s(t)$.

Optionally, there is the *reference trajectory*, marked as $r(t|k)$. This starts at current output $y(k)$ and is defined as an ideal trajectory along which the plant should return to the set-point trajectory, in the case for example that a disturbance occurs. It is frequently assumed that the reference trajectory approaches the set-point exponentially from the current output value, where the time constant of the exponential defines speed of the response.

A predictive controller utilizes an *internal model* to predict the behaviour of the plant, starting at the current time, over the *prediction horizon*, H_p. This predicted behaviour depends on the assumed input trajectory $\hat{u}(k+i|k)$, with $i = 0, 1, ..., H_p - 1$. It is assumed that the internal model is linear. The notation $\hat{u}$ is used instead of u to denote that at time k there is only prediction of what the input at time $k+i$ shall be; the actual input at that time, $u(k+i)$, shall probably be different from $\hat{u}(k+i|k)$.

The input trajectory is chosen so as to bring the plant output at the end of prediction horizon $k+H_p$ to the required value $r(k+H_p)$. There are several input trajectories $\hat{u}(k|k), \hat{u}(k+1|k), ...\hat{u}(k+H_p-1|k)$ which achieve this and we could choose one of them. In Figure 4.1 it is shown that the input can vary over the first three steps of the prediction horizon and to remain constant thereafter: $\hat{u}(k+2|k) = \hat{u}(k+3|k) = ..., \hat{u}(k+H_p-1|k)$, so that

there are three parameters to choose, namely $\hat{u}(k|k), \hat{u}(k+1|k), \hat{u}(k+2|k)$. These parameters are chosen so as to minimize some *cost function*.

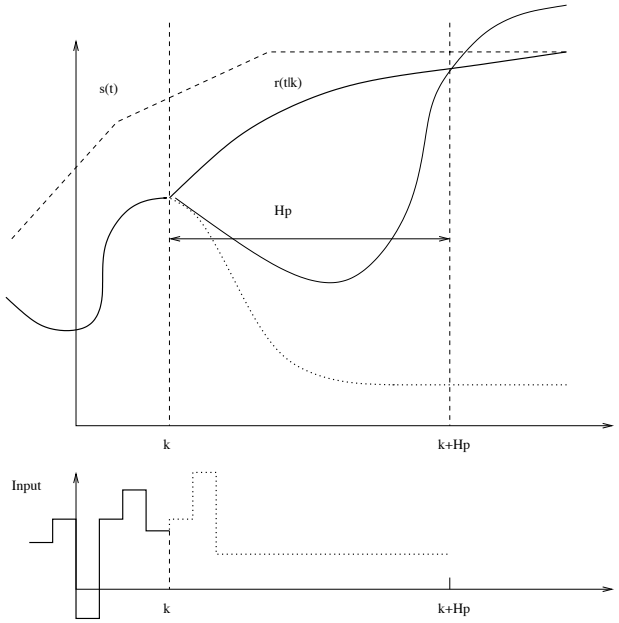

Figure 4.1: Predictive control: the basic idea

Once the future input trajectory has been chosen, only the first element of that trajectory is applied as input signal to the plant. Then the complete cycle of the output measurement, prediction, and input trajectory determination is repeated, one sampling interval later. Since the prediction horizon maintains the same length as before, but slides along by one sampling interval at each step, the *receding horizon* control strategy applies.

Constraints are the other major remaining characteristic of MPC. This affects the choice of future input trajectory $\hat{u}(k+i|k)$, with $i = 0, 1, ..., H_p-1$, in such a way that the input signals and their rates remain within allowed constraints and such that the outputs, and possibly *inferred* variables in the case that these are not measured directly, also remain within allowed constraints.

Proper choice of prediction and control horizons can be beneficial for the system performance. A common choice of parameters is first to choose the control interval about 20-30 sampling periods, and then choose prediction

horizon H_p equal to that number. The control horizon H_u equals a small number, e.g. 3-5. In the case of constraints, a long prediction horizon allows the controller to anticipate the constraint and avoid it or minimize its effects. In the case of non-minimum phase plants (those with zero at right half plane and exhibit in the beginning response to the opposite direction) a long prediction horizon would allow the controller to move in longer-term direction.

The output variables are referred to as controlled variables (CV), while the input variables are called manipulated variables (MV). Measured disturbances are called disturbance variables (DV).

In the present work, unconstrained MPC was implemented in the engine testbed with controller type MPC I.

4.1.3 Unconstrained MPC

It is standard to assume a linear and time-invariant plant, which after discretisation of time at a single sampling rate, gives the following state-space system

$$x(k+1) = Ax(k) + Bu(k) + Ew(k) \tag{4.1}$$

$$y(k) = C_y x(k) + v(k) \tag{4.2}$$

$$z(k) = C_z x(k) \tag{4.3}$$

where x is the state vector, u is the control input vector, y is the measured output vector, z is the vector of outputs to be controlled and w, v are the vectors of unknown state disturbances and measurements errors respectively. A, B, C_y, C_z and E are constant matrices.

The future input trajectory is chosen as one that minimises a cost function V. The cost function V penalizes deviations of the predicted controlled outputs $\hat{z}(k+i|k)$ from a reference trajectory $r(k+i|k)$. The cost function is defined as

$$V(k) = \sum_{i=H_w}^{H_p} \|z(k+i|k) - r(k+i|k)\|^2_{Q(i)} + \sum_{i=0}^{H_u-1} \|\Delta u(k+i|k)\|^2_{R(i)} \tag{4.4}$$

where H_p and H_u are the prediction and control horizons respectively, H_w is the window parameter, Q and R are weights.

If the plant has a linear model and a quadratic cost function like above, then the problem that has to be solved is a standard finite-horizon *linear quadratic* (LQ) problem[1].

If the cost function is changed from quadratic to '1-norm' or '∞-norm' then one penalizes absolute values of errors, or the peak error respectively, then finding the optimal solution becomes a *linear programming*, (LP), problem [MGK07].

Common choices of stage cost can be

$$l(y, r, u) = \|Q^{1/2}(y - r)\|_2^2 + \|R^{1/2}(u - \bar{u})\|_2^2 \tag{4.5}$$

$$l(y, r, u) = \|Q(y - r)\|_1 + \|R(u - \bar{u})\|_1 \tag{4.6}$$

$$l(y, r, u) = \|Q(y - r)\|_\infty + \|R(u - \bar{u})\|_\infty \tag{4.7}$$

where $Q = Q^T \geq 0$ and $R = R^T > 0$ typically, and $\bar{u}$ is an equilibrium value of u that is compatible with set point r.

The optimal value of the cost is

$$J^0 = x_k^T P x_k \tag{4.8}$$

where P is symmetric positive semi-definite solution of the algebraic Riccati equation

$$P = A^T PA - A^T PB(B^T PB + R)^{-1} B^T PA + Q \tag{4.9}$$

The cost equation is rewritten in

$$V(k) = \|Z(k + i|k) - T(k + i|k)\|_Q^2 + \|\Delta U(k + i|k)\|_R^2 \tag{4.10}$$

Recall that Z has the form

$$Z(k) = \Psi x(k) + \Upsilon u(k - 1) + \Theta \Delta U(k) \tag{4.11}$$

for suitable matrices Ψ, Υ and Θ.

[1]The idea is to pose control problems as problems of constrained optimization. The 'classical' theory of Optimal Control mainly developed between 1955 and 1970, was driven by problems coming from the needs of aerospace industry, namely by the problems of launching, guiding and landing space vehicles and also of needs in flight and missile control [Mac04]

Then the error $\mathcal{E}$ can be defined as

$$\mathcal{E}(k) = \mathcal{T}(k) - \Psi x(k) + \Upsilon u(k-1) \tag{4.12}$$

A block diagram of a model predictive controller is presented in Figure 4.2, from [Mac04].

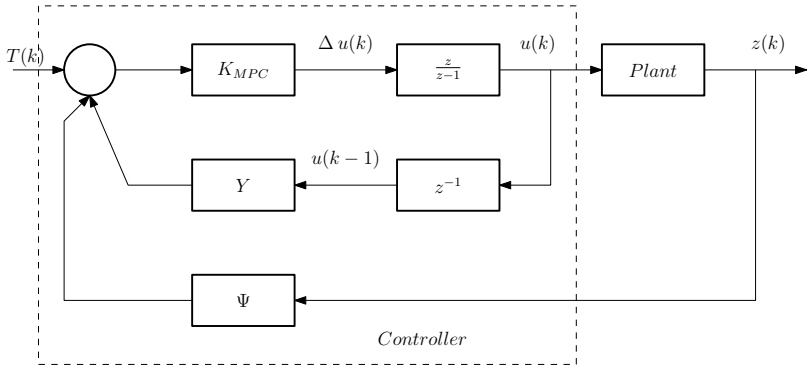

Figure 4.2: Block diagram of a MPC with state feedback without constraints

Following a successful initial controller setup with unconstrained MPC, the remaining tests in the engine with the two different controllers (MPC I and MPC II), incorporated constrained MPC. These controllers are presented in Section 5.4.

4.1.4 Constrained MPC

Inequality constraints on input and output variables are important characteristics for MPC applications; being a motivation for the early developments of MPC. Input constraints (on manipulated variables) can be considered as a result of physical limitations of plant equipment, like control valve travel limits or rate-of-change in variables like actuator movement or flow rates. Output constraints are related to the plant operational strategy.

In constrained MPC, the control action can be computed subject to hard constraints on the manipulated variables and/or the outputs.

Manipulated variable constraints:

$$u_{min}(l) \leq u(k+l) \leq u_{max}(l) \tag{4.13}$$

Manipulated variable rate constraints:

$$|\Delta u(k+l)| \leq \Delta u_{max}(l) \tag{4.14}$$

Output variable constraints:

$$y_{min}(l) \leq y(k+1|k) \leq y_{max}(l) \tag{4.15}$$

The cost function is defined as

$$V(k) = \sum z(k+i|k) - r(k+i|k)^2_{Q(i)} + \sum \Delta u(k+i|k)^2_{R(i)} \tag{4.16}$$

with the form

$$min \frac{1}{2}\theta^T \Phi \theta + \phi^T \theta \tag{4.17}$$

subject to $\Omega\theta \leq \omega$.

which is a standard optimization problem known as the *Quadratic Programming* (QP) problem [2].

Two methods for solving QP problems can be *Active Set* and *Interior Point* [Mac04]. More information about linear and quadratic programming can be found in [Fle96].

A major problem that may occur with constraint optimization is that the problem may be infeasible; in which case the solver stops. Various approaches are used in practice, such as avoiding hard constraints on z, actively manage constraint definition in every step k or actively manage horizons in every step k.

A block diagram of a model predictive controller with constraints is presented in Figure 4.3, from [Mac04].

Several types of future behaviour of controlled variables (CV) exist [QB03]. Usually the CV are set to a *fixed set point*, and the deviations on both sides are penalized by the cost function. A drawback of this type is that the control action can be very aggressive, with large input adjustments; with a

[2] Expressions like $x^T Qx$ and $u^T Ru$, where x, u are vectors and Q, R are symmetric matrices are called quadratic forms, If $x^T Qx \geq 0$ for every x, except $x = 0$, then this quadratic form is called positive definite.

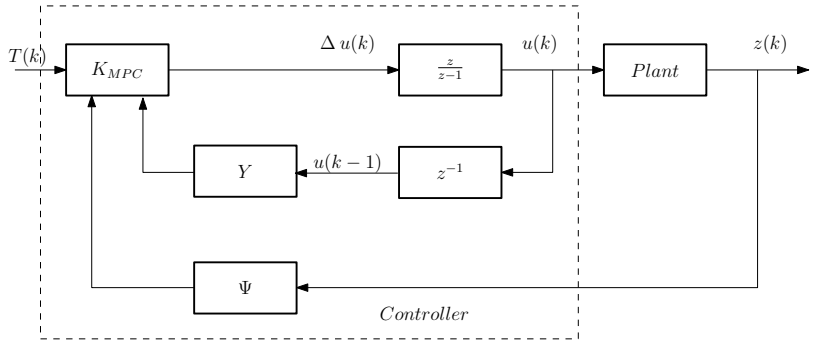

Figure 4.3: Block diagram of a MPC with constraints and state feedback

possible remedy to detune the controller. Another option is the *zone* control, where upper and lower boundaries are defined and are usually implemented as upper and lower soft constraints. This is the case when the objective is to keep CVs within boundaries, neglecting their exact values. A third option is to define the CV as a *reference trajectory*. From the current CV to the setpoint, a curve of first or second order is specified and a quadratic cost function penalizes deviations. Finally objectives are represented as *funnels*, which are similar to zones but become narrower over the prediction horizon.

4.1.5 State Estimation

In order to compute the solution to the optimal control problem, the knowledge of the state of the system is required. In practice, the states are not directly measured and a state estimator is used to reconstruct the state from the available measurements. Disturbances affect both the states and the measurements. Kalman Filter is capable of recursively estimating the state of a linear system, as follows.

$$\hat{x}_{k|k} = \hat{x}_{k|k-1} + L_k(y_k - C\hat{x}_{k|k-1}) \tag{4.18}$$

$$\hat{x}_{k+1|k} = A\hat{x}_{k|k} + Bu_k \tag{4.19}$$

where $\hat{x}_{k|k}$ is the state estimate at sample time k given k. L_k is the filter gain matrix, and multiplies the difference between the measured output y_k output, and predicted output $C\hat{x}_{k|k-1}$ to produce a filtered state estimate by correcting the predicted state estimate at previous sample time. When

disturbances are normally distributed random variables, Kalman Filter produces the optimal estimate of state [Mac04].

Kalman Filter is used for the state estimation of controllers MPC I and MPC II, which are presented in Chapter 5.

4.1.6 Tuning Parameters

The parameters that can be tuned in MPC are the sampling time, the control horizon H_u, the prediction horizon, H_p, and the output and input matrices Q and R respectively.

For stable, minimum phase systems, the sampling time does not affect stability; however for good performance of the closed loop system, the sampling time must be small enough to capture process dynamics, and large enough to allow for on-line computations [HS97].

The control and prediction horizon affect the performance of the controlled system and influence robustness. A long prediction horizon results in better performance, is essential for systems with slow dynamics, but will result in long computation time for the control input. The control horizon when short, provides robustness to uncertainties due to parameter variations.

The output matrix Q penalizes tracking errors and ensures that output constraints are not violated. The input matrix R penalizes control increments and helps to keep control inputs within bounds, ensuring that smooth control actions are provided [KM99]. Increment in R will reduce the control activity. These parameters are usually tuned by iterations and simulation, although theories exist that provide choices which guarantee stability and robustness characteristics.

Tuning of parameters that affect the performance of the controllers were used in the simulation study, as shown in Section 5.2.

4.1.7 Advantages, Drawbacks, Limitations

Two important factors determine the success of an MPC application. First the availability of a suitable plant model and second the ability to solve the quadratic programming problem within the prescribed sampling period (on

line). The latter becomes an issue when it is required to solve QP problem online for complex systems with fast response times, where computational resources may be limited. But as modern computer power is increasing, MPC can be considered for high-bandwidth applications like aerospace, automotive and robotics [MGK07].

Most MPC applications are in refineries and petrochemical applications, and some in food, pulp and paper industries.

Some factors for success are:

1. The process model captures the static and dynamic interactions between input, output and disturbance variables
2. Constraints on inputs/outputs are handled in a systematic manner
3. The basic ideas are easy to explain and understand
4. Accurate model predictions can provide early warning of potential problem

The drawback is the large on-line computational load required to perform the optimization.

Current industrial algorithms suffer from limitations [QB03].

1. Limited model choices
2. Sub-optimal feedback
3. Lack of nominal stability
4. Inefficient solution of dynamic optimization

4.2 Models for MPC

The relation between the linear model and the real plant needs careful consideration in predictive control. In most control methodologies the linear model is used off-line, for analysis and controller design purposes. In predictive control it is used as part of the control algorithm, and the resulting signals are applied directly to the plant [Mac04]. It is considered the most

critical and time consuming step; the view in a commissioning project is that it can take up to 90% of cost and time [ML99].

Phenomenological modeling can be expensive and may lead to unnecessarily complicated system descriptions; on the other hand empirical input-output descriptions require appropriate selection of model structures, test signals and validation procedures [KC01].

Typically models are derived from step tests or Pseudo Random Binary Signals (PRBS), and impulse response coefficients are fitted with least squares. Input channels are excited one at a time but this practice may not give a multivariable model of the required accuracy. There were cases where although SISO models were very accurate, when combined, they represented a very poor MIMO model.

In the following the various types of models used in MPC shall be outlined. In the first applications, step and pulse response models were used; later GPC introduced the transfer functions and difference equations. Today most of the formulations utilize models in state space formats.

4.2.1 Step and Pulse Response

Although manufacturing processes are inherently nonlinear, the vast majority of MPC applications to date are based on linear dynamic models, the most common being step and impulse response derived from the convolution sum in discrete time. There are potential reasons for this. Linear empirical models can be identified in a straightforward manner from process test data. In addition, in refinery processing the goal is mainly to maintain process at a desired steady state (regulator problem) rather than moving rapidly from one operating point to another (as in a servo problem). For such applications a carefully identified linear model is sufficiently accurate [KC01].

In practice it is difficult to perform pulse tests, as large pulse amplitudes are required to excite the plant sufficiently [Mac04].

If a step or pulse response model exists, then it is possible to assemble a *block-Hankel* matrix to derive a state-space model, that can match the step responses exactly. This model will be of large state dimension, but it is possible with the use of *Singular Value Decomposition* (SVD) to obtain a still

accurate model of lower state dimension. Subspace identification methods [vOdM96] are preferable to the above path 'step test-step response-state space model' as one can use arbitrary input-output data.

4.3 Stability and Robustness

4.3.1 Stability in Predictive Control

There is well-developed theory that leads to the formulation of MPC problem in such a way that closed-loop stability is guaranteed. Two popular choices are to impose terminal constraints at the end of prediction horizon and to use an infinite prediction horizon [MGK07].

In the first approach, if a terminal constraint of the form $\hat{x}_{k+H_p|k} = 0$ is imposed, it always gives closed loop stability, but proves to be a strong constraint and it can be relaxed to $\hat{x}_{k+H_p|k} \in \mathcal{X}_F$, on the assumption that $\mathcal{X}_F$ has suitable properties. In the latter approach, when using infinite prediction horizon, closed-loop stability is guaranteed. The drawback in this case is that there are infinite decision variables, $\hat{u}_{k+i|k}$, with $i = 0, 1, ...$ The quadratic program for an infinite open-loop horizon is an infinite-dimensional optimization problem. To overcome this, a horizon length N is selected, such that constraints are inactive for $i \geqslant N$. Then $\hat{u}_{k+i|k}$, with $i = 0, 1, ..., N-1$ is choosen and fixed feedback law $u_{k+i} = \mu(x_{k+i})$ for $i \geqslant N$ is assumed .

4.3.2 Robustness in Predictive Control

A control system is robust when the stability is maintained and performance specifications are met for a specified range of model variations (uncertainty range). Although robust control theory is rich for linear systems, little is known for linear systems with constraints [ML99].

Various approaches exist that check robustness of the designed predictive controller. These can be norm-bounded uncertainty, polytope uncertainty, the tuning procedure of Lee and Lu, the LQG/LTR tuning procedure and LMI approach [Mac04] and [ML99].

The main interest is in *norm-bounded* uncertainty method. $P_0(z)$ is the

nominal model of the plant and Δ is the uncertainty, as a stable bounded operator. Then the real plant $P(z)$ is given by

$$P(z) = P_0(z) + \Delta \tag{4.20}$$

for additive uncertainty.

The feedback combination of the system with uncertainty block Δ will remain stable if the following holds

$$\bar{\sigma}[K(e^{j\omega T_s})S(e^{j\omega T_s})]\|\Delta\|_\infty < 1 \tag{4.21}$$

where $\bar{\sigma}[.]$ denotes the largest singular value. This inequality will be used in a controller tuning procedure, so that the frequency response is affected.

4.4 Nonlinear Model Predictive Control

In case that the plant exhibits nonlinearities, the linear model used in MPC is no longer useful; one has to use a nonlinear model and techniques from Nonlinear Model Predictive Control (NMPC) [Mac04]. Main active research is towards this area.

The main disadvantage is that the convexity of the optimization is lost which is a serious drawback for on-line applications.

One approach is to replace the linear model with a nonlinear one, and then use suitable optimization methods to overcome the loss of convexity. It is usually very difficult to analyze the applications. A popular optimization algorithm is *Sequential Quadratic Programming* (SQP). An other method is *Multiple Shooting*, which is suitable for first principle models, consisting of large sets of differential or differential-algebraic equations. More details can be found in [FAD$^+$01], [ML99] and [AFN04].

As an alternative, the nonlinear model can re-linearized (or perform successive linearizations [vEL01]), as the plant moves from one operating point to another, and use the latest linear model as the internal model at each step. This results in solving a QP problem at each step. Re-linearization or adaptation of the linear internal model is the most common way to deal

with plant nonlinearities in practice. This is not always adequate if the nonlinearities are severe.

Nonlinear models used in NMPC can be obtained from first principles modeling or can be based on Hammerstein-Wiener, neural nets or Volterra models. Hammerstein-Wiener models describe dynamic systems using one or two static nonlinear blocks in series with a linear block. Only the linear block contains dynamic elements. The linear block is a discrete-time transfer function and the nonlinear blocks are implemented using nonlinearity estimators, such as saturation, wavenet, and dead zone. Hammerstein-Wiener models were used in [PK08], as presented briefly in Section 3.4.5.

4.5 Summary

The basic structure of a model predictive controller was introduced in this chapter: the necessary models, the cost function and the constraints. Also introduced were the issues of stability and the theoretical and computational difficulties of nonlinear MPC. MPC with these elements was implemented for the opacity control problem; this is the subject of Chapter 5.

Chapter 5

Control of Smoke Density (Opacity)

Once a mathematical model of the engine that incorporates the dominant process features is identified, then this model can be used in model predictive control (MPC). Optimal control theory provides the tools to determine suitable control commands, subject to constraints on outputs.

The objective in the present work is the reduction of opacity in the exhaust gas of a marine diesel engine, during transient loading. Chapter 5 describes the achievement of this objective, through the application of optimal air injection profiles. Reduction in opacity was verified by comparison of opacity values achieved when optimizing the supply of air injection to those corresponding without any air injection operation.

Two controllers were designed and implemented in the engine testbed. With the first controller (MPC I), control of pressure in the intake manifold was achieved, while the second controller (MPC II) was used for the control and reduction of opacity. Both schemes used constraint on the intake pressure, with the aim to avoid compressor instability that may appear with the supply of compressed air in the manifold downstream the compressor.

5.1 Control Systems in Marine Diesel Engines

Manufacturers of internal combustion engines often use maps to represent the relation between some measured values (e.g. speed and torque) and the required actions (e.g. the injection timing values). Using this example, at any speed and load condition, the corresponding injection timing is calculated using an interpolation algorithm. Furthermore, the control system may depend on a series of look-up tables, and is then referred as *scheduled*. Modern engine control systems have a large number of tables and demand substantial effort to fill-in those tables (i.e. *calibrate* them).

Engine control and calibration is a costly task of the engine development program. Traditional solutions rely largely on heuristics and the determination of complex maps with feed-forward strategies to compensate for a wide range of operating conditions. Control and calibration has evolved into this process partly because of the inherent drawbacks of conventional control and optimization techniques. The main problem with the traditional approach is an inability to handle system constraints and large system delays. This means that controller gains have to be limited to avoid oscillatory control which in turn leads to compromised engine performance.

In the last two decades more advanced control solutions have been developed in the process industry which avoid these problems. The new direction in control systems is to follow a model-based approach, where the design of the control algorithms would be based on the modeling of the principal elements in the control loop.

Along these lines, and as a prelude to the present work, the author has applied Hinfinity robust control method to a Wartsila marine diesel engine [PK06], [Pap06a], [Pap07], and [Pap06b] and nonlinear plant linearization and PID control in [LPKC07].

5.2 Controller Design

5.2.1 Control Objectives

The control objective in the present work is to minimize exhaust opacity during engine transients, with the supply of external air, subject to the

constraint of keeping pressure in the intake manifold below a certain value, in order to avoid compressor instability.

The application is considered as a possible retrofit to an existing engine, under the assumption that the fuel control system in place and operating will not be altered. The air injection is considered as input variable (or manipulated variable), the fuel as measured disturbance and the opacity and pressure in intake manifold (Pengin) in as outputs (or controlled variables).

The design cycle for the controller was as follows, in accordance with [QB03]. First the MPC controller was configured and initial tuning parameters were selected. Second, the controller was tested off-line using closed-loop simulation to verify the controller performance. This was a repetitive task, until the performance was acceptable. Third, the controller with filters and additional elements was downloaded to the destination machine and was tested on-line. The tuning of the controller parameters was repeated, as needed.

5.2.2 Tuning

The choices of controller parameters like prediction horizons, weight matrices and sampling times, have a considerable effect on the performance and stability of the model predictive controller. References [HS97] and [HM97] provide information regarding the tuning of MPC parameters.

In the present work, the parameters which were tuned were the sampling time, the control horizon M, the prediction horizon, P, and the output and input matrices Q and R respectively.

Simulations provided information about the system responses, and involved the linear models.

The constrained Model Predictive Controller was designed with function `mpc` from MATLAB MPC Toolbox, v.2. Sampling time was 0.1 sec. A Prediction horizon smaller than the maximum delay of 6 samples must be avoided. Final choice was 20 samples. The control horizon M was 2 samples. The input weights were set to 0 while the output weights were 1 and 0. For constraints on the manipulated variables, maximum one and minimum zero were used. The constraint for the output variable *pengin* was set to 0.7. All

the above parameters required a scaled plan, as defined in Section 3.4.1.The system model was in the format of discrete transfer functions. For state estimation, a standard Kalman Filter was used.

The simulation setup presents a controller similar with the one that was implemented in the test engine. The internal model of the controller was the same with the plant model. The closed-loop simulation with the plant and the predictive controller is shown in the block diagram of Figure 5.1.

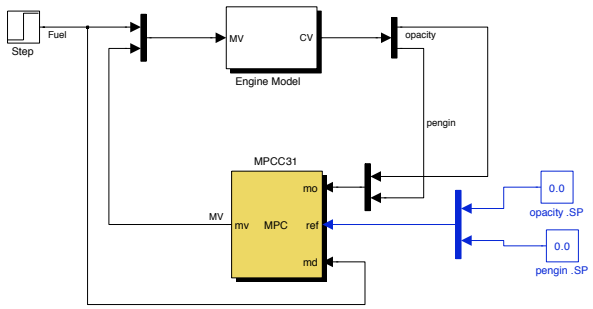

Figure 5.1: The simulated MPC in closed-loop configuration

The responses and the input of the MPC controller are shown in Figure 5.2. Prediction horizon was $P = 20$, control horizon $M = 2$ and sampling time $T_s = 0.1$ sec. Input weights Q were set to zero, and output weights were equal to one and zero. A constraint was applied in output 2, i.e. the pressure in intake manifold, $pengin = 0.7$.

A disturbance is applied in the fuel and the responses in opacity and intake manifold pressure are observed. The opacity decays back to its initial zero value, and the intake manifold pressure acquires its steady state value of 0.7 in less than a second. The respective constraint of 0.7 in pressure is not violated during the transient. The delay in the response of opacity is also evident. For the manipulated variable, i.e. the actuator command for the the air injection, the action takes place for a duration of less than a second.

Various tuning parameters were used in simulation studies, with the same models for controller and plant as before. In the first case, the effect of the prediction horizon is studied. The responses and the input of the

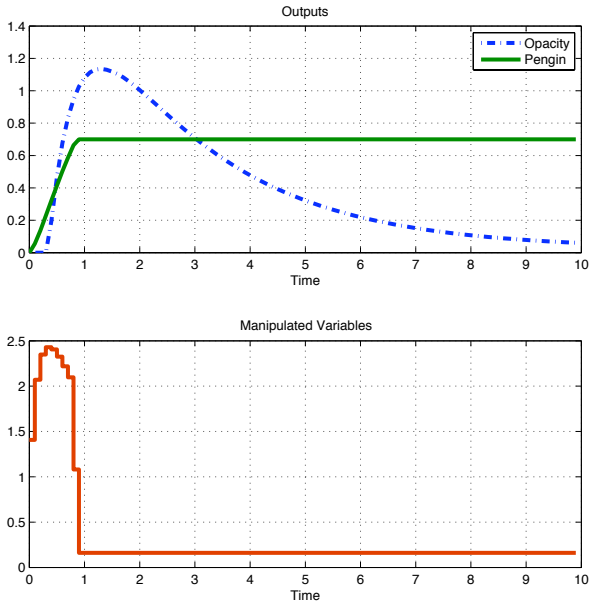

Figure 5.2: Simulated MPC, standard

MPC controller with $P = 10$, $P = 20$ and $P = 50$ are shown in Figure 5.3. The remaining controller parameters are the same. No effect can be seen for the controlled variable opacity. For pressure, the response for the horizon of 50 samples is the fastest, while for all the three cases the steady state value remains the same. It can be seen that for the manipulated variable, i.e. the air injection, and for the largest horizon, the control action is very aggressive and short in duration; behavior not very favourable for actuators. The chosen value of 20 samples, seems an adequate compromise, between the response time for pressure and the actuator command.

In the second case, the effects of the output weight are shown. The response and the input of the MPC controller with weights $R = 10$, $R = 100$ are shown in Figure 5.4. No effect can be seen for the controlled variable opacity. For pressure, the response for the penalty of 1 shows the slowest response, while for the cases of the larger penalties, the response is the same. For the manipulated variable, i.e. the air injection, for the smallest penalty the control action is very smooth in comparison with the aggressive

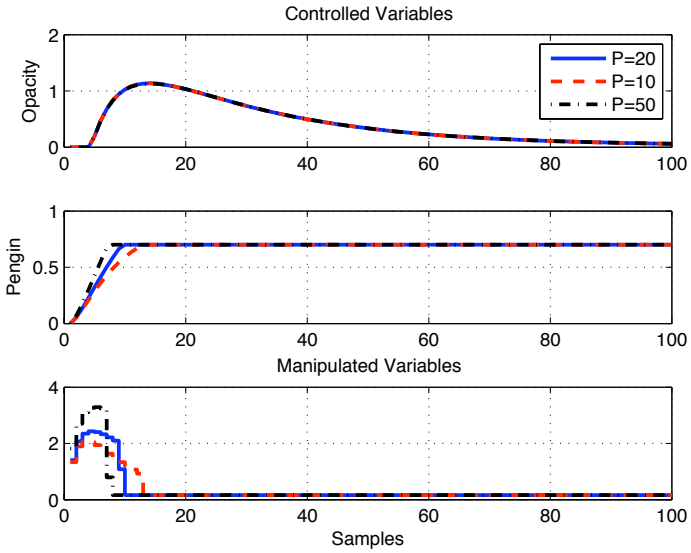

Figure 5.3: Simulated MPC, with $P = 10,\ 20,\ 50$

responses of the higher penalties. The chosen value of $R = 1$ eventually will supply less air, while the opacity is not affected by the choice of penalty values.

Finally, the effects of the sampling time are simulated. The response and the input of the MPC controller with $T_s = 0.05,\ 0.1,\ 0.2$ sec are shown in Figure 5.5. Significant differences in the controlled variables can be observed. The fastest sampling time of 0.05 sec causes a sluggish response, with delay in opacity increase and longer settling time. Respectively, the actuator for air injection, remains active about double and three-times more for the cases of 0.1 and 0.2 sec. The chosen value of 0.1 sec exhibits a performance almost in-between the fastest and the slowest sampling times.

5.3 Implementation of Control Algorithms

MPC requires the process model that will forecast the future values of outputs like opacity and pressure, when inputs like the air injection and the fuel will be altered. MPC uses this forecast to calculate the adjustment in the manipulated variable that is needed to keep 'opacity' at its set point.

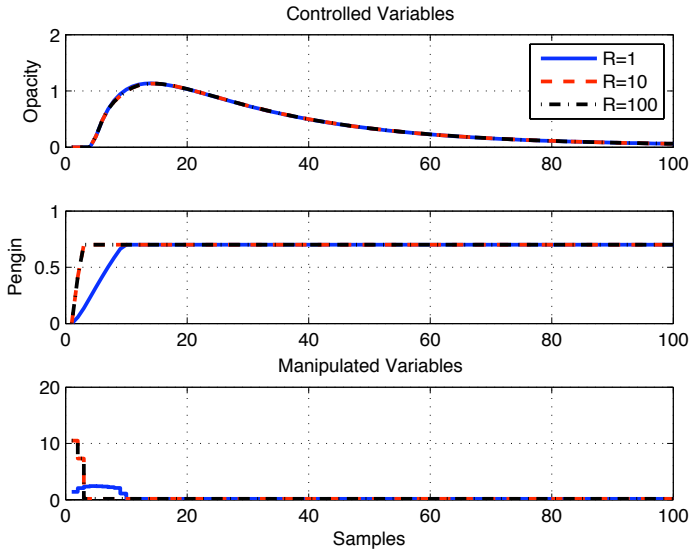

Figure 5.4: Simulated MPC, $R = 1,\ 10,\ 100$

The control calculation considers the effect of any known constraints on this adjustment (pressure has an upper bound that cannot be exceeded).

The controller receives a measured disturbance signal (position of fuel rack) directly, which allows to compensate for this disturbance's impact on opacity, rather than wait until the effect appears on the opacity measurement. This is feed-forward control. It effectively anticipates the delay of 0.6 sec observed in the opacity measurement response.

The MPC controller is shown in Figure 5.6.

Relay Element

The actuator for the air injection is a solenoid valve, which switches either on or off. In order to respond to the analog command of the controller, a relay element interfaces the analog and switching part. The relay element allows its output to switch between two specified values. When the relay is on, it remains on until the input drops below the value of the Switch off point parameter. When the relay is off, it remains off until the input exceeds the value of the Switch on point parameter. The thresholds were

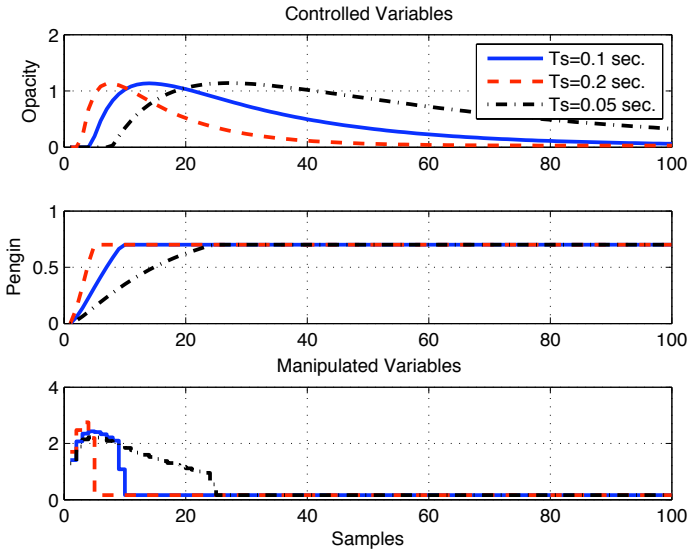

Figure 5.5: Simulated MPC, $T_s = 0.05,\ 0.1,\ 0.2$ sec

selected after trial-and-error. Thus the valve switches on when the analog command is larger than 1.5 Volt and switches off when the analog command is lower than 0.8 Volt. These settings are specific to the application and affect directly the operation of the air injection system, as the thresholds can start the supply of air to the engine earlier or later.

The relay element is shown in Figure 5.7.

Filtering

A digital filter was incorporated in the feedback loop of pressure in the intake manifold. Figure 5.8 shows the effect of filter on the signal of inlet manifold pressure, for two different engine loading cases. The filter succeeds in removing the higher frequency signal distortion, before this signal is fed-back to the controller.

The choice and effect of filter is system dependent. After some trial-end-error, a forth-order, low pass filter, with cut-off frequency at 1 rad/s was selected. The frequency response of the filter is shown in the Bode diagram of Figure 5.9.

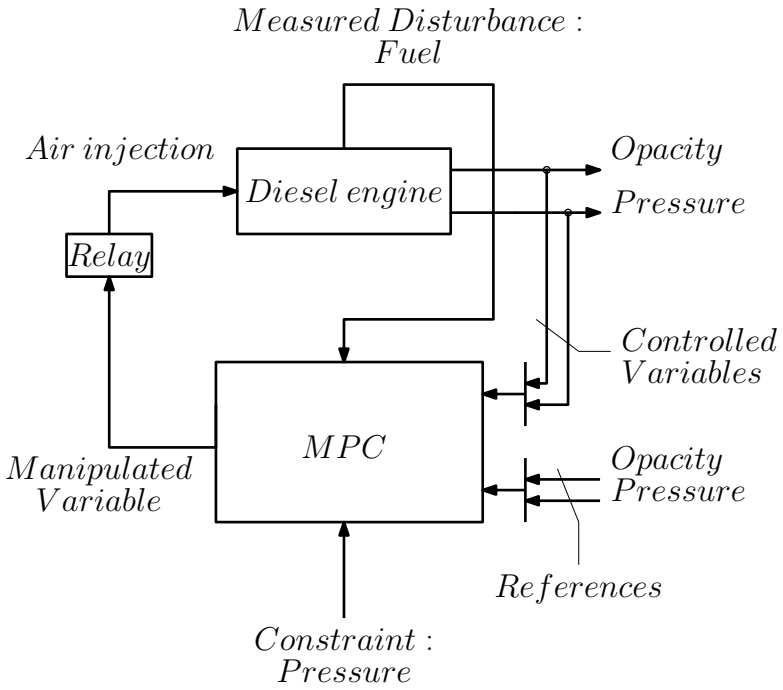

Figure 5.6: MPC block diagram

The filter type was Butterworth, which is an Infinite Impulse Response (IIR) filter [OS75]. The basic advantage of IIR filters over other types like the Finite Impulse Response (FIR) is the much lower filter order with which one can achieve the required specifications. For the design of the filter, the MATLAB Signal Processing Toolbox was used [Mat07].

For the other measured signals in the control loop, i.e. opacity, air injection pressure and fuel, filtering was not required, as the signals had suitable characteristics for interfacing with the controller.

5.4 Performance of Predictive Controllers

In the present work, two different predictive control controllers were designed and tested. The first controller, MPC I, was simpler as it had a model which related injected air to intake manifold pressure. This is a Single-Input-Single-Output (SISO) model. The second controller, MPC II, used a model that related injected air and fuel to opacity and pressure in intake

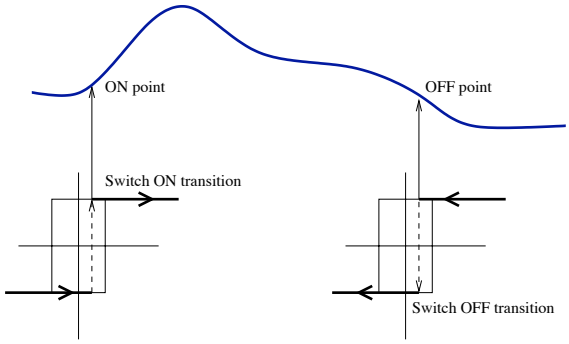

Figure 5.7: Relay element in controller for air injection

manifold. The fuel was considered a measured disturbance. Table 5.1 shows the characteristics of the two controllers that were implemented in the test engine.

Table 5.1: Parameters of the experimental controllers

Controller Type	Controlled Variable	Manipulated Variable	Disturbance Variable	Constraints	Model
MPC I	pressure	air injection	–	pressure	Sub
MPC II	opacity	air injection	fuel	pressure	TF

Samples of results are shown from the multitude of the test made. The total number of tests was 60. During the tests, the different configurations in the two predictive controllers were tested.

In general the engine was loaded in a single step. The engine operated in its nominal speed of 1200 rpm. The dynamometer applied a torque load from 0% to 47.5% (1890 Nm), with a maximum duration of 30 to 40 sec. With this load, the engine speed was decreased by about 10%.

During a test session, after the warm up of the testbed and opacimeter, the different settings in the air injection control system, engine control system, data acquisition system were entered in the respective computers through application interfaces. The data capture from the data acquisition

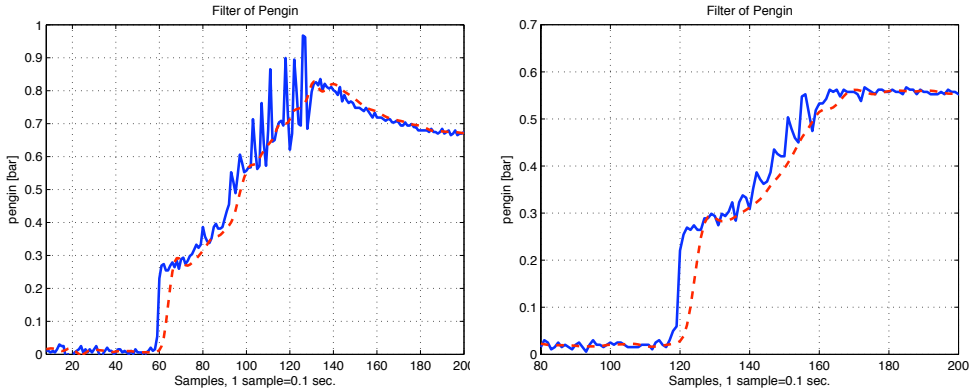

(a) Raw, filtered pressure

(b) Raw, filtered pressure

Figure 5.8: The digital filter for Pengin channel in action, compared with the raw signal, in two different cases

system was triggered by the start command for the load application from the engine control system. The air injection control system was in stand-by mode: during the transient, the set points of pressure or opacity were followed with appropriate control action through the air injection action. After the end of the test session, data from 36 channels with the engine parameters were stored for further processing.

5.4.1 Results from Pressure Control

The first controller, MPC I, had a model which related injected air to pressure in intake manifold. This is a Single-Input-Single-Output (SISO) model. The configuration of model predictive controller MPC I is shown in Figure 5.10.

The reason for using this type of controller was twofold. As it was based on a SISO model, it was simpler than MPC II, allowed quick shakedown of the experimental arrangement, and familiarization with the engine testbed under air injection control and provided valuable experience for the control of pressure in the engine intake manifold. It must again be stressed that safety and testbed integrity was a primary concern in the experiments. Apart from the cost of any possible breakdown, the cost of the testbed operation is also

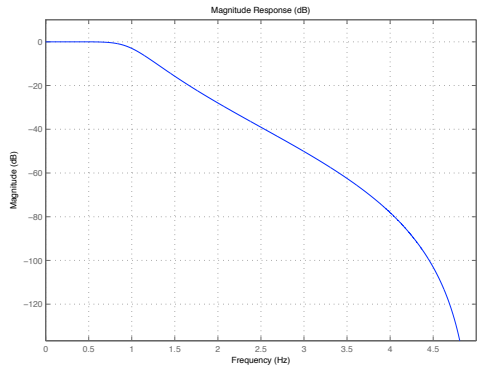

Figure 5.9: Bode plot of the digital filter for pressure

substantial and the run times had to be minimized.

Another reason was that MPC I provided the opportunity to use a different model structure, coming from subspace identification method, as was presented in Section 3.2.2.

Here the pressure was used indirectly to manipulate the exhaust opacity. As the opacity measurement was not part of the control loop, the associated delay was not present and therefore the measurement of fuel as feedforward contribution in the controller was not necessary. As explained earlier, the elements of relay in the output and the Butterworth filter in pressure signal were also present.

For this type of controller, two different pressure set points were chosen. In the first case the set point in pressure in the intake manifold was 1.7 bar, while in the second case the set point was 2.0 bar.

With the first set point, pressure set at 1.7 bar, the engine operation was normal, without any significant signs of compressor instability.

The responses of the controlled and manipulated variables are shown in Figure 5.11. Presented in the figure is the pressure signal, the filtered pressure signal which enters the controller and the set point of pressure during the transient. Time is shown in samples, where each sample equals to 0.1 sec.

A step load from 0 to 47.5 % was applied to the engine, with the speed set at 1200 rpm. The set point of the pressure in intake manifold is applied

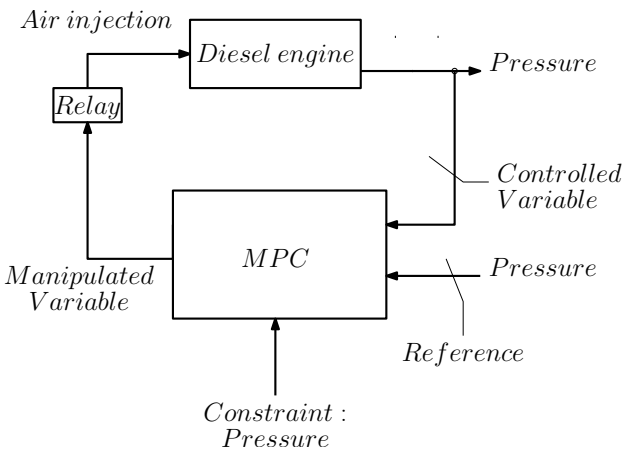

Figure 5.10: Predictive controller for pressure in intake manifold (MPC I)

during the start of the transient, and starts from almost 1.1 bar up to set point value which is 1.7 bar. During the engine transient, the aim is to maintain the pressure in the intake manifold around this value. The air injection controller will provide the necessary command to the solenoid actuator for the air admission.

The set point of 1.7 bar was chosen after some testing, and was used to show the behavior of the control system to a step point that will not bring the compressor close to instability. The set point of 1.7 bar was set as a constraint, whose value was not allowed to be exceeded during the transient.

It can be seen from Figure 5.11 that the control can be considered satisfactory. The set point is followed quite closely, and at the points where the actual value of pressure violates the constraint of 1.7 bar, the command is stopped. The effect of the solenoid valve is present, with its on-off switch pattern, distinguished in the bottom graph, which shows the actual air pressure in the air injection line.

The responses of fuel rack position and opacity are shown in Figure 5.12.

Opacity reached immediately its highest value of 80% but quickly the effect of the air injection brought a reduction in opacity to a value of almost 50%. The delay in the response of opacity measurement is evident.

For the fuel rack position, the effect of the fuel limiter operation can

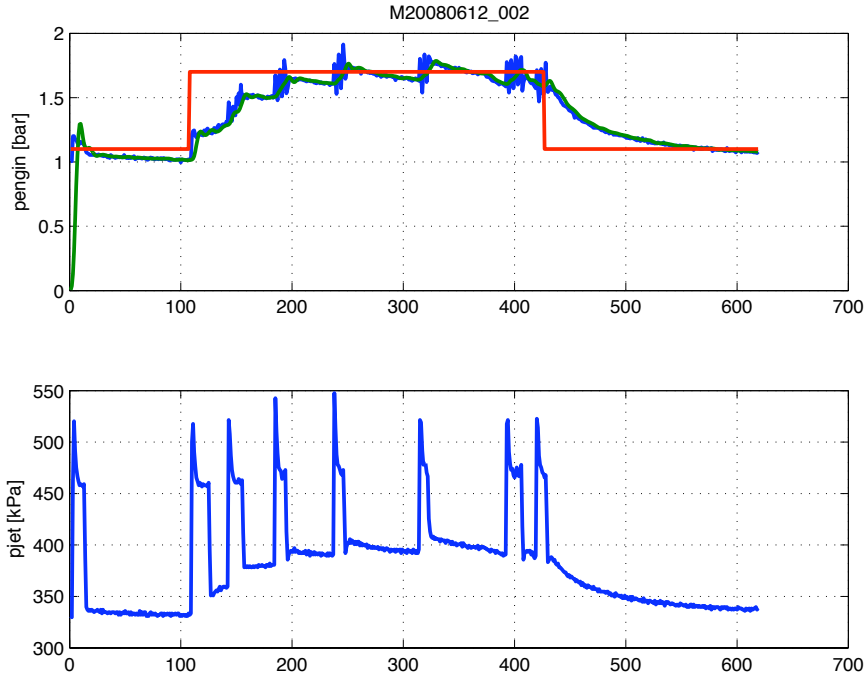

Figure 5.11: Controlled and manipulated variables, MPC I, set point 1

be observed. Although the load was applied rapidly, the action of the fuel actuator followed an inclined response at about 0.5 (equal to 50% actuation) and supplied considerable less fuel.

The control output and the relay switching are shown in Figure 5.13.

The particular responses were taken with the relay switching set to open and close the solenoid valve when the threshold of 3, in the command, was exceeded. The control output, labeled as xmpc, remained within operating limits from the start of the disturbance during the transient, and only at the end, at time 420, during the stop of the command took momentarily a negative value.

As mentioned in Chapter 4, constrained model predictive control effectively keeps the controlled variable, in this case the pressure in intake manifold, to its set value.

With the second set point, with pressure set at 2.0 bar, the engine oper-

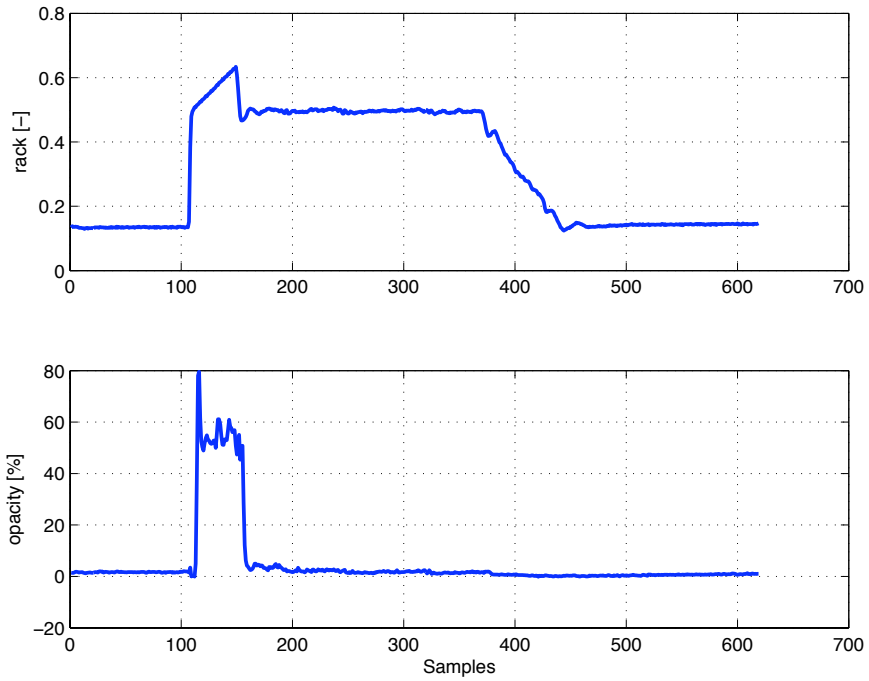

Figure 5.12: Opacity and fuel rack variables, MPC I, set point 1

ation was affected by compressor instability. The instability was manifested both in the measurement of pressure, speed, and mass flow, but also as loud 'banging' and vibrations of the testbed intake system. The responses of the controlled and manipulated variables are shown in Figure 5.14.

The same load scenario was applied in this case. The set point of the pressure in intake manifold is applied during the start of the transient, and starts from almost 1.1 bar up to set point value which is now 2.0 bar. With this set point, the compressor is clearly brought to instability. The set point of 2.0 bar was set as a constraint, whose value was not allowed to be exceeded during the transient.

It can be seen from Figure 5.14 that the control can be considered rather satisfactory. The set point was followed in an average, and as in the previous test with the lower set point, at the points where the actual value of pressure violated the constraint of 2.0 bar, the command was stopped. The effect of

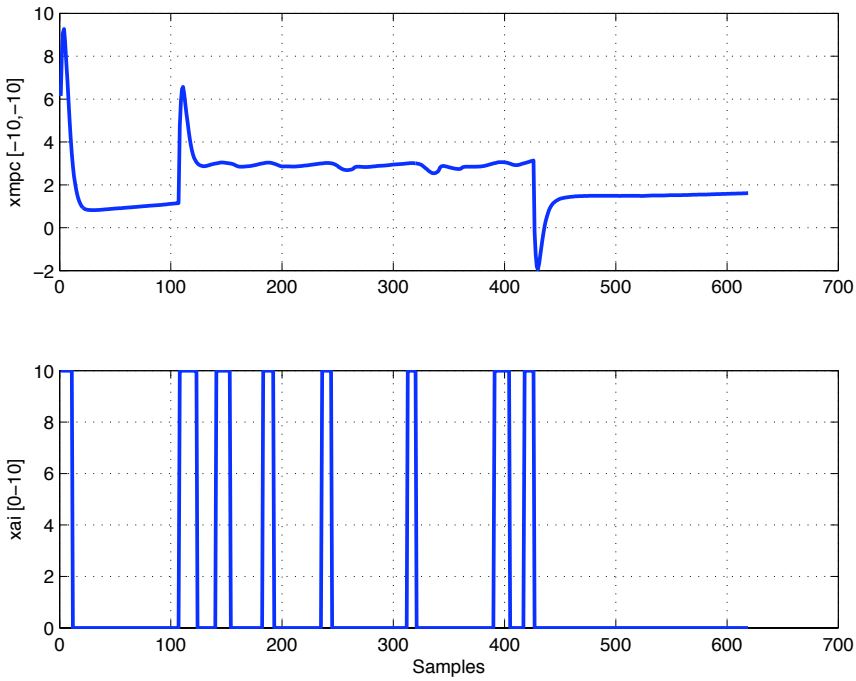

Figure 5.13: Control output and the relay switching, MPC I, set point 1

the solenoid valve was present, with its on-off switch pattern, displayed in the bottom graph, which shows the actual air pressure in the air injection line. When pressure in the intake manifold exceeded 1.5 bar, oscillations could be observed. The oscillations were present in the whole manifold volume, reaching even the area close to the solenoid valve, as one can notice in the oscillations in the air injection pressure.

The responses of fuel rack position and opacity are shown in Figure 5.15.

It can be seen that opacity reached immediately its highest value of 70% but quickly the effect of the air injection brought a reduction to a value of almost 40%. The delay in the response of opacity measurement was evident, as in the previous test. In the current test though, the air in the first moments of transient, from samples 70 to 120, was not adequate and the opacity reached a higher value of about 55% within the next 50 time units or 5 seconds.

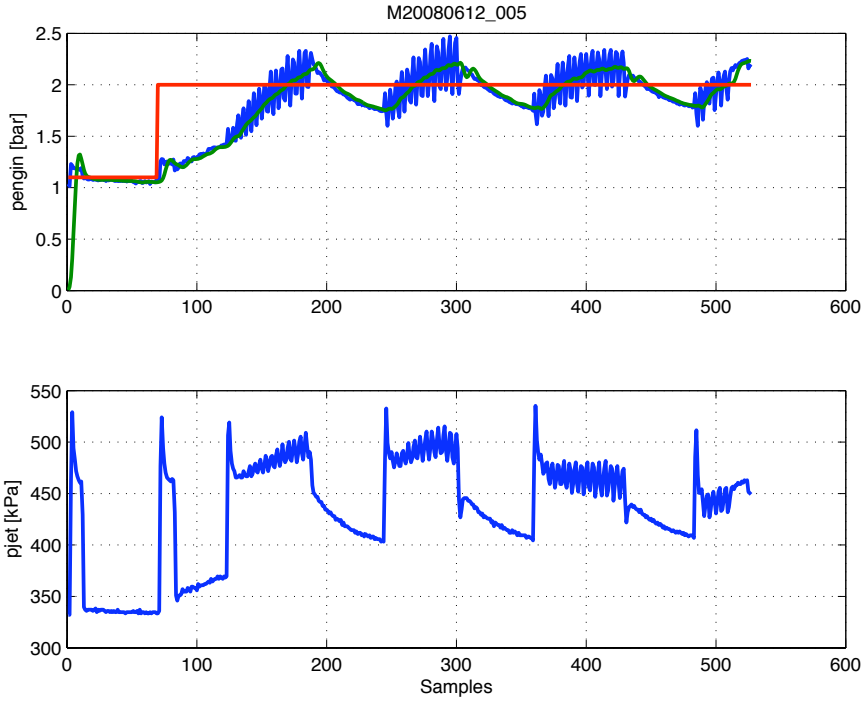

Figure 5.14: Controlled and manipulated variables, MPC I, set point 2

For the fuel rack position, the effect of the fuel limiter operation can be observed as in the previous test. Small oscillations were present, due to pulsations of supplied air for combustion, resulted from the instability in the compressor as described earlier.

The control output and the relay switching are shown in Figure 5.16.

The particular responses were taken with the relay switching set to open and close the solenoid valve when the threshold of 3, in the command, was exceeded. The control output, labeled as xmpc, momentarily exceeded limits in the beginning, in an effort to provide more action in the start of the disturbance. The controller showed proper corrective action in an effort to reach fast the pressure set point; but the outcome in the actual pressure and further in opacity was not very satisfactory. This results from the setting of the relay switching. The particular value of threshold allowed efficient modulation of air from time 100 until the end of transient, but had the

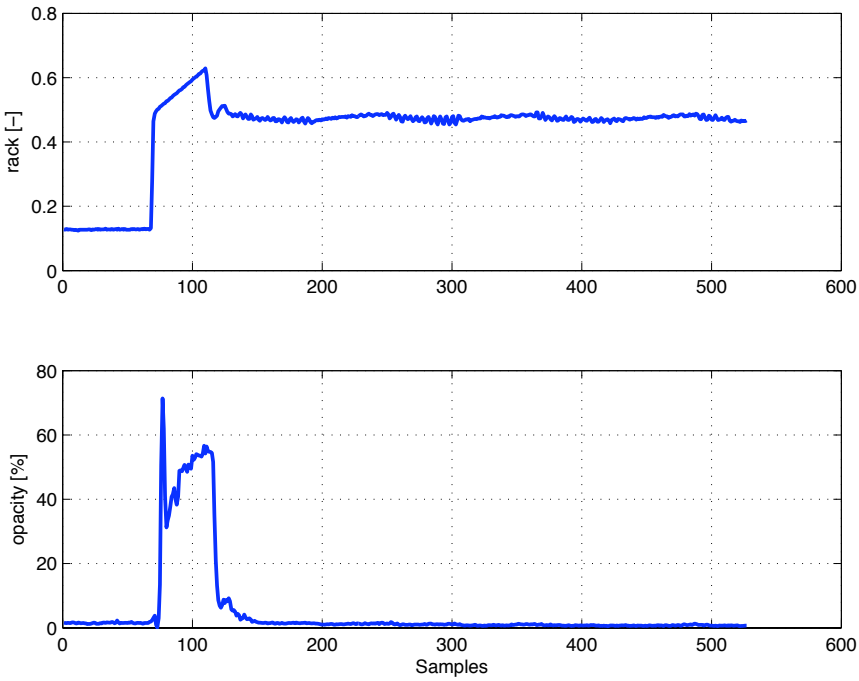

Figure 5.15: Opacity and fuel rack variables, MPC I, set point 2

drawback of early closure in the beginning, at time 70 until about 80.

5.4.2 Results from Opacity Control

The second controller, MPC II, used a model that related injected air and fuel to opacity and pressure in intake manifold. The fuel was considered a measured disturbance.

The configuration of model predictive controller II (MPC II) is shown in Figure 5.17.

In this setup, the measurement of opacity was taken into consideration from the feedback control system. In addition, the signal from fuel rack position, also taken into consideration from the feedback control system, will be used for feedforward control action: the controller will respond to changes in fuel, before it gets the (delayed by 0.6 sec) signal from opacity.

The model structure which is used by the predictive controller comes

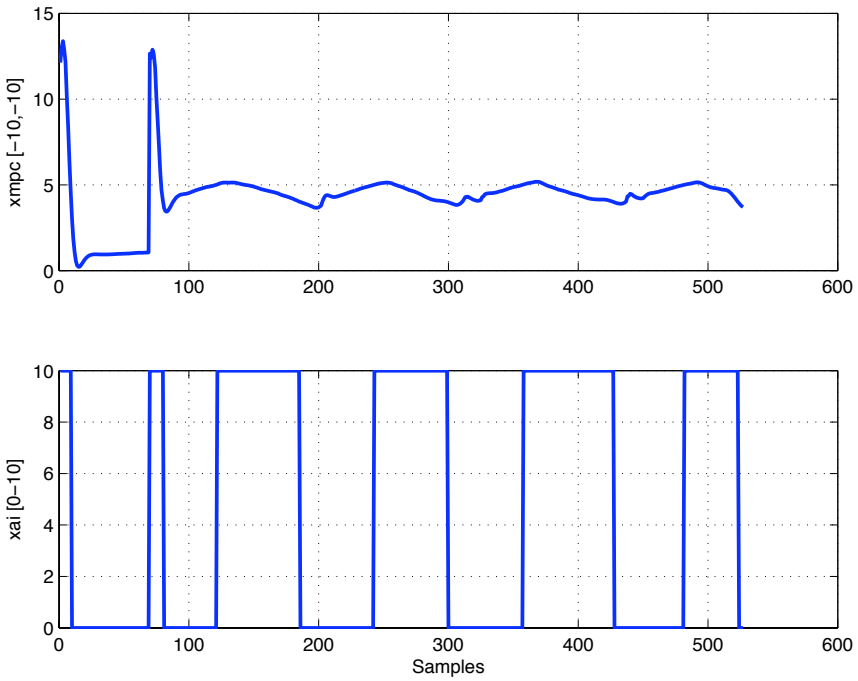

Figure 5.16: Control output and the relay switching, MPC I, set point 2

from prediction error method, in the form of transfer functions, discretized at 0.1 sec. Results from the prediction error method were presented in Section 3.4.3.

As explained earlier, the elements of relay in the output and the Butterworth filter in pressure signal were also present.

For this type of controller, two different settings for the relay switching were chosen. These settings affect the on/off sequence in the air injection actuator; practically affect the modulation of air the intake manifold. In the first case, setting a, the solenoid valve opens in the threshold of 0.6 of command signal and closes in the threshold of 0.3. In the second case, setting b, the solenoid valve opens in the threshold of 1.5 of command signal and closes in the threshold of 0.8. In both cases the intake manifold pressure constraint is set to 0.7 of a scaled value, which corresponds to 1.7 bar in actual pressure.

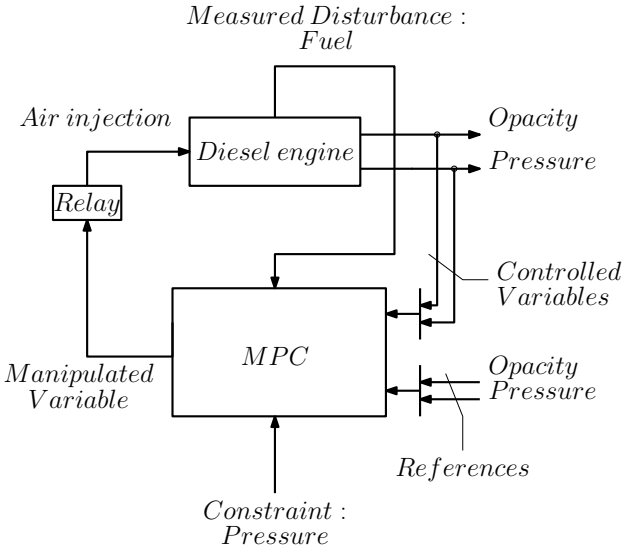

Figure 5.17: Predictive controller for opacity (MPC II)

For the first type of settings, setting a, the responses of the controlled and manipulated variables are shown in Figure 5.18.

A step load from 0 to 47.5 % was applied to the engine, with the speed set at 1200 rpm. The set point of opacity was set to zero, as it is a disturbance rejection case. The air injection controller provided the necessary command to the solenoid actuator for the air admission. The set point of 1.7 bar for intake manifold pressure was set as a constraint, whose value was not allowed to be exceeded during the transient. With this set point, the compressor was brought to a intermediate instability.

It can be seen from Figure 5.18 that the control can be considered rather satisfactory.

Opacity reached immediately its highest value of 75% but quickly the effect of the air injection brought a reduction. After the peak value, the opacity dropped to about 30% for a very short time and then increased to a final value of almost 55%. The delay in the response of opacity measurement is evident. It is obvious that that some improvement in order to avoid the increase to a higher value from 30% to 50% must be provided.

The responses of intake manifold pressure and fuel rack position are

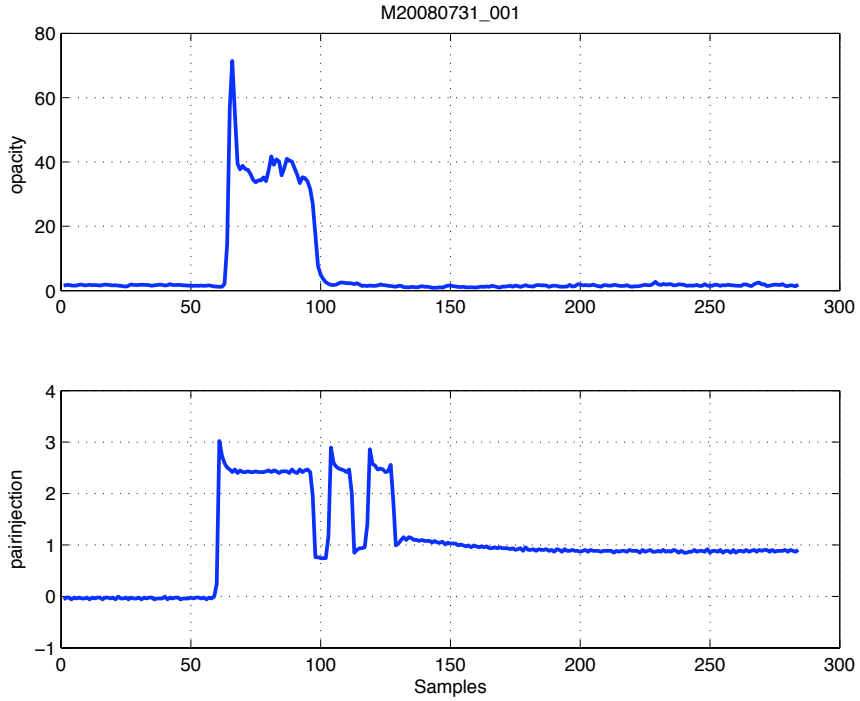

Figure 5.18: Controlled and manipulated variables, MPC II, setting a

shown in Figure 5.22.

During the disturbance, the air injection increased pressure in intake manifold, and the constraint of 0.7 (about 1.7 bar in actual pressure) was violated only for a short period, between time unit 120 and 130. For the rest of the disturbance, the pressure was kept below the constraint. The control can be considered satisfactory, for two reasons. First, it can be seen that the filtered signal does not overcome the constraint value of 0.7. This means that the controller is aware of the actual constraint violation. Second, although the oscillation in pressure is significant, the internal controller model forecasts the pressure behavior satisfactorily.

For the fuel rack position, the effect of the fuel limiter operation can be observed as in previous cases.

The control output and the relay switching are shown in Figure 5.23.

It can be seen that the solenoid valve opens in the threshold of 0.6 of

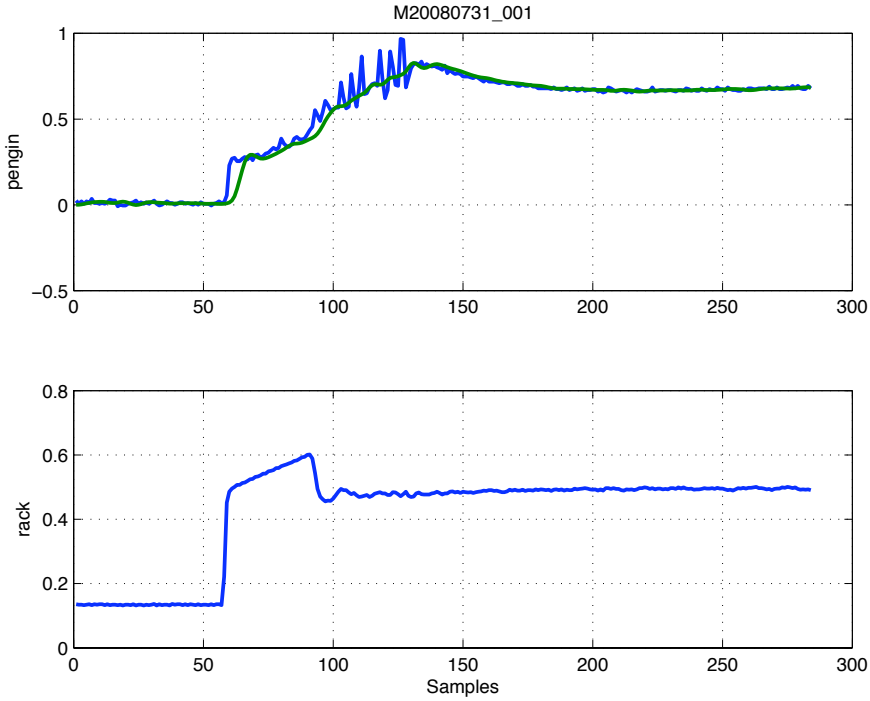

Figure 5.19: Constraint and fuel rack variables, setting a

command signal and closes in the threshold of 0.3. The command does not reach the maximum allowed level of 10 (equal to 100%).

For the second type of settings, setting b, the responses of the controlled and manipulated variables are shown in Figure 5.21.

A step load from 0 to 47.5 % was applied to the engine, with the speed set at 1200 rpm. The set point of opacity was set to zero, as it is a disturbance rejection case. The air injection controller provided the necessary command to the solenoid actuator for the air admission. The set point of 1.7 bar for intake manifold pressure was set as a constraint, whose value was not allowed to be exceeded during the transient. With this set point, the compressor was brought to a intermediate instability.

It can be seen from Figure 5.21 that the control can be considered rather satisfactory.

Opacity reached immediately its highest value of 85% but quickly the

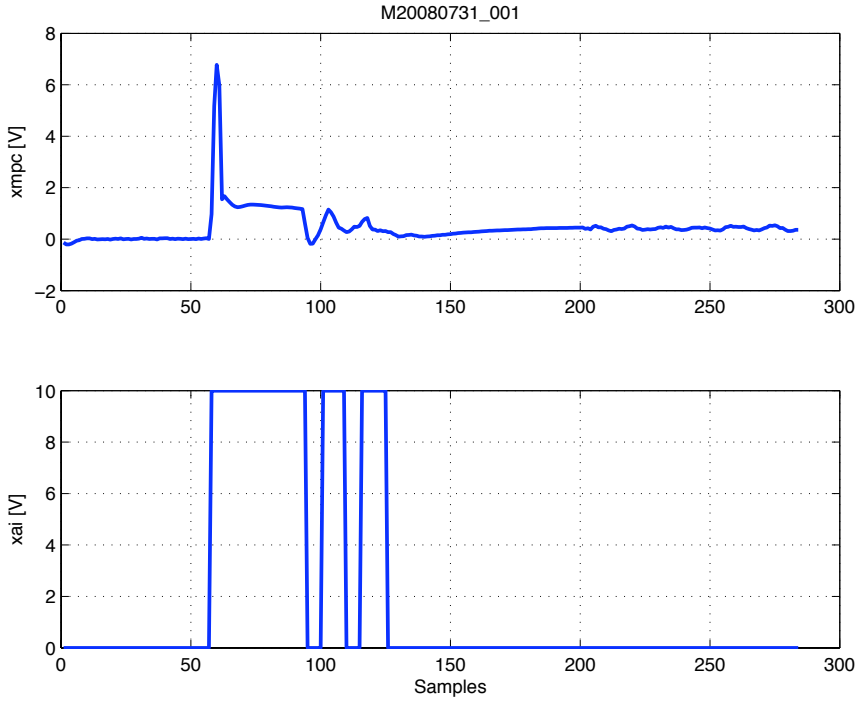

Figure 5.20: Control output and the relay switching a

effect of the air injection brought a reduction. After the peak value, the opacity dropped to about 40% after by the end of disturbance. The delay in the response of opacity measurement is evident.

The responses of intake manifold pressure and fuel rack position are shown in Figure 5.22.

During the disturbance, the air injection increased pressure in intake manifold, and the constraint of 0.7 (about 1.7 bar in actual pressure) was not violated during the transient. The control can be considered satisfactory, as the internal controller model forecasts the pressure behavior satisfactorily. Oscillation in pressure was present also in this test. However, the magnitude was lower than the in the previous case.

For the fuel rack position, the effect of the fuel limiter operation can be observed as in previous cases.

The control output and the relay switching are shown in Figure 5.23.

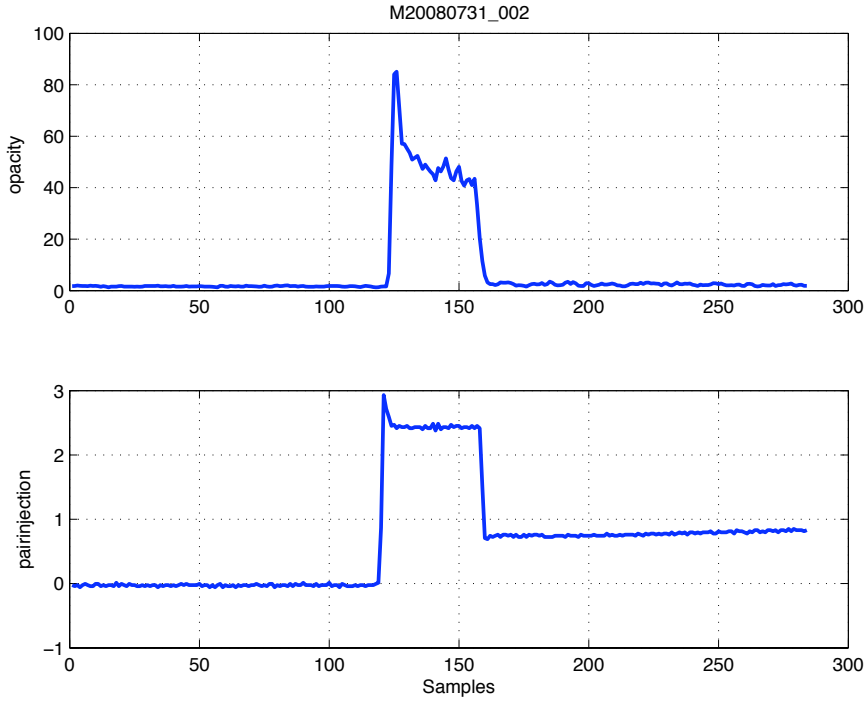

Figure 5.21: Controlled and manipulated variables, MPC II, setting b

It can be seen that the solenoid valve opens in the threshold of 0.6 of command signal and closes in the threshold of 0.3. The command does not reach the maximum allowed level of 10 (equal to 100%). In comparison with the case of setting a, with current setting b, the actuator provides less air.

The comparison in performance for achieved opacity is shown in Figure 5.24.

It can be seen that controller MPC II, with setting a, achieved bigger reduction in opacity. Controller with setting b, had a higher peak, at 85% and dicreased up to 40%, while controller with setting a, had a high peak, at 70% and dicreased for most of the time under 40%.

The comparison in performance for intake manifold pressure is shown in Figure 5.25.

It can be seen that controller MPC II, with setting b, caused less instability in the intake manifold pressure. Controller with setting a, caused

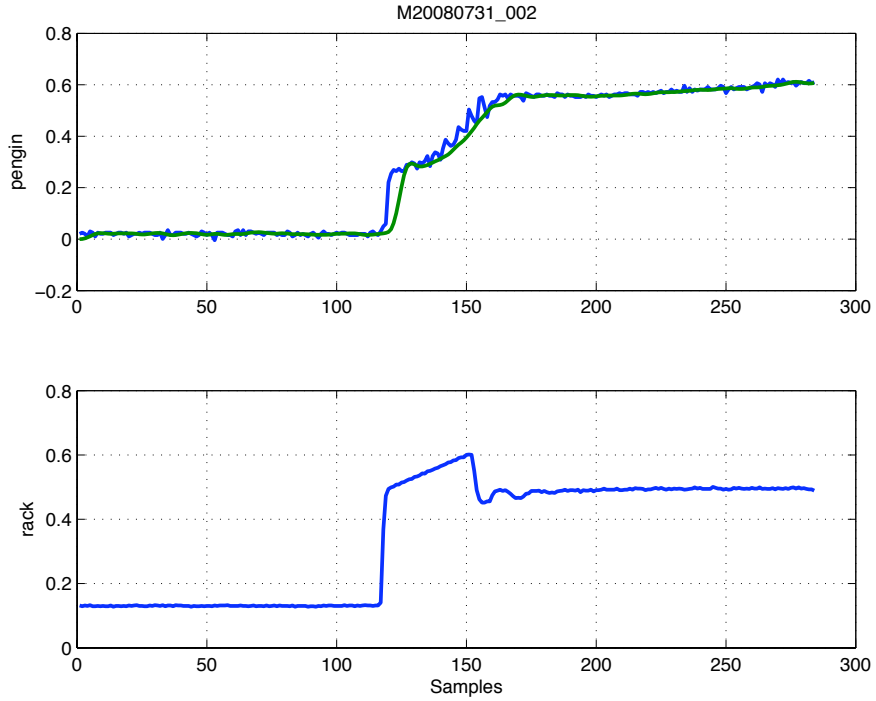

Figure 5.22: Constraint and fuel rack variables, setting b

more instability, but increased the pressure higher. Since the controller with the constraint feature achieves in not violating the pressure limit, controller MPC II is a better choice.

A comparison of opacity under MPC control is shown in Figure 5.26. It can bee seen that in the case with air injection, the opacity was reduced considerably. The initial peak value in both cases remained the same, around 80% for this type of loading 0% up to 47.5%. However when the air was injected in the manifold, after about 5 time samples (0.5 sec) the peak dropped at about 40% and remained in this lower level until the end of the disturbance.

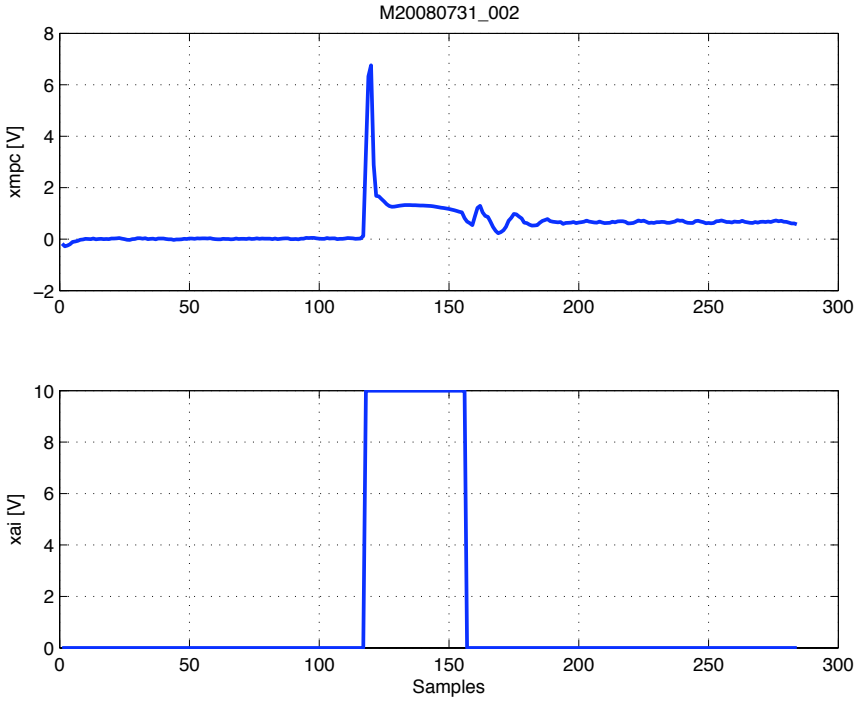

Figure 5.23: Control output and the relay switching b

5.5 Summary

In this chapter the main results of this work were presented. Based on the identified models for the inputs-outputs, the model predictive controller was implemented on the engine. Simulations with the model inputs and outputs in closed loop, allowed for appropriate choices of the tuning parameters of the controller. The most important parameters that were selected were the prediction horizon, controller weights and sampling times. This practice contributed to minimize the required testbed operation. At the same time, instabilities or poor closed-loop system performance were avoided.

Two different controllers were implemented in the testbed, MPC I and MPC II. Both controllers had as manipulated variable the air injection supply. Controller MPC II had the fuel as measured disturbance. Controller MPC I had as controlled variable the pressure in intake manifold. Con-

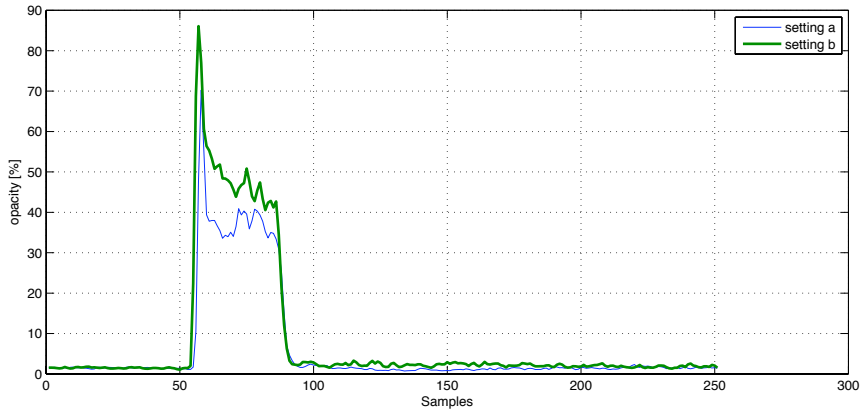

Figure 5.24: Comparison for opacity, MPC II

troller MPC II, respectively had as controlled variable the opacity. The control strategy was successful in the opacity reduction and the achievement of the desired pressure in intake manifold, which was formulated in the controller as a constraint. Based on the responses of opacity and intake manifold pressure during the transient, controller MPC II showed better performance.

Results comparing the opacity under air injection model predictive control with the standard engine operation, i.e. without air injection, during the same transient were presented.

Based on the above results, it can be seen that with air injection, opacity was reduced considerably. The peak value remained the same in both cases, about 80%. However, in the case with air injection, this peak dropped considerably after about 0.5 sec to a steady value of about 40%, until the end of disturbance.

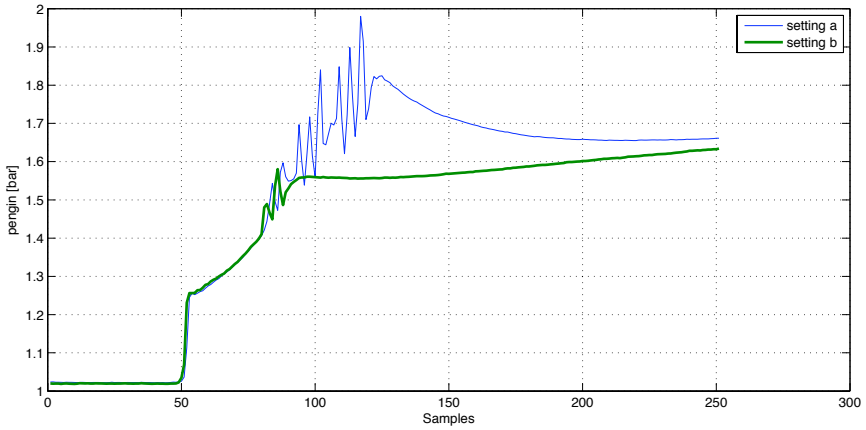

Figure 5.25: Comparison for intake manifold pressure, MPC II

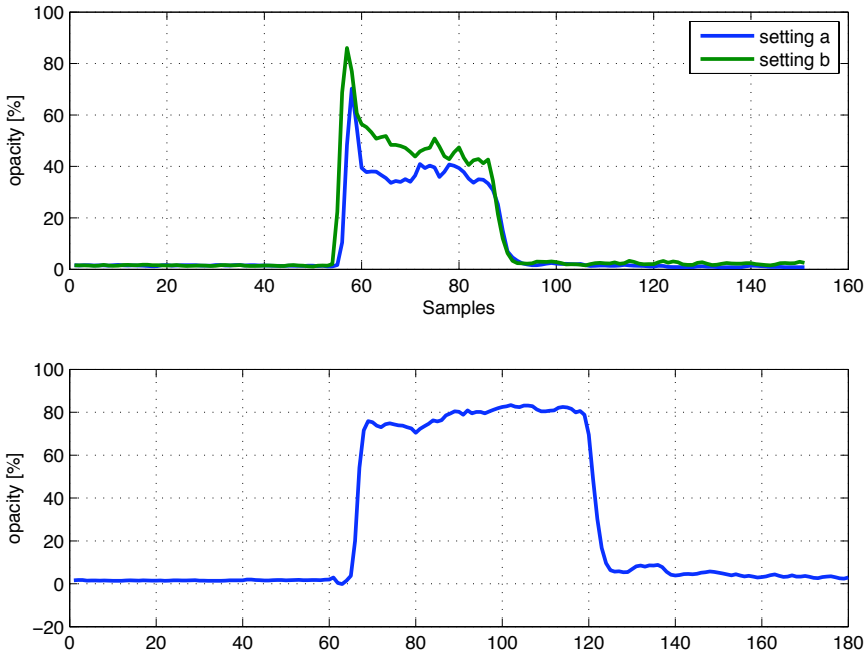

Figure 5.26: Comparison of opacity with air injection under MPC control (top) and without air injection

Chapter 6

Conclusions and Future Work

Two main ideas were followed in this research work: system identification and predictive control. The model construction from experimental data, based on system identification, provided successful models for the predictive control operation. It can be noted from the results of the controlled variables, that the identified models did not provide perfect forecasts, and in several cases a better model could improve the performance of the closed-loop control system. However, the models captured the dominant dynamics of the process under control, and have led to a satisfactory overall control performance.

From the three types of identified models, parametric methods in the form of transfer function models and subspace identification methods in the form of state-space models, were finally implemented on the experimental engine. The third nonlinear model of Hammerstein-Wiener type, was used only in simulations, but provided promising results for a possible direction towards nonlinear model predictive control in the future.

The uncertainty of the identified models in transfer function form was provided and evaluated. It showed for some model parameters that their estimate was not precise. This is due to the extend that the particular identification data for that combination of input-output did not provide adequate or rich information, so that the errors were significant. For the

cases that the fuel is involved as variable in identification[1], the problem in identification becomes ill-conditioned, as the respective fuel data come from closed-loop control operation.

Having identified parameters that relate opacity and pressure in manifold to air injection and fuel, model predictive control was used for opacity control, under the constraint of high pressure in manifold.

Simulations with the model inputs and outputs in closed loop, allowed for appropriate choices of the tuning parameters of the controller. The most important parameters that were selected were the prediction horizon, controller weights and sampling times. The simulation phase was an import and contribution towards the decrease of testbed operation time and avoidance of instabilities or poor closed-loop system performance.

Based on the identified models for the inputs-outputs, the model predictive controller was implemented on the engine.

Two different controllers were implemented in the testbed, MPC I and MPC II. Both controllers had as manipulated variable the air injection supply. Controller MPC I had as controlled variable the pressure in intake manifold. Controller MPC II had the fuel as measured disturbance and the opacity as controlled variable.

The use of MPC I allowed quick shakedown of the experimental arrangement, provided familiarization with the engine testbed under air injection control as well as valuable experience for the control of pressure in the engine intake manifold. The model used based on subspace identification method. Two different pressure set points were chosen, 1.7 bar and 2.0 bar.

With controller MPC II, the measurements of opacity and fuel rack position were taken into consideration from the feedback control system. The model structure which was used by the predictive controller comes from prediction error method, in the form of transfer functions, discretized at 0.1 sec. For this type of controller, two different settings for the relay switching were tested.

Based on the responses of opacity and intake manifold pressure during

[1]From a control point of view, fuel was used as disturbance variable, air injection was used as manipulated variable, opacity was the controlled variable and intake manifold pressure was used as constraint

the transient, controller MPC II showed better performance.

Results comparing the opacity under air injection model predictive control with the standard engine operation, i.e. without air injection, during the same transient were presented.

Based on the above results, it can be seen that with air injection, opacity was reduced considerably. The peak value remained the same in both cases, about 80%. However, in the case with air injection, this peak dropped considerably after about 0.5 sec to a steady value of about 40%, until the end of disturbance. This significant reduction obtained in the full scale testbed experiments demonstrated the effectiveness of the proposed system of controlled air injection for smoke abatement during engine transients, as well as the suitability of the control method used.

Future Work

- During the air injection operation, the engine boost pressure is rapidly increased and oxygen is admitted to the engine for combustion. This could cause a considerable increase in NOx formation. In this work, the role of NOx formation was not taken into consideration, as this could cause complexity in the control approach. It remains of interest to incorporate NOx, with measurements and respective modelling, in an approach similar to the opacity, to the control problem of emissions for a diesel engine.

- In the particular setup of the present work, envisioned as a possible retrofit application for smoke reduction, fuel was considered as an independent control variable. In a possible integrated scheme, the fuel/engine speed control could be incorporated in the model predictive control. In practice, the fuel control receives the highest attention for engine operation, as it affects both the engine performance and emissions.

- In this work only one control objective at a time was used, that of minimising the opacity or the pressure in the manifold. Relevant with the earlier point on fuel/speed problem, a possible extension could be

to use multiple control objectives, depending on the operating point. In this case the objective function is no longer a quadratic function and quadratic programming algorithms cannot be used.

- Another area of potential study is to incorporate robustness in the engine model through uncertainties. Analysis of robust stability is of great importance and analytical tools are not available to guarantee stability for constrained model predictive control. Therefore, there is considerable related work that could be applied to the control study of diesel engines.

- In this work, the state estimation part in the predictive controller was performed with a standard Kalman Filter, for the linear models which were used in the two types of controllers. In the case that a nonlinear model is used in order to describe the air dynamics in the intake manifold and opacity, then relevant work can be carried out with an extended Kalman filter, applicable to nonlinear models.

- Approaches involving active surge control may be of interest but system reliability issues must be carefully considered in any approach, since in large engines turbocharger compressor surge cannot be tolerated.

- The plant type in this work, contains many elements that are discrete in nature: the control of air injection was through the solenoid valve, the fuel command had considerable limiting action, etc. These types of problems today are considered as 'hybrid' [Bem04], and it would be challenging to provide a solution for the various controls of the experimental engine under this point of view with the implementation of predictive control.

References and Bibliography

[AFN04] F. Allgower, R. Findeisen, and Z. Nagy. Nonlinear model predictive control: From theory to application. *J. Chin. Inst. Chem. Engrs*, 35(3), 2004.

[Age08] Environmental Protection Agency. Control of emissions of air pollution from locomotive engines and marine compression-ignition engines less than 30 liters per cylinder. EPA-HQ OAR 2003 0190, FRL-85453, Federal Register, www.regulations.gov, May 2008.

[Ale06] N. Alexandrakis. Shaft power measurement on the testbed MAN B&W 5 L16/24. Technical Report LME/TR-118, Laboratory of Marine Engineering, NTUA, March 2006.

[AVLa] AVL List GmBH. *AVL 439 Opacimeter Operating Manual*, 11/2003 edition.

[AVLb] AVL List GmBH. *AVL Indiset 620 User Manual*, 1/2002 edition.

[AVLc] AVL List GmBH. *TDC Sensor 428 Operating Instructions*, 1/2002 edition.

[BBA02] B. Brunell, R. Bitmead, and Connolly A. NMPC of an aircraft gas turbine engine. In *Proceedings of 41st IEEE Conference om Decision and Control*, volume 6, 2002.

[Bem04] A. Bemporad. *Hybrid Control Toolbox*, first edition, 2004.

[Ben04] J. Bengtsson. *Closed loop control of HCCI engine dynamics*. PhD thesis, Lund University, 2004.

[BM99] A. Bemporad and M. Morari. Robust model predictive control: A survey. In A. Vicino, A. Garulli, and A. Tesi, editors, *Robustness in identification and control, Lecture notes in control and information sciences*, volume 245. Springer, 1999.

[BMR07] A. Bemporad, M. Morari, and N. Ricker. *Model predictive control toolbox 2.* The Mathworks, second edition, 2007.

[BO03] M. Bai and K. Ou. Design and implementation of electromagnetic active control actuators. *Journal of Vibration and Control*, 9:997–1017, 2003.

[Boc94] H. Bockhorn. *Soot Formation in Combustion.* Springer-Verlag, 1994.

[CB00] E. Camacho and C. Bordons. *Model Predictive Control.* Springer, 2000.

[CIM08] CIMAC. CIMAC guide to diesel exhaust emissions control of NOx, SOx, particulates, smoke and CO2- seagoing ships and big stationary diesel power plants. Technical report, CIMAC Working Group on Exhaust Emissions, draft for publication, August 2008.

[CMT87a] D. Clarke, C. Mohtadi, and P. Tuffs. Generalized predictive control. Part I. The basic algorithm. *Automatica*, 23(2):137–148, 1987.

[CMT87b] D. Clarke, C. Mohtadi, and P. Tuffs. Generalized predictive control. Part II. Extensions and interpretations. *Automatica*, 23(2):149–160, 1987.

[CVKA05] E. Codan, I. Vlaskos, N. Kyrtatos, and N. Alexandrakis. Controlled pulse turbocharging of medium speed 5-cylinder diesel engine. In *Proceedings of 10th Turbocharger Conference, Dresden, 22-23 September 2005*, Paris, France, 2005.

[dJ95] B. de Jager. Rotating stall and surge control: A survey. In *Proceedings of the 34th Conference on Decision and Control*, December 1995.

[FAD+01] R. Findeisen, F. Allgower, M. Diehl, G. Bock, P. Schloder, and Z. Nagy. Efficient nonlinear model predictive control. In *Proceedings of Chemical Process Control*, volume 6, 2001.

[FLD06] H. Ferreau, G. Lorini, and M. Diehl. Fast nonlinear model predictive control of gasoline engines. *Proceedings of the 2006 IEEE International Conference on Control Applications*, 2006.

[Fle96] R. Fletcher. *Practical Methods of Optimization.* John Wiley, 1996.

[GO04] L. Guzzella and C. Onder. *Introduction to Modelling and Control of Internal Combustion Engine Systems.* Springer, 2004.

[HB85] C. Harris and S. Billings, editors. *Self-Tuning and Adaptive Control: Theory and Applications.* Peter Peregrinus, 1985.

[Hey98] J. Heywood. *Internal Combustion Engine Fundamentals.* McGraw Hill, 1998.

[HM97] M. Huzmezan and J. M. Maciejowski. RCAM design challenge presentation document: the model based predictive control approach. Technical Report GARTEUR/TP-088-20, GARTEUR, 1997.

[HOO+06] S. Hashimoto, H. Okuda, Y. Okada, S. Adachi, S. Niwa, and M. Kajitani. An engine control systems design for low emission vehicles by generalized predictive control based on identified model. In *Proceedings of the 2006 American Control Conference*, 2006.

[HRFA06] M. Herceg, T. Raff, R. Findeisen, and F. Allgower. Nonlinear model predictive control of a turbocharger diesel engine. *Proceedings of the 2006 IEEE International Conference on Control Applications*, 2006.

[HS97] M. Henson and D. Seborg. *Nonlinear Process Control*. Prentice Hall, 1997.

[Jua94] J.N. Juang. *Applied System Identification*. Prentice Hall, 1994.

[Jun03] M. Jung. *Mean value modelling and robust control of the airpath of a turbocharged diesel engine*. PhD thesis, University of Cambridge, 2003.

[KC01] B. Kouvaritakis and M. Cannon. Nonlinear predictive control: theory and practice. In B. Kouvaritakis and M. Cannon, editors, *Introduction*. IEE Control Engineering Series, 2001.

[KCM02] E. Kerrigan, H. Chen, and J. M. Maciejowski. CUDSID 1.0 System Identification Toolbox-User's Guide. Technical report, Cambridge University Engineering Department, 2002.

[KJB00] R. Kvaternik, J-N. Juang, and R. Bennet. Exploratory studies in generalized predictive control for active aeroelastic control of tiltrotor aircraft. In *American Helicopter Society Northeast Region Active Controls Technology Conference*, 2000.

[KM99] E. Kerrigan and J. M. Maciejowski. Fault tolerant control of a ship propulsion system using model predictive control. In *Proceedings of European Control Conference*, Karlsruhe, Germany, August 1999.

[Kyr07] N. P. Kyrtatos. Marine engines and atmospheric pollution (presentation in greek). Athens, Greece, December 2007. Meeting at Evgenidou Foundation.

[Lju99] L. Ljung. *System Identification: Theory for the User, second edition*. Prentice Hall, 1999.

[Lju07] L. Ljung. *System Identification Toolbox 7*. The Mathworks, 2007.

[LKK05] G. Livanos, E. Kanellopoulou, and N. P. Kyrtatos. Marine diesel engine rapid load acceptance without smoke. In *Proceedings*

of 7th International Symposium on Marine Engineering. ISME, Tokyo, Japan, October 2005.

[LLG+08] D. Lack, B. Lerner, C. Granier, T. Baynard, E. Lovejoy, P. Massoli, A. Ravishankara, and E. Williams. Light absorbing carbon emissions from commercial shipping. *Geophysical Research Letters*, 35(11), 2008.

[LPKC07] G. Livanos, G. Papalambrou, N. P. Kyrtatos, and A. Christou. Electronic engine control for ice operation of tankers. In *Proceedings of 25th CIMAC World Congress, Vienna, Austria, May 2007*, Vienna, Austria, 2007. CIMAC.

[LTK03] G. Livanos, G. Theotokatos, and N. P. Kyrtatos. Simulation of large marine two-stroke diesel engine operation during fire in the scavenging air receiver. *Journal of Marine Engineering and Technology*, (A3), 2003.

[LYM06] K. Ling, S. Yue, and J. M. Maciejowski. A FPGA implementation of model predictive control implementation of model predictive control. In *Proceedings of the 2006 American Control Conference*, June 2006.

[Mac04] J.M. Maciejowski. *Predictive Control with Constraints*. Prentice Hall, 2004.

[Mat07] The Mathworks. *Signal Processing Toolbox 6 - User's Guide*, sixth edition, 2007.

[MGK07] J. M. Maciejowski, P. Goulart, and E. Kerrigan. *Advanced Strategies in Control Systems with Input and Output Constraints*, volume 346, chapter : Constrained Control Using Model Predictive Control. Springer, 2007.

[MIO94] I. Mkilaha, M. Inoue, and K. Ohtake. Reduction of emissions in IDI diesel engine by air injection. In *Proceedings of the International Symposium COMODIA 94*, 1994.

[MK06] W. Majewski and M. Khair. *Diesel Emissions and Their Control*. SAE International, 2006.

[ML99] M. Morari and J. Lee. Model predictive control: Past, present, and future. *Computers and Chemical Engineering*, 23(667), 1999.

[Moh51] K. Mohr. Development and today's state of the archaouloff fuel injection process for compressorless diesel engines. In *Proceedings of 1st International Congress on Combustion Engines*, Paris, France, 1951. International Congress on Combustion Engines.

[Mos95] E. Mosca. *Optimal, Predictive and Adaptive Control*. Prentice Hall, 1995.

[OdR07] P. Ortner and L. del Re. Predictive control of a diesel engine air path. *IEEE Transactions on Control Systems Technology*, 15(3), May 2007.

[OR94] B. Ogunnaike and W. Ray. *Process Dynamics Modeling and Control*. Oxford University Press, N.Y., 1994.

[OS75] A. Oppenheim and R. Schafer. *Digital Signal Processing*. Prentice Hall, 1975.

[PAK+07] G. Papalambrou, N. Alexandrakis, N. P. Kyrtatos, E. Codan, I. Vlaskos, V. Pawils, and R. Boom. Smokeless transient loading of medium/high speed engines using a controlled turbocharging system. In *Proceedings of 25th CIMAC World Congress*. 25th CIMAC World Congress, Vienna, Austria, May 2007.

[Pap06a] G. Papalambrou. Power Take In (PTI) system on compressor for small gen-set engines during transient operation-Part A, Task 11.1. Technical Report D11.1a, I.P. HERCULES, www.ip-hercules.com, January 2006.

[Pap06b] G. Papalambrou. Reduced order engine models in MATLAB. Technical Report LME/TR-123, Laboratory of Marine Engineering, NTUA, Athens, Greece, March 2006.

[Pap06c] G. Papalambrou. Torque control of AEG GC 40.22M motor/generator of LME. Technical Report LME/TR-122, Laboratory of Marine Engineering, NTUA, Athens, Greece, March 2006.

[Pap07] G. Papalambrou. Power Take In (PTI) system on compressor for small gen-set engines during transient operation-Part B. Technical Report D11.1a, HERCULES Task 11.1, August 2007.

[PK06] G. Papalambrou and N. Kyrtatos. Hinfinity robust control of marine diesel engine equipped with Power-Take-In system. In *Proceedings of 11th IFAC Symposium on Control in Transportation Systems*, Delft, The Netherlands, August 2006.

[PK08] G. Papalambrou and N. P. Kyrtatos. NMPC for load acceptance without smoke in marine diesel engines. In *Proceedings of International Workshop on Assessment and Future Directions of Nonlinear Model Predictive Control (NMPC08)*, Pavia, Italy, September 2008.

[QB03] S. Qin and T. Badgewell. A survey of industrial model predicitve control technology. *Control Engineering Practice*, 11, 2003.

[Raw00] J. Rawlings. Tutorial overview of model predicitve control. *IEEE Control systems magazine*, 6 2000.

[SEM04] D. Seborg, T. Edgar, and D. Mellicamp. *Process Dynamics and Control*. Wiley, second edition, 2004.

[Sou04] J. Souder. *Closed-loop control of a multi-cylinder HCCI engine*. PhD thesis, University of California at Berkeley, 2004.

[SP96] S. Skogestaad and I. Postlethwaite. *Multivariable Feedback Control*. Wiley, 1996.

[SS00] A. Stafanopoulou and R. Smith. Maneuverability and smoke emission constraints in marine diesel propulsion. *Control Engineering Practice*, (8), 2000.

[Sti03] G. Stiesch. *Modeling Engine Spray and Combustion Processes.* Springer, 2003.

[TK02] G. Theotokatos and N.P. Kyrtatos. Analysis of a large two-stroke marine diesel engine transient behaviour during compressor surging. In *Proceedings of the 7th International Conference on Turbochargers and Turbocharging*, 2002.

[VCM99] E. Vinuela, J. Cubillos, and C. Moraga. Linear model-based predicitve control of the LHC 1.8 K cryogenic loop. In *Proceedings of the 1999 Cryogenic Engineering and International Cryogenic Materials Conference*, 1999.

[vEL01] H. van Essen and H. Lange. Nonlinear model predictive control experiments on a laboratory gas turbine installation. *Journal of Engineering for Gas Turbines and Power*, 123, April 2001.

[vOdM96] P. van Overschee and B. de Moor. *Subspace Identification for Linear Systems.* Kluwer Academic Publishers, 1996.

[VSP04] A. Vahidi, A. Stefanopoulou, and H. Peng. Model predicitve control for starvation prevention in a hybrid fuel cell system. In *IEEE Proceedings of 2004 American Control Conference.* IEEE, 2004.

[Wel93] P. Wellstead. Notes on signal processing. UMIST, Control Systems Centre, 1993.

[WMD99] J. Warnatz, U. Maas, and R. Dibble. *Combustion: Physical and Chemical Fundamentals, Modeling and Simulation, Experiments, Pollutant Formation.* Springer, second edition, 1999.

[WZ91] P. Wellstead and M. Zarrop. *Self-Tuning Systems.* Wiley, 1991.

[ZB93] Y. Zhu and T. Backx. *Identification of Multivariable Industrial Processes for Simulation, Diagnosis and Control.* Springer, London, 1993.

Appendices

.1 Instrumentation and Controllers

Pressure sensors

The testbed engine is equipped with four types of pressure sensors, depending on the accuracy and response requirements of the measured pressure channel.

One type is KISTLER 4075A10, where pressure acts via a thin steel diaphragm on a silicon measuring element. The latter contains diffused piezo-resistive elements connected in the form of a Wheatstone measuring bridge. The effects of pressure unbalance the bridge and produce an output signal of 0-500 mV. These sensors are suitable for inlet/outlet pressure measurements of combustion engines, like the sensor PE 303 for charge-air pressure. Range is 0-10 bar abs (refereed to vacuum and not to atmospheric pressure), with natural frequency of 45 kHz, for rapid changes in pressure. It is mounted on the engine with suitable cooling adapter.

For in-cylinder pressure AVL GU21D uncooled transducer was used, with M7 thread. The natural frequency is 85 kHz, with measurement range of 0-250 bar. Sensing element is AVL GaP04 (gallium orthophosphate) crystal, whose compactness and thermal stability allows it to be mounted to the combustion chamber and makes capable to give high precision measurements without interference from pipe oscillations.

There is also pressure transducer from GE DRUCK PTX1400, absolute pressure, range 0-10 bar, 0.15 % accuracy, with silicon pressure diaphragm.

The various sensors are shown in 1.

The AVL amplifiers: rack and individual 2 units are shown in 2.

Shaft torque measurement

Mechanical torque is measured by strain-gauge bridges placed on the inner surface of the hub which connects the brake shaft with the rubber coupling. In order to convert the shaft deformation in an instant torque signal, it is required to convert the principal surface strains into an electrical voltage. Telemetry is used in order to transfer the signal from the rotating shaft to the inductive pick-up and further on with cables to the signal electronics

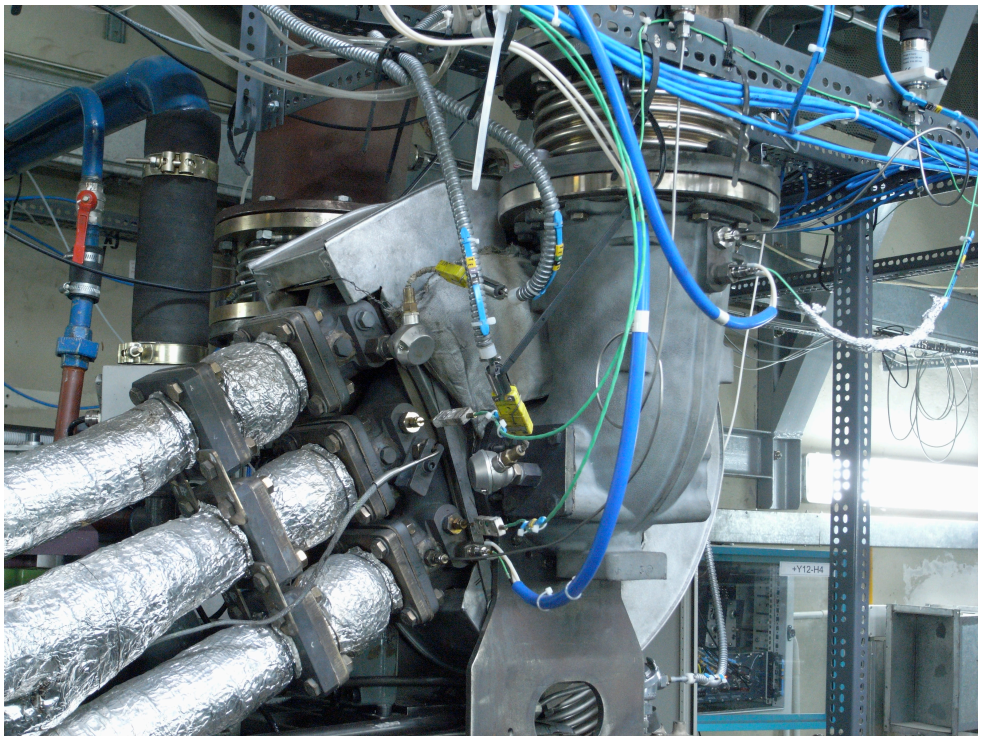

Figure 1: The various sensors at engine

that produce the final analog torque signal.

The torque signal passes through an isolator with 30 Hz bandwidth and a first-order filter with time constant of 0.8 sec before is fed to the closed-loop torque controller in the ATLAS system. The relative uncertainty coefficient is 0.35%. Details of the torque measurement configuration can be found in [Ale06].

The brake torque controller was tuned experimentally as described in [Pap06c].

Temperature

Temperatures are measured at various points at the engine. Sensors are thermocouples and RTDs. A thermocouple consists of two different types of metals, joined together at one end. When the junction of the two metals is heated or cooled, a voltage is created that can be correlated back to the

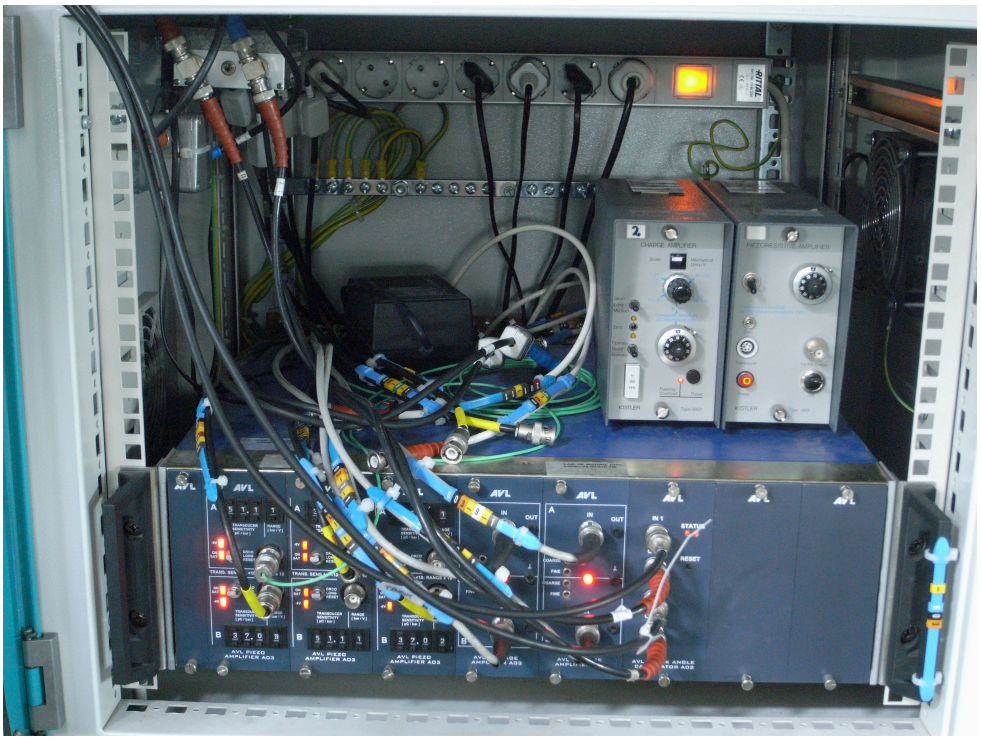

Figure 2: The AVL amplifier rack

temperature. Resistance Temperature Detectors (RTD) are sensors that contain a resistor that changes resistance value as its temperature changes, usually made of platinum.

TDC sensor

In the thermodynamic evaluation of pressure curves measured in internal combustion engines, the exact determination of the top dead centre (TDC) is required. As the rigid construction of an engine is not ideal, a statically determined TDC can involve uncertainties. Therefore a TDC determination with the engine motored in the speed of 1200 rpm is determined, with a TDC sensor, model TDC-428 from AVL List [AVLc]. The sensor evaluates the variation in capacitance between the piston and the sensor probe head, and with an electronic circuit, an analog signal corresponding to the piston lift is sent to the DAQ system.

The air injection controller

The host computer is equipped with an ASUS P5V-VM-DH motherboard with a Pentium 4 processor and 448 KB RAM[2] , while the target computer is equipped with an ASUS CUV-4X-E motherboard with a Pentium 3 processor and 640 KB RAM. Both computers have Compaq NC3120 network interface cards. The two computers are connected point to point through an ethernet TCP/IP [3] network at 100 Mbps with a crossover cable. The host PC runs Windows XP, MATLAB/Simulink and Real Time Workshop. The target PC runs only the xPC Target kernel and the control application. It also contains a National Instruments PCI-6024E data acquisition board providing the input and output signals, connected to the PCI bus. The board provides up to eight differential analog input channels, with 12-bit resolution, with configurable sampling rate up to 200 kS/s for all channels, up to two analog outputs, also with 12-bit resolution, at rates of up to 10 kS/s for both channels. The analog signal ranges are from -10V to +10V. In addition eight input/output digital lines, at 5 volts TTL are available.

The xPC toolbox forms the core of the air injection controller. The toolbox provides analog-to-digital (A/D), digital-to-analog (D/A), Digital Input (DIN) and Digital Output (DOUT) device drivers for the selected hardware. The language is C and S-functions. The host PC compiles the Simulink models and downloads them to the target PC. The host computer controls the model execution and allows change of parameters on the fly. The compilation from Simulink to xPC code is performed with RealTime Workshop and uses OpenWatcom C compiler.

The BIOS [4] is the only software component required by the xPC kernel. After BIOS is loaded it searches for a bootable image (executable) which starts the kernel. After the kernel is loaded, the target PC does not many make any other calls to BIOS; the resources on the CPU motherboard are addressed entirely through I/O addresses. The kernel activates the application loader and waits to download the target application from the host PC. The loader receives the code, copies the different code sections to their

[2]Random Access Memory

[3]Transmission Communication Protocol/Internet Protocol

[4]Basic Input Output System: system software loaded by PC at boot time.

designated addresses and sets the target application ready to start. The executable target application provides full 32-bit power. The choice of the PC components and the 32-bit Intel or AMD processor, ensure compatibility with the xPC OS.

.2 Compressor Instability

Description of instability

Surge and rotating stall are flow instabilities which occur in turbomachinery. Surge is a self-excited cyclic phenomenon, affecting the compression system as a whole, characterized by large amplitude pressure rise and mass flow fluctuations. Even flow reversal is possible. This type of behavior is a large amplitude limit cycle oscillation. It starts to occur in a region of the compressor map where the pressure rise and mass flow characteristics for constant speed have a positive slope that exceeds a certain value determined by characteristics of the compressor and slope of the load line. The slope of instantaneous mass flow/pressure rise characteristic is important. As a consequence, the onset of surge not only depends on the compressor characteristics, but also on the flow/pressure characteristic of the system it discharges into [dJ95].

Surge has a more complex topology than rotating stall. At least four different categories of surge, with respect to flow and pressure fluctuations, can be distinguished: mild, classic, modified and deep surge.

As shown in Figure 3, the cycle starts at 1 where the flow becomes unstable. It then goes very fast to the negative flow characteristic at 2 and descends until approximately zero flow 3. Then it proceeds very fast to the normal characteristic at 4 where it starts to climb to point 1. Arriving at point 1 the cycle repeats unless measures are taken to stop it.

Rotating surge and stall phenomena restrict the performance (pressure rise) and efficiency (specific power consumption) of the compressor. This may lead to rapid blade heating and to an increase in the exit temperature of the compressor.

Blade vibration and shaft torque reversals may lead to compressor failure.

On the compressor map the line/barrier that separates regions of stable and unstable operations is called *surge line* and it is characterized by three variables: compressor rotating speed, n, mass flow, ϕ, non-dimensional flow coefficient or mass flow divided by the choked mass flow and pressure ratio, Ψ, the non-dimensional pressure coefficient or the pressure ratio between

exit and inlet of the compressor.

Anti-Surge Measures

Measures that have been suggested to cope with surge are as follows [dJ95].

- Surge control, surge avoidance, where the machine is prevented to operate in a region near and beyond the surge line. It is an open loop strategy.

- Surge detection and avoidance, where the surge avoidance starts acting when the onset of surge is detected. It is a closed loop strategy.

- Active surge control, where the flow instabilities are stabilized by one or more actuators who under closed loop control take input from a controller that receives relevant information from suitable sensors.

The accuracy of the detection of surge depends on the instrumentation that should measure quantities that eventually could lead to surge. Due to the small time scales involved, the sensors and actuators should have small time constants and delays. Also the instrumentation should not be intrusive, with low maintenance cost, easily repaired and the reliability of the machine must be ensured.

A surge-avoidance line (or surge control line) which the compressor is not allowed to cross in the compressor map is introduced some distance, e.g. 10% of flow rate, from the actual surge line, although this margin can be altered dynamically. This margin does not follow from a detailed analysis of the influence of disturbances and uncertainties on the surge behavior, but is fixed by empirical rules on an ad-hoc basis. The aim is to achieve under no circumstances, that the turbomachine does not go into surge, despite all uncertainties. On the other hand, this restriction of the feasible operating region unduly restricts the capabilities of the machine. The surge line constraint is a nonlinear inequality constraint; it is approximated by one or more linear constraints [Mac04]. Control systems currently used in industry are based on this control strategy.

Surge avoidance is adopted in the present work, according to which the compressor is allowed to operate at an appropriate pressure and flow so as to avoid the instability. This is shown in Figure 3.

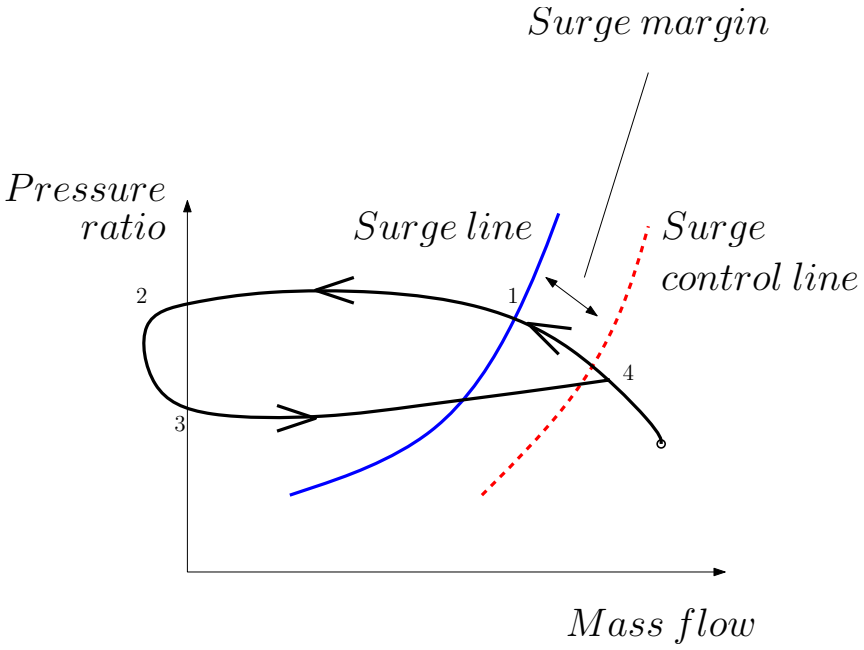

Figure 3: Surge avoidance